Institut für Physikalische und Theoretische Chemie
der Technischen Universität München

ParaGauss — A Parallel Implementation of the Density Functional Method: Spin-Orbit Interaction in the Douglas–Kroll–Hess Approach and a Novel Two-Component Treatment of Spin-Independent Interaction Terms

Alexei V. Matveev

Vollständiger Abdruck der von der Fakultät für Chemie zur Erlangung des akademischen Grades eines

Doktors der Naturwissenschaften (Dr. rer. nat.)

genehmigten Dissertation.

Vorsitzende: Univ.-Prof. Dr. S. Weinkauf
Prüfer der Dissertation
1. Univ.-Prof. Dr. N. Rösch
2. Univ.-Prof. Dr. M. Kleber
3. Univ.-Prof. Dr. W. Domcke

Die Dissertation wurde am 24.09.2003 bei der technischen Universität München eingereicht und durch die Fakultät für Chemie am 30.10.2003 angenommen.

Contents

List of abbreviations

BLYP	Becke–Lee–Yang–Parr
BP	Becke–Perdew
CG	Clebsch–Gordan
CSCO	Complete Set of Commuting Operators
DF	Density-Functional
DFT	Density-Functional Theory
DK	Douglas–Kroll
DKH	Douglas–Kroll–Hess
DKS	Dirac–Kohn–Sham
ee	Electron-Electron
EFM	Eigenfunction Method
EPR	Electronic Paramagnetic Resonance
FF	Fitting Function
fpFW	free-particle Foldy–Wouthuysen
FW	Foldy–Wouthuysen
GGA	Generalized Gradient Approximation
HF	Hartree–Fock
irrep	irreducible representation
KS	Kohn–Sham
LCAO	Linear Combination of Atomic Orbitals
LCGTO	Linear Combination of Gaussian-Type Orbitals
LDA	Local Density Approximation
NMR	Nuclear Magnetic Resonance
PBE	Perdew–Burke–Ernzerhof
PW91	Perdew–Wang, year 1991
QM	Quantum Mechanics
revPBE	Zhang and Yang revision of PBE
RPBE	Hammer, Hansen, and Nørskov revision of PBE
SCF	Self-Consistent Field
SO	Spin-Orbit
SR	Scalar Relativistic
VWN	Vosko–Wilk–Nusair
xc	exchange-correlation
ZORA	Zeroth Order Regular Approximation

Chapter 1

Introduction

Electronic structure calculations evolved from illustrative numerical applications of the Schrödinger equation to a scientific area of predictive strength [1, 2, 3, 4, 5, 6, 7]. Quantum chemistry, the theoretical treatment of the electronic structure of molecular systems, nowadays is one of the major subfields in the area of numerical calculations of the electronic structure of matter. Whether specific problems can be solved by quantum chemistry depends much on the availability of suitable methods which incorporate the relevant interactions so that pertinent characteristics of the system can be modeled. Relativistic quantum chemistry, which by now covers a vast variety of methods and approximations [8], is a field that grew with the attempts to account for relativistic effects in the quantum mechanics (QM) of molecular systems. Such effects are due to the fact that the speed of light is finite, but large enough so that in most cases it can be assumed to be essentially infinite. Relativistic effects are often thought of as unimportant for "normal" molecular system. Very many purely chemical applications of quantum chemistry are successful without accounting for relativity. However, modern chemistry could hardly be imagined without such spectroscopic techniques as electron paramagnetic resonance (EPR), nuclear magnetic resonance (NMR) or other high-resolution methods where relativistic interactions often play an important role. The chemistry of heavy elements cannot be described theoretically without, in some way, accounting for relativistic effects.

A well known example of a relativistic effect is the spin-orbit (SO) interaction in atoms and molecules. One of the observable effects of SO interaction is the fine structure of atomic and molecular spectral lines [9, 10]. The term "spin-orbit" was originally used to describe the coupling $\zeta(r)\boldsymbol{ls}$ of the orbital angular momentum $\boldsymbol{l}$ of an electron and its spin $\boldsymbol{s}$ in atoms. The eigenfunctions of the spherically symmetric SO Hamiltonian are eigenfunctions of the total angular momentum $\boldsymbol{j} = \boldsymbol{l} + \boldsymbol{s}$. The energy dependence on quantum numbers $j = l \pm \frac{1}{2}$ is able to describe the fine structure of atomic levels. The radial function $\zeta(r)$ determines the strength of the SO coupling in atomic shells localized at

different separations from the nucleus and thus the magnitude of the fine structure in atoms. The expectation values of the electron magnetic moment $\boldsymbol{\mu} = \boldsymbol{l} + 2\boldsymbol{s}$, responsible for the interaction with an external magnetic field, has to be taken with eigenfunctions of the total angular momentum $\boldsymbol{j}$ to determine properly the g factor, an EPR parameter of an unpaired electron. SO interaction plays an important role also in molecules although the orbital angular momentum is often not a good quantum number there. The SO interaction renders the g factor of an electron in a radical different from the exact $g = 2$ of a free electron [11]. In molecular compounds where the orbital interplay involves the SO interaction, structural parameters, e.g. the geometry, can be notably affected by the SO interaction. The so-called scalar relativistic (SR) effects, the counterpart of the SO relativistic effects, always make notable contributions to the physics and chemistry of the heavy elements and their compounds. However, these effects are rather of quantitative than qualitative nature.

One of the common approximations assumes a simple form for the SO coupling constant $\zeta(r) = dV/dr$, where V is a effective electronic potential function. For a hydrogen-like atom, the potential is $V = -Z/r$ with Z being the nuclear charge; such a radial potential is not that good an approximation for heavier atoms where the screening effects of the electron density has to be accounted for. The screening effects of the electron density reduce the effective nuclear charge Z, hence they also reduce SO effects, the more so the higher in energy (and, therefore, more diffuse) an atomic state is. In actual implementations, the form of the SO (relativistic) interaction terms may differ from the simple form $\zeta(r)\boldsymbol{ls}$, as for example in the Douglas–Kroll (DK) formalism [12]. As in the simplest case, neglecting the relativistic effects of the electron-electron interaction often limits the accuracy of a formal description.

A basic task for a quantum chemical calculation is to determine approximately the many-electron wavefunction and the density of the ground state of a system. For computational efficiency, the equations of quantum mechanics are often cast into algebraic form by representing the wavefunctions as linear combinations of some finite set of simple basis functions. Effectively, a wavefunction is represented by a vector of coefficients; concomitantly, quantum operators are expressed by matrices. A strait-forward, "wavefunction" based approach, e.g. the Hartree–Fock (HF) formalism [1, 2, 3] followed by configuration interaction [7], can become computationally very demanding even for a moderate-size system.

Density functional theory (DFT), by now well founded [4, 5, 13], avoids many bottlenecks of wavefunction-based approaches at the expense of having a closed analytic form of the total energy of a system. DFT in its most popular form of the Kohn–Sham (KS) formalism [14] was proven to perform well in quantum chemistry, both in terms of accuracy and computational efficiency [15]; it was successfully applied to many physical and chemi-

cal problems. The accuracy of a KS calculation depends significantly on the quality of the approximation for the exchange and correlation (xc) energies as functionals of the density. Much effort was spent to find and investigate rigorous expressions of such xc functionals for some limit cases of the electron density and to develop practical expressions for use in the whole domain of the electron density values [15]. Because of the complex dependence of the xc functionals on the density, as a rule it is only possible to evaluate the necessary quantities by numerical integration. In fact, in some setups, the accuracy of the entailed numerical integration can demand a substantial computational effort, it can even turn into a bottleneck of the whole computation.

Relativistic extensions of DFT present an efficient way to account for relativistic and correlation effects on the same footing [16, 17]. One of the most reliable and cost-efficient relativistic methods of quantum chemistry is the Douglas–Kroll (DK) approach [12]. The DK strategy reduces the fully relativistic Dirac equation for four-spinor wavefunctions to an equation for two-component spinors [12]. In combination with a technique of Hess et al. [18] for an approximate evaluation of the momentum-dependent operators in a finite basis set, the DK formalism evolved to the practical Douglas–Kroll–Hess (DKH) computational method [16, 19, 17].

For larger molecular systems exhibiting some symmetry, it is advantageous to exploit its consequences to reduce the computational cost of the electronic structure calculation, applying e.g. selection rules for matrix elements. The power of a group-theoretical analysis helps much in the interpretation of the interactions in the system, for instance, when analyzing orbital interaction in molecular or super-molecular systems. Similarly, a symmetry analysis allows to eliminate completely the spin degrees of freedom in a closed-shell non-relativistic calculation. However, if SO (relativistic) coupling terms are included in the Hamiltonian, is is no longer possible to separate off spin and spatial components of the wavefunctions. Inclusion of the SO interaction forces one to retreat to two-component (or four-component) complex-valued spinors, and to projective (double-valued) group representations. This turns into significant computational overhead in quantum chemistry programs. Fortunately, most operators in a quantum chemistry calculation that includes SO interaction still exhibit the symmetry of the non-relativistic Hamiltonian which also entails invariance with respect to rotations of the spin coordinates. Such operators are often referred to as "spin-free" or "spinless". It is, therefore, possible to treat such operators in a more efficient (and cheaper) way than via general spin-coupling. However, some measures to ensure a consistent simultaneous usage of the operators of two kinds, spin-free and spin coupled ones, as well as a unifying framework, e.g. transformations back and forth between single- and double-valued representations, is required.

ParaGauss is a general purpose quantum chemistry program package for carrying out

density functional (DF) calculations on molecular many-electron systems [20, 21]. Several approximations of the *xc* functional, the kernel of a KS calculation, are implemented in the program; they exhibit different accuracy and applicability domains. It was one of the tasks of this work [22] to implement the newly proposed PBE functional [23] and several of its variants [24, 25] and to evaluate its accuracy for molecular systems.

With ParaGauss, one is also able to perform relativistic DFT calculations, at both the SR and the SO level. SO interaction was treated in the approximation that only the nuclear attraction part of the effective potential was assumed to contribute to the relativistic effects [26]. A consistent and variational incorporation of the relativistic effects of the screening terms of the Coulomb (Hartree) potential of the density into the relativistic model formed another major task of the present work [27].

The third task of the work was to derive and implement an efficient symmetry treatment of relativistic SO calculations, in a framework where one can exploit the spin-free character of the operators. In particular, limitations of the numerical integration of the spin-free *xc* potential had to be removed to overcome performance restriction of SO calculations.

Chapter 2 presents the formalism of the well-known Douglas–Kroll–Hess approach to the relativistic KS problems and its extension to a variational incorporation of the screening effects of the Hartree potential (Sections 2.1 and 2.2). Applications to validate the quality of the approximation are presented in Section 2.3. Next, in Chapter 3, the theory underlying the symmetry treatment in ParaGauss is described. In particular the procedures of a consistent spinor and orbital symmetrization are discussed. In Section 3.5, the numerical integration of the *xc* potential as an example for spin-free operators in SO calculations is presented. Finally, Chapter 4 is devoted to *xc* functionals of the PBE family; the performance of several *xc* functionals is investigated for a set of small molecules and some transition metal carbonyl complexes.

Chapter 2

The Electron-Electron Interaction in the Douglas–Kroll–Hess Approach to the Dirac–Kohn–Sham Problem

Compounds of heavy elements present a challenge to computational chemistry because both electron correlation and effects of relativity have to be accounted for when a reliable description is to be achieved [28, 29]. Relativistic methods based on density functional theory (DFT) are suitable for reaching this dual goal [16, 17]. The appropriate framework for discussing a relativistic electronic system is quantum electrodynamics, also within DFT [30, 31]. A relativistic extension of the Hohenberg–Kohn theorem [32] has been formulated with reference to the covariant four-current density [33]. The corresponding Kohn–Sham (KS) problem [14] results in a Dirac-type equation for four-component one-electron wavefunctions, so-called *four-spinors* (or *bi-spinors*) [34, 35]. In the KS approach to DFT, the effect of the electron-electron (ee) interaction is described by an effective field (to be determined self-consistently) which comprises the classical Coulomb interaction of the electron charge density as well as exchange-correlation (xc) contributions. In conventional formulations of relativistic DF schemes, the same xc functionals as in the non-relativistic methods are applied, but in a fully relativistic description the xc functional changes as well [31, 36].

From the non-relativistic (Schrödinger) limit it is known that for most chemical problems a formalism employing two-component spinors is able to provide a reasonably accurate description of electrons in light atoms and molecules. Therefore, the idea of incorporating relativistic effects as small corrections into a two-component picture is very attractive. Several methods exist to reduce the four-component theory to a two-component Schrödinger-like formalism with an effectively relativistic Hamiltonian by decoupling electronic and positronic degrees of freedom [37, 12, 38, 39, 40, 41, 42]. The change of picture underlying this decoupling procedure entails a modification of pertinent operators, such as

the kinetic energy, the nuclear attraction, and the *ee* interaction. Relativistic corrections arising from this modification can be classified into scalar-relativistic (SR) and spin-orbit (SO) terms [43]. If one neglects SO interaction, one arrives at a SR formalism, effectively a one-component theory [16, 38], which nowadays can be applied almost in routine fashion [17]. For KS calculations, an SR formalism involving transformed operators of the kinetic energy and the nuclear attraction energy has proven to be very successful [16, 17, 44].

It is well known that *ee* contributions are very important for a quantitative description of relativistic effects on numerous properties of many-electron systems [45, 46, 47, 48, 49]. Spin-orbit interaction provides one such example which has been studied in detail. The corresponding one-electron term is screened in part by an effective two-electron contribution [50]. For very light elements, the two-electron contribution to the spin-orbit splitting was found to be of the same order as the one-electron term [45, 48, 51, 9, 52]. Recently, the relative importance of one- and two-electron contributions to the spin-orbit interaction was discussed in general [53] and, in particular, with regard to the NMR shielding tensor, both within an conventional quantum chemistry (*ab initio*) description [54] and a DFT-based formalism [46, 47]. In those studies, the effect of the SO interaction was explored by a perturbation approach at either the non-relativistic or scalar relativistic (SR) level. The importance of the *ee* contribution for the proper calculation of the g-tensors of molecular systems was very recently demonstrated [55], using the theoretical approach developed here; the SO interaction was also included in a self-consistent fashion. The SO interaction often is described in a perturbation approach or by more elaborate post-SCF methods [45]. A self-consistent treatment of the SO interaction is much less frequent; this holds for both HF-based *ab initio* methods [45] and DF calculations [39, 26].

A rigorous description of the SO interaction implies a relativistic treatment of the *ee* interaction. In HF-based methods, the two-electron integrals have to be corrected relativistically which becomes quite expensive for larger systems [53, 56], but also in a DF treatment the computational effort increases notably when the SO interaction is taken into account. Therefore, further approximations to the *ee* contributions are sometimes invoked, e.g. a single-center SO approach with adjusted atomic parameters [57] and a mean-field SO approach [56] which recently was employed also in DF calculations of NMR shifts and g-tensors [46, 47]. A complete mean-field SO technique also requires a transformation of the two-electron integrals, but an efficient approximation hardly sacrificing any accuracy is obtained when the SO interaction is restricted to one-center contributions [56].

In the following, we will discuss the relativistic *ee* contributions in the KS method and, in particular, the self-consistent treatment of the SO interaction. In Section 2.1, we introduce the pertinent notation of the Douglas–Kroll (DK) method for obtaining a two-component version of the relativistic Dirac–Kohn–Sham (DKS) Hamiltonian. Then

we shall describe the relativistic extension of the algebraic form of the DK formalism, as pioneered by Hess and Buenker [38, 18], to a consistent treatment of the *ee* interaction, Section 2.1.4. We will pay special attention to the relativistic formulation of the fitting function approach to the KS method [58, 59, 60]. In Section 2.2.3, we will describe and discuss pertinent details of the implementation in the program PARAGAUSS. Finally, in Section 2.3, we shall supplement these methodological discussions with selected applications, concerning the spin-orbit splitting of the KS one-electron energies of the Hg atom, g-tensor shifts of NO_2, and various properties of the diatomic molecules TlH, PbO, Bi_2, and Pb_2.

2.1 The Relativistic Kohn–Sham Problem

2.1.1 The Four-Component Formalism

Relativistic density functional theory emerges from a covariant renormalized density functional of the four-current density [31]. In the absence of an external vector potential (i.e. without an external magnetic field), the ground state energy of the system is a functional $E[\rho]$ of the electron density ρ only. To minimize this energy functional by means of the variational KS or DKS approach, it is convenient to separate the energy functional as usual:

$$E^{(4)}[\rho] = T_S^{(4)}[\rho] + E_{ext}[\rho] + E_{ee}[\rho] \tag{2.1}$$

where the superscript (4) indicates the four-component picture of the operator in question. $T_S^{(4)}$ is the relativistic kinetic energy,

$$T_S^{(4)}[\rho] = \sum_{\varepsilon}^{occ} \int d^3\boldsymbol{r}\, \psi_\varepsilon^{(4)\dagger}(\boldsymbol{r})(\boldsymbol{\alpha p}c + \beta c^2)\psi_\varepsilon^{(4)}(\boldsymbol{r})\,, \tag{2.2}$$

of the non-interacting DKS reference whose electron density ρ is constructed from the four-component DKS eigenfunctions $\psi_\varepsilon^{(4)}$:

$$\rho(\boldsymbol{r}) = \sum_{\varepsilon}^{occ} |\psi_\varepsilon^{(4)}(\boldsymbol{r})|^2\,. \tag{2.3}$$

$E_{ext}[\rho]$ is the interaction energy of the electron density ρ with an external potential which, for a molecular system, usually is the potential V_{nuc} set up by the nuclei:

$$E_{ext}[\rho] = \int d^3\boldsymbol{r}\, \rho(\boldsymbol{r}) V_{nuc}(\boldsymbol{r})\,. \tag{2.4}$$

The *ee* interaction is represented by the functional $E_{ee}[\rho]$ [13]:

$$E_{ee}[\rho] = E_H[\rho] + E_{xc}[\rho]\,. \tag{2.5}$$

It is convenient to separate the classical Coulomb self-interaction energy (Hartree energy) of the electronic charge density ρ,

$$E_H[\rho] = \frac{1}{2}\int d^3\boldsymbol{r}\, d^3\boldsymbol{r}'\frac{\rho(\boldsymbol{r})\rho(\boldsymbol{r}')}{|\boldsymbol{r}-\boldsymbol{r}'|}\,, \tag{2.6}$$

and the exchange-correlation (xc) contribution. Actually, Eqs. (2.4) and (2.6) define the xc functional $E_{xc}[\rho]$. Its detailed form is unknown; in a relativistic system this energy functional also contains relativistic contributions [31, 61, 30] which are of little importance for many chemical properties of molecules [38, 56, 62, 36, 63, 49]. Variation of the energy functional with respect to the orbitals $\psi_\varepsilon^{(4)}$ yields the Dirac–Kohn–Sham equation [31, 16]

$$h_{DKS}^{(4)}\psi_\varepsilon^{(4)} = \varepsilon\,\psi_\varepsilon^{(4)} \tag{2.7}$$

with the DKS Hamiltonian

$$h_{DKS}^{(4)}[V_{eff}] = \boldsymbol{\alpha}\boldsymbol{p}c + \beta c^2 + V_{eff}. \tag{2.8}$$

The effective potential

$$V_{eff} = V_{nuc} + V_{ee} = V_{nuc} + V_H + V_{xc} \tag{2.9}$$

is the sum of the external contribution V_{nuc}, the Hartree potential of the electron density ρ,

$$V_H(\boldsymbol{r}) = \int d^3\boldsymbol{r}'\,\frac{\rho(\boldsymbol{r}')}{|\boldsymbol{r}-\boldsymbol{r}'|} \tag{2.10}$$

and the xc potential

$$V_{xc} = \frac{\delta E_{xc}[\rho]}{\delta\rho}. \tag{2.11}$$

2.1.2 The Douglas–Kroll Two-Component Formalism

Operators in the DKS Hamiltonian such as the kinetic energy of a free particle $t_S^{(4)} = \boldsymbol{\alpha}\boldsymbol{p}c + \beta c^2$, the effective potential V_{eff} and its constituents V_{nuc}, V_H and V_{xc} are 4×4 operators. However, only the free-particle kinetic energy has a nontrivial four-component structure; the other operators are diagonal in the four-spinor space. Most relevant for the following is the block structure of operators implied by the partitioning of four-spinor

components into electronic (large, L) and positronic (small, S) spinors:

$$\psi^{(4)} = \begin{pmatrix} \psi^L \\ \psi^S \end{pmatrix}. \tag{2.12}$$

This partitioning is based on the fact that for *positive* energy solutions (in the regions where the potential is not extremely strong) one finds $|\psi^L| \gg |\psi^S|$. In this sense, diagonal operators like V_{eff} are block-diagonal, but the kinetic energy operator $t_S^{(4)}$ is not because it couples large and small components. Any 4×4 operator Q can be represented as a sum of its *even* and *odd* parts $\mathcal{E}[Q]$ and $\mathcal{O}[Q]$, respectively:

$$\mathcal{E}[Q] = \begin{pmatrix} Q_{LL} & 0 \\ 0 & Q_{SS} \end{pmatrix}, \qquad \mathcal{O}[Q] = \begin{pmatrix} 0 & Q_{LS} \\ Q_{SL} & 0 \end{pmatrix}. \tag{2.13}$$

$$Q = \begin{pmatrix} Q_{LL} & Q_{LS} \\ Q_{SL} & Q_{SS} \end{pmatrix} = \mathcal{E}[Q] + \mathcal{O}[Q] \tag{2.14}$$

where the even part is block-diagonal in large and small spinors and the odd part has only off-diagonal nonzero 2×2 blocks. Such a decomposition is trivial for the kinetic energy operator $t_S^{(4)}$ because βc^2 is even and $\boldsymbol{\alpha p} c$ is odd.

To construct a two-component representation of the DKS equation, one applies a unitary transformation U which brings the DKS Hamiltonian to even (block-diagonal) form [37]:

$$\psi^{(\pm)} = \begin{pmatrix} \psi^+ \\ \psi^- \end{pmatrix} = U \begin{pmatrix} \psi^L \\ \psi^S \end{pmatrix} = U\psi^{(4)} \tag{2.15}$$

As a consequence, the four components of the DKS four-spinors are decoupled into two two-component spinors, so-called positive and negative energy solutions $\psi^{(\pm)}$. In chemistry, we are interested only in the electronic block (upper left-hand or "++") of the DKS Hamiltonian. The other block on the diagonal ("−−"), a representation of the DKS Hamiltonian in the basis of negative energy (positronic) solutions, is of negligible interest in the context of chemical problems. This transformation U, sometimes referred to as the "exact" Foldy–Wouthuysen (FW) transformation [41, 42], unfortunately results in a Hamiltonian which is highly singular, hence not suitable for numerical calculations. A transformation suggested by Douglas and Kroll (DK) [12] avoids this problem by a series of successive approximations that, at each the step, yield an effective Hamiltonian which entails only well-behaved operators. The first step in a series of DK transformations is the free-particle Foldy–Wouthuysen (fpFW) transformation, an exact decoupling transformation of the free-particle Dirac Hamiltonian. An alternative transformation strategy to

a two-component relativistic Hamiltonian that is successfully used in many applications relies on the "zeroth-order regular" approximation ZORA [39, 40, 64, 65].

Not only the Kohn–Sham Hamiltonian and its constituents change their form with the picture change $(\psi^L, \psi^S) \rightarrow (\psi^{(+)}, \psi^{(-)})$, but also the energy expression changes its algebraic form. Yet, to preserve the variational nature of the Kohn–Sham construction, the total energy expression and the effective DKS Hamiltonian must be consistent. This consistency is not only important for formal reasons, but should also be ensured in practical implementations of the formalism, e.g. when one constructs displacement derivatives (forces) of the total energy. We will return to this topic in Section 2.1.5.

The "zeroth-order" DK approximation is identical to the fpFW decoupling transformation which is exact for the free-particle Hamiltonian, namely of the kinetic energy operator [12, 18, 66]:

$$\hat{E} = U_0 t_S^{(4)} U_0^\dagger = \beta E_p = \begin{pmatrix} E_p & 0 \\ 0 & -E_p \end{pmatrix} \tag{2.16}$$

where

$$E_p = c^2 \sqrt{1 + (p/c)^2}\,. \tag{2.17}$$

The fpFW transformation can be expressed analytically:

$$U_0 = A_p(1 + \beta R_p) \tag{2.18}$$

with $R_p = K_p \boldsymbol{\alpha p}$ and the kinematic factors $A_p = \sqrt{(E_p + c^2)/2E_p}$ and $K_p = c/(E_p + c^2)$. Any even operator V (e.g. V_{eff}, V_H or V_{xc}) transforms to

$$\begin{aligned} U_0 V U_0^\dagger &= \mathcal{E}_1[V] + \mathcal{O}_1[V] \\ \mathcal{E}_1[V] &= A_p(V + R_p V R_p)A_p \\ \mathcal{O}_1[V] &= \beta A_p(R_p V - V R_p)A_p \end{aligned} \tag{2.19}$$

The even term $\mathcal{E}_1[V]$ represents the fpFW transformed potential V. Together with the transformed kinetic energy operator it forms the fpFW transformed Hamiltonian, also referred to as first-order DK Hamiltonian:

$$U_0 h_{DKS}^{(4)}[V] U_0^\dagger = \hat{E} + \mathcal{E}_1[V] + \mathcal{O}_1[V] \tag{2.20}$$

$$= h_{DK,1}^{(2)} \oplus h_{DK,1}^{(-2)} + \mathcal{O}_1[V]. \tag{2.21}$$

Here, the even terms $\hat{E}$ and $\mathcal{E}_1$ were separated into electronic and positronic Hamiltonians, $h_{DK,1}^{(2)}$ and $h_{DK,1}^{(-2)}$, respectively. The odd term $\mathcal{O}_1[V]$ couples electronic and positronic solutions in the case of a non-vanishing effective potential V; it is of first order in the

potential V. Eigenfunctions of the electronic two-component Hamiltonian $h^{(2)}_{DK,1}$ for heavy atoms exhibit a large contamination by negative energy solutions with eigenvalues that lie lower than those of the corresponding DKS problem [67, 68]. Therefore, it is advisable to take the decoupling to further steps, to improve the handling of strongly relativistic systems [12, 69].

The first-order DK transformation can be represented by a unitary operator [12]

$$U_1 = \sqrt{1+\hat{W}^2} + \hat{W} = 1 + \hat{W} + \frac{1}{2}\hat{W}^2 + O(\hat{W}^3) \tag{2.22}$$

with an anti-Hermitean generator $\hat{W} = -\hat{W}^\dagger$ that is assumed to be small. If applied to the one-particle DKS Hamiltonian $h^{(4)}_{DKS}[V]$ together with the fpFW transformation U_0, $U = U_1U_0$, one obtains the second-order DK Hamiltonian which exhibits approximately block-diagonal form:

$$Uh^{(4)}_{DKS}U^\dagger = h^{(2)}_{DK,2} \oplus h^{(-2)}_{DK,2} + \mathcal{O}_2[V] \tag{2.23}$$

Here, the two-component operators $h^{(2)}_{DK,2}$ and $h^{(-2)}_{DK,2}$ represent the decoupled electronic and positronic second-order DK Hamiltonians, respectively. The coupling term $\mathcal{O}_2$, Eq. (2.23), is of second order in V/E_p where E_p is the relativistic kinetic energy operator for a free particle, Eq. (2.17). The generator $\hat{W}$ depends on potential V in first order of V/E_p, Eq. 2.28. The diagonal blocks $h^{(\pm 2)}_{DK,2}$ are accurate to third order in V/E_p [12]. The DK transformation can be viewed as a mapping of four-component operators $h^{(4)}_{DKS}[V]$, parametrized by the potential V, onto two-component operators:

$$\text{1st order DK transf.: } h^{(4)}_{DKS}[V] \to h^{(2)}_{DK,2}[V] \tag{2.24}$$

with the trivial limiting case of a free particle: $h^{(4)}_{DKS}[0] \to E_p$. To derive an expression for the second-order DK Hamiltonian with a general potential V one will need an explicit form of the transformation generator $\hat{W}$.

Application of U_1 to any operator C yields

$$U_1CU_1^\dagger = C + [\hat{W}, C] + \frac{1}{2}[\hat{W}, [\hat{W}, C]] + O(\hat{W}^3) \tag{2.25}$$

$$= C + [\hat{W}, C] + \frac{1}{2}\{\hat{W}^2, C\} - \hat{W}C\hat{W} + O(\hat{W}^3). \tag{2.26}$$

Here, square brackets denote a commutator and curly brackets an anti-commutator. For an even operator C and an odd operator $\hat{W}$, the first correction term $[\hat{W}, C]$ of this equation is odd and the remaining correction terms are even. One chooses $\hat{W}[V]$ such that this first, odd term resulting from the first-order transformation U_1 of the relativistic kinetic energy

$\hat{E}$ cancels $\mathcal{O}_1[V]$:

$$[\hat{W}, \hat{E}] + \mathcal{O}_1 = 0\,. \tag{2.27}$$

This equation is solved by an odd, anti-Hermitean operator best expressed in terms of its matrix elements in a plane-wave basis [12]

$$\hat{W}_{pp'}[V] = \beta\mathcal{O}_{1\,pp'}[V]/(E_p + E_{p'}). \tag{2.28}$$

The weighting with $(E_p+E_{p'})^{-1}$ can be conveniently accounted for by formally substituting

$$V \to \widetilde{V}_{pp'} = V_{pp'}/(E_p + E_{p'}) \tag{2.29}$$

in Eq. (2.19). After application of the second unitary transformation $U_1[V]$ and canceling terms according to Eq. (2.27) one has:

$$U_1 U_0 h^{(4)}_{DKS} U_0^\dagger U_1^\dagger = \hat{E} + \mathcal{E}_1 + \frac{1}{2}[\hat{W}, [\hat{W}, \hat{E}]] + [\hat{W}, \mathcal{O}_1] + [\hat{W}, \mathcal{E}_1] + \dots\,. \tag{2.30}$$

Here all terms of $O(\hat{W}^3) = O((V/E_p)^3)$ have been dropped. The new (odd) coupling term $\mathcal{O}_2 = [\hat{W}, \mathcal{E}_1]$ is of second order in potential, $O((V/E_p)^2)$, and will be neglected in this work. Alternatively, one can continue with further transformations to reduce the order of the coupling term [12] and produce DK Hamiltonians of higher orders. Recently, applications of the third-order DK transformation were reported to improve the energies of the lowest-lying s levels of superheavy atoms [70, 71, 72], but for chemical properties of molecules the second-order DK formalism is usually a good approximation [70, 71, 72]. With help of Eq. (2.27) we expand the commutator

$$[\hat{W}, \mathcal{O}_1] = -[\hat{W}, [\hat{W}, \hat{E}]] \tag{2.31}$$

which is also of second order in the potential, $O((V/E_p)^2)$ and is twice the double commutator already present in Eq. (2.30) with the opposite sign. The Hamiltonian $h^{(4)}_{DK,2}[V]$ DK-*decoupled* to second order is:

$$h^{(4)}_{DK,2}[V] = \hat{E} + \mathcal{E}_1[V] + \mathcal{E}_2[V] \tag{2.32}$$

$$\begin{aligned} \mathcal{E}_2[V] &= -\frac{1}{2}[\hat{W}, [\hat{W}, \hat{E}]] \\ &= \hat{W}\hat{E}\hat{W} - \frac{1}{2}\{\hat{W}^2, \hat{E}\} \end{aligned} \tag{2.33}$$

The DK method allows one to continue with further transformations, e.g. U_2, U_3, ... each defined similarly to U_1, Eq. (2.22), via transformation generators $\hat{W}_2$, $\hat{W}_3$, ... and aimed

at eliminating the remaining odd coupling terms of lower-order DK Hamiltonians. For example, the transformation U_2 may be applied to eliminate the odd term $\mathcal{O}_2 = [\hat{W}_1, \mathcal{E}_1]$ of Eq. (2.30). Its transformation generator $\hat{W}_2$ will be defined similarly to Eq. (2.28) as

$$\hat{W}_{2,pp'}[V] = \beta \mathcal{O}_{2,pp'}[V]/(E_p + E_{p'}) \tag{2.34}$$

Let us, however, continue with the second-order DK Hamiltonian. If one now substitutes $\hat{E}$ in Eq. (2.32) by βE_p and restricts the decoupled operators $\mathcal{E}_1$ and $\mathcal{E}_2$ to the electronic 2×2 blocks, one obtains the corresponding two-component DK Hamiltonian of second order:

$$h^{(2)}_{DK,2}[V] = E_p + \mathcal{E}^{(2)}_1[V] + \mathcal{E}^{(2)}_2[V]\,. \tag{2.35}$$

Note that the two-component "potential" terms $\mathcal{E}^{(2)}_1[V]$ and $\mathcal{E}^{(2)}_2[V]$ (which are of first and second order in V, respectively) have a more general origin. For instance, $\mathcal{E}^{(2)}_2$ also contains corrections to the kinetic energy operator that are induced by the picture change. This separation is a result of the convention where one isolates the kinetic energy operator E_p in its simple fpFW representation (DK transformed to first order) and assigns all kinetic terms induced by further DK transformation to the term $\mathcal{E}^{(2)}_2$. With Eqs. (2.19) and (2.32) the explicit forms of the 2×2 terms $\mathcal{E}^{(2)}_1[V]$ and $\mathcal{E}^{(2)}_2[V]$ read:

$$\begin{aligned} \mathcal{E}^{(2)}_1[V] &= A(V + RVR)A \\ \mathcal{E}^{(2)}_2[V] &= -\frac{1}{2}\{W, \{W, E_p\}\} \\ &= -WE_pW - \frac{1}{2}\{W^2, E_p\} \end{aligned} \tag{2.36}$$

with

$$W[V] = A(R\tilde{V} - \tilde{V}R)A\,. \tag{2.37}$$

and

$$R = K\boldsymbol{\sigma p} \tag{2.38}$$

In summary, to construct a two-component picture of the four-component DKS Hamiltonian $h^{(4)}_{DKS}[V] = t^{(4)}_S + V$, one applies a unitary transformation U that decouples an effective DK Hamiltonian $h^{(4)}_{DK,2}[V] = Uh^{(4)}_{DKS}[V]U^\dagger$ to a certain order (here: second order) in the potential V. The transformation $U[V]$ depends on the effective one-electron potential V. Finally, employing the projection operator B onto the space of the electronic solutions $\psi^{(+)}$, the corresponding two-component Hamiltonian is:

$$h^{(2)}_{DK,2}[V] = Bh^{(4)}_{DK,2}[V]B^\dagger \tag{2.39}$$

For many applications to chemical problems [16, 44, 26] one obtains a satisfactory approximation by further simplifying the DK Hamiltonian $h^{(2)}_{DK,2}[V_{eff}]$, Eq. (2.35). To this end, one takes only V_{nuc} into account, both when constructing the decoupling transformation $U[V_{nuc}]$ and when transforming the DKS Hamiltonian. Thus, one applies the DK transformation machinery to the "reduced" DKS Hamiltonian with $V = V_{nuc}$, by formally invoking the mapping in Eq. (2.24), and adds the electronic parts of the potential *a posteriori*:

$$h^{(2)}_{DKnuc,2} = h^{(2)}_{DK,2}[V_{nuc}] + V_{ee}\,. \tag{2.40}$$

This popular variant of a two-component DK method [16, 44, 70, 73, 74] is commonly referred to as DK formulation "in the nuclear field only". In the work, we will present the first formalism which goes beyond this "nuclear only" approximation, referred to as DKnuc, of the DK formalism.

Thus far, we used the "square root" parametrization of the unitary rotation matrix $U_n = \sqrt{1 + \hat{W}_n^2} + \hat{W}_n$, Eq. (2.22). However, there are alternatives to this original proposition of Douglas and Kroll [12]. For example, three other analytical definitions

$$U_n = \left(\frac{1 + \hat{W}_n}{1 - \hat{W}_n}\right)^{1/2} \tag{2.41}$$

$$U_n = \frac{2 + \hat{W}_n}{2 - \hat{W}_n} \tag{2.42}$$

$$U_n = \exp(\hat{W}_n) \tag{2.43}$$

are equivalent to that of Eq. (2.22) when expanded up to second order in the generator $\hat{W}_n$ [72]. In many implementations, including this work, only these expansion terms up to second order are included. The three expressions represented by series in $\hat{W}_n$ differ by their radii of convergence. The exponential ansatz for the transformation matrix is convenient to construct higher-order expansions because of its well known property [75], [cf. Eq. (2.26) for a "square root" parametrization]:

$$\begin{aligned}\exp(\hat{W})\, C\, \exp(-\hat{W}) = C + [\hat{W}, C] + \frac{1}{2}[\hat{W}, [\hat{W}, C]] \\ \ldots + \frac{1}{n!}[\hat{W}, \ldots, [\hat{W}, C]] \ldots] + \ldots\end{aligned} \tag{2.44}$$

Moreover, the transformation matrix U_n may be defined directly by an expansion series in $\hat{W}_n$ with the optimal coefficients to account for maximum unitarity of a truncated expansion [72]. The coefficients of such an optimal expansion were recently given [72]. Maximum unitarity ensures that eigenvalues and eigenvectors of the two-component DK Hamiltonian

are the best approximation to their DKS counterparts.

2.1.3 Scalar Relativistic Treatment and Spin-Orbit Interaction

The spin operator $\boldsymbol{s} = \boldsymbol{\sigma}/2$ does not commute with the two-component DK Hamiltonian $h^{(2)}_{DK,2}$, Eq. (2.35). In a relativistic atomic Hamiltonian, $\boldsymbol{s}$ and the orbital angular momentum $\boldsymbol{l} = [\boldsymbol{r} \times \boldsymbol{p}]$ are coupled by the SO interaction. For molecules the SO interaction terms can be approximated either by a superposition of atomic contributions of the type $\zeta(\boldsymbol{r})\boldsymbol{ls}$, eventually adjusted for inter-atomic interactions [57], or, more generally, by a term proportional to $\boldsymbol{s} \cdot [\boldsymbol{\nabla} V \times \boldsymbol{p}]$. Therefore, the spin coordinates cannot be separated from the spatial coordinates and a genuine two-component treatment is necessary. As a consequence, the symmetrization of DKS orbitals has to be achieved with the help of complex-valued *double-group* representations or, more appropriately, by *projective* representations, e.g. by representations generated by half-integer angular momentum eigenfunctions (see Chapter 3) [76, 77]. The additional computational effort concomitant to the intrinsic two-component formalism induced by the inclusion of SO interaction in the Hamiltonian often motivates a further approximation, namely the SR approximation which results in a spin-free, effectively one-component formalism. Any Hermitian 2×2 operator $C^{(2)}$ can be uniquely represented as $C^{(2)} = C_{SR} + \boldsymbol{c\sigma}$; in the SR approximation one neglects the term $\boldsymbol{c\sigma}$.

As an example, consider the term $\boldsymbol{\sigma p} V \boldsymbol{\sigma p}$ which is part of the first-order correction $\mathcal{E}^{(2)}_1$ of the DK Hamiltonian, Eq. (2.36). Invoking the identity $\sigma_i \sigma_j = \delta_{ij} + i\epsilon_{ijk}\sigma_k$ for Pauli spin matrices [78], the last expression leads to

$$\boldsymbol{\sigma p} V \boldsymbol{\sigma p} = \boldsymbol{p} V \boldsymbol{p} + i[\boldsymbol{p} \times V \boldsymbol{p}]\boldsymbol{\sigma} \,. \tag{2.45}$$

Here, the first term represents the SR part of the operator and the second term, attributed to the SO part of the operator, is neglected in the SR approximation. Finally, we mention some debate whether the separation of relativistic effects into SR and SO contributions is rigorous and physical [43, 79]. Visscher and van Lenthe showed [43] that there is more than one way to derive a *spin-free* form of a Dirac equation and, hence, more than one way to separate spin-coupling terms.

2.1.4 Relativistic Transformation of the Coulomb Potential

In the DKS formalism a system of "noninteracting" electrons moves in an effective field V_{eff} which is the sum of the nuclear potential V_{nuc} and the electron-electron interaction V_{ee}, Eq. (2.9). In regions close to the nuclei, relevant for the relativistic characteristics, one usually has $V_{ee} \ll V_{nuc}$. Mainly due to this fact it has become an efficient practical approach to

exclude the *ee* interaction from relativistic transformations. The DK Hamiltonian [see Eq. (2.40)]

$$h^{(2)}_{DKnuc,2} = E_p + \mathcal{E}^{(2)}_1[V_{nuc}] + \mathcal{E}^{(2)}_2[V_{nuc}] + V_{ee} = E_p + V_{nuc,rel} + V_{ee} \tag{2.46}$$

takes the SO interaction into account in an approximate fashion. In a recent study it was shown that $h^{(2)}_{DKnuc,2}$ provides a satisfactory description of various molecular properties [26]. At this level of approximation, matrix elements of V_{ee} are interpreted as $\langle\psi^{(2)}_\varepsilon|V_{ee}[\rho^{(2)}]|\psi^{(2)}_\varepsilon\rangle$ where $\rho^{(2)} = \Sigma_\varepsilon|\psi^{(2)}_\varepsilon|^2$ is a "two-component" density, generated directly from the Kohn–Sham solution in analogy to the non-relativistic Schrödinger picture.

The *a posteriori* addition of V_{ee}, Eq. (2.40), requires a justification because it represents an additional approximation. After the picture change induced by the relativistic decoupling transformation, the functional form of the operator V_{ee} changes. Moreover, the effective potential $V \equiv V_{eff} = V_{nuc}+V_{ee}$ defines the second-order DK transformation $U_1[V]$. Treating V_{ee} as an external "add-on" is only justified if the relativistic effects due to it are relatively small. This is not always the case [45, 46, 47, 48, 49] as is also demonstrated in the following discussion and by some applications in Section 2.3.

Therefore, we shall now discuss how to include relativistic effects due to V_{ee}. Of course, formally, there is no difference between V_{ee} and V_{nuc}: only their sum $V = V_{eff}$ matters and defines relativistic corrections as described in Section 2.1.2. The question then is how to construct an efficient approach for evaluating relativistic corrections due to V_{ee} in the light of its *specific* features. As mentioned above, the fact that V_{ee} is relatively weak compared to the V_{nuc} presents an advantage. At variance with V_{nuc}, V_{ee} is not known at the outset and has to be determined self-consistently during the SCF process. This aspect and the fact that the relativistic corrections depend in a nonlinear fashion on the *ee* potential complicate the task.

For computational algorithms that deal efficiently with the complications induced by V_{ee} (see Section 2.1.5), it seems worth to preserve a linear dependence of the effective relativistic DKS Hamiltonian on V_{ee}. Several options come to mind how to achieve this. Instead of simply adding V_{ee} *unchanged* to the DK Hamiltonian $h^{(2)}_{DKnuc,2}$ *after decoupling* to second order in the nuclear field, one can subject V_{ee} to the transformations U_0. Formally, this results in replacing V_{ee} by $\mathcal{E}_1[V_{ee}]$ in Eq. (2.32). More accurately, one can transform V_{ee} by $U[V_{nuc}] = U_1[V_{nuc}]U_0$. Obviously, the substitution

$$V_{ee} \rightarrow U[V_{nuc}]V_{ee}U^\dagger[V_{nuc}] \rightarrow V^{(2)}_{DK\,ee,2} \tag{2.47}$$

yields a two-component form of the *ee* interaction, decoupled in the same picture as the rest of operators, $U = U[V_{nuc}]$, that includes only correction terms linear in V_{ee}; see Eq. (2.19). However, because the transformation U depends on the nuclear potential, some

of the correction terms are of second order in the *effective* potential V_{eff}, namely those which are proportional to $V_{nuc} \times V_{ee}$. Such terms are absent if the zeroth-order DK (or free-particle FW) transformation is applied to V_{ee}. Finally, one can invoke a straightforward Taylor expansion of the DK Hamiltonian, Eq. (2.32), to first order in V_{ee} as an accurate representation of relativistic effects at that level.

In summary, the two-component DKS model Hamiltonians just discussed are in order of increasing complexity and rigor:

$$h^{(2)}_{DKnuc,2} = h^{(2)}_{DK,2}[V_{nuc}] + V_{ee} \tag{2.48}$$

$$h^{(2)}_{DKee1,2} = h^{(2)}_{DK,2}[V_{nuc}] + BU_0 V_{ee} U_0^\dagger B^\dagger = h^{(2)}_{DK}[V_{nuc}] + \mathcal{E}^{(2)}_1[V_{ee}] \tag{2.49}$$

$$h^{(2)}_{DKee2,2} = h^{(2)}_{DK,2}[V_{nuc}] + BU[V_{nuc}] V_{ee} U^\dagger[V_{nuc}] B^\dagger = h^{(2)}_{DK,2}[V_{nuc}] + V^{(2)}_{DK\,ee,2} \tag{2.50}$$

$$h^{(2)}_{DKee3,2} = h^{(2)}_{DK,2}[V_{nuc}] + \frac{\delta h^{(2)}_{DK,2}}{\delta V_{nuc}}\{V_{ee}\} \tag{2.51}$$

$$h^{(2)}_{DK,2} \equiv h^{(2)}_{DK,2}[V_{eff}] = E_p + \mathcal{E}^{(2)}_1[V_{eff}] + \mathcal{E}^{(2)}_2[V_{eff}] \tag{2.52}$$

The two-component Hamiltonian $h^{(2)}_{DK,2}[V_{nuc}]$ is obtained when the four-component DKS Hamiltonian $h^{(4)}_{DKS}[V_{nuc}]$ is decoupled to second order in the nuclear field; see Eq. (2.40). The Hamiltonian $h^{(2)}_{DKnuc,2}$, Eq. (2.48), augmented by the untransformed *ee* interaction V_{ee}, was recently used successfully for an approximate self-consistent treatment of the SO interaction [26]. The next two approximate Hamiltonians $h^{(2)}_{DKee1,2}$ and $h^{(2)}_{DKee2,2}$ exhibit variants of V_{ee} that result when DK transformations of increasing order are applied. On the other hand, $h^{(2)}_{DKee3,2}$ is obtained when one linearizes the Hamiltonian $h^{(2)}_{DK,2}$, Eq. (2.52), consistently in the quantity V_{ee}. The term added to $h^{(2)}_{DK,2}[V_{nuc}]$ in Eq. (2.51) is a linear functional of V_{ee}; in other words, the functional derivative $\delta h^{(2)}_{DK,2}/\delta V_{nuc}\{\cdot\}$ is a linear operator acting on V_{ee}.

Next, we derive an explicit expression for $h^{(2)}_{DKee3,2}$ by carrying out the Taylor expansion of the two-component DK Hamiltonian $h^{(2)}_{DK,2}[V]$. The potential term $\mathcal{E}^{(2)}_1 = \mathcal{E}^{(2)}_1[V]$ of the DK Hamiltonian is linear in V; hence

$$\mathcal{E}^{(2)}_1[V_{nuc} + V_{ee}] = \mathcal{E}^{(2)}_1[V_{nuc}] + \mathcal{E}^{(2)}_1[V_{ee}] \tag{2.53}$$

where the second term is of first order in V_{ee}; see Eq. (2.19). On the other hand, the second-order term $\mathcal{E}^{(2)}_2[V]$ cannot be represented as a straightforward sum of nuclear and *ee* contributions. Formally, the correction terms to $\mathcal{E}^{(2)}_2$ due to V_{ee} can be obtained using

$$\mathcal{E}^{(2)}_2[V_{nuc} + V_{ee}] \approx \mathcal{E}^{(2)}_2[V_{nuc}] + \frac{\delta \mathcal{E}^{(2)}_2}{\delta V_{nuc}}\{V_{ee}\} \tag{2.54}$$

but we prefer a different derivation. The transformation generator $W[V]$, Eq. (2.37), depends linearly on the potential V; thus

$$W[V_{eff}] = W[V_{nuc}] + W[V_{ee}] \equiv W_{nuc} + W_{ee}\,. \tag{2.55}$$

The terms of $\mathcal{E}_2^{(2)}$, Eq. (2.36), split accordingly. As an example, we note for the term $\frac{1}{2}\{W^2, E_p\}$ that

$$W^2 = W_{nuc}^2 + \{W_{nuc}, W_{ee}\} + W_{ee}^2 \tag{2.56}$$

The assumption $W_{ee} \ll W_{nuc}$ implies the ordering $W_{ee}^2 \ll \{W_{nuc}, W_{ee}\} \ll W_{nuc}^2$. With Eqs. (2.35) and (2.36), we obtain the effective DK Hamiltonian to first order in V_{ee} if we keep the terms linear in W_{ee}:

$$h^{(2)}_{DKee3,2} = h^{(2)}_{DKnuc,2} + \mathcal{E}_1^{(2)}[V_{ee}] - \frac{1}{2}\{W_{ee}, \{W_{nuc}, E_p\}\} - \frac{1}{2}\{W_{nuc}, \{W_{ee}, E_p\}\} \tag{2.57}$$

In the Hamiltonian $h^{(2)}_{DK,2}$, Eq. (2.52), the terms of order W_{ee}^2, neglected in Eq. (2.57), are retained.

We could also have obtained the result of Eq. (2.57) by separating the terms of the double anti-commutator form of the second-order potential term $\mathcal{E}_2^{(2)}$, Eq. (2.36). After substitution $W = W_{nuc} + W_{ee}$, the term $\{W, \{W, E_p\}\}/2$ may be split into three parts. The first and largest one, $\{W_{nuc}, \{W_{nuc}, E_p\}\}/2$, is the unmodified nuclear only contribution $\mathcal{E}_2^{(2)}[V_{nuc}]$ assigned to $h^{(2)}_{DKnuc,2}$. The second part, linear in W_{ee}, is $\{W_{nuc}, \{W_{ee}, E_p\}\}/2 + \{W_{ee}, \{W_{nuc}, E_p\}\}/2$ which matches the V_{ee}-dependent terms in Eq. (2.57). The last contribution, $\{W_{ee}, \{W_{ee}, E_p\}\}/2$, is of second order in V_{ee}; it is discarded in the Hamiltonian $h^{(2)}_{DKee3,2}$ but not in the full second-order Hamiltonian $h^{(2)}_{DK,2}$, Eq. (2.52). Thus, the relation between these two Hamiltonians reads:

$$h^{(2)}_{DKee3,2} = h^{(2)}_{DK,2} + \frac{1}{2}\{W_{ee}, \{W_{ee}, E_p\}\} \tag{2.58}$$

Next, we compare $h^{(2)}_{DKee3,2}$, Eq. (2.57), with $h^{(2)}_{DKee2,2}$ of Eq. (2.50), where V_{ee} is subjected to a DK transformation in the field of the nuclei only and then added to $h^{(2)}_{DKnuc,2}$. They obviously differ because the approximate Hamiltonian $h^{(2)}_{DKee2,2}$ does not comprise any contributions linear in V_{ee} that result from applying the decoupling transformation $U[V_{nuc} + V_{ee}]$ to the Hamiltonian $h^{(4)}_{DKS}[V_{nuc}]$; see Eq. (2.40). Rather, $h^{(2)}_{DKee2,2}$ contains only those contributions that emerge when V_{ee} undergoes a DK transformation $U[V_{nuc}]$ in the

nuclear field only, Eq. (2.47):

$$U[V_{nuc}]V_{ee}U^\dagger[V_{nuc}] = U_1[V_{nuc}](\mathcal{E}_1[V_{ee}] + \mathcal{O}_1[V_{ee}])U_1^\dagger[V_{nuc}] \tag{2.59}$$

$$\simeq \mathcal{E}_1[V_{ee}] + [\hat{W}_{nuc}, \mathcal{O}_1[V_{ee}]] \tag{2.60}$$

$$= \mathcal{E}_1[V_{ee}] - [\hat{W}_{nuc}, [\hat{W}_{ee}, \hat{E}]] \tag{2.61}$$

With $\mathcal{O}_1[V_{ee}] = -[\hat{W}_{ee}, \hat{E}]$, Eq. (2.27), and after projection B onto the electronic 2×2 block, we get

$$V^{(2)}_{DK\,ee,2} = \mathcal{E}^{(2)}_1[V_{ee}] - \{W_{nuc}, \{W_{ee}, E_p\}\}\,. \tag{2.62}$$

Here, W_{ee} is explicitly defined by Eq. (2.37) whereas the picture change used to transform V_{ee} is induced by the nuclear field V_{nuc} only, i.e. with $\hat{W}_{nuc}$. With this definition of $V^{(2)}_{DK\,ee,2}$, the Hamiltonian $h^{(2)}_{DKee2,2}$, Eq. (2.50), becomes

$$h^{(2)}_{DKee2,2} = h^{(2)}_{DKnuc,2} + \mathcal{E}^{(2)}_1[V_{ee}] - \{W_{nuc}, \{W_{ee}, E_p\}\}\,. \tag{2.63}$$

Comparison of the ee-dependent terms of this equation with those of Eq. (2.57) establishes a relation between the two approximate Hamiltonians:

$$h^{(2)}_{DKee3,2} = h^{(2)}_{DKee2,2} - \frac{1}{2}[[W_{ee}, W_{nuc}], E_p] \tag{2.64}$$

Thus, one pathway where the general expression of $h^{(2)}_{DK,2}[V_{nuc} + V_{ee}]$ is linearized in V_{ee} according to Eq. (2.51), and another pathway, Eq. (2.50), where $h^{(2)}_{DKnuc,2}$ is supplemented by V_{ee}, but transformed with $U[V_{nuc}]$ to the same picture, differ only by the double commutator $[[W_{ee}, W_{nuc}], E_p]/2$. This difference is expected to be minor as we will confirm for some atomic and molecular properties when we compare the two variants of the final two-component DK Hamiltonians $h^{(2)}_{DKee2,2}$ and $h^{(2)}_{DKee3,2}$; see Section 2.3.

It may be useful to compare the five approximate Hamiltonians of Eqs. (2.48-2.52) by listing explicitly the defining additional term compared to the pertinent reference Hamiltonian:

$$h^{(2)}_{DKnuc,2} = h^{(2)}_{DK,2}[V_{nuc}] + V_{ee} \tag{2.65}$$

$$h^{(2)}_{DKee1,2} = h^{(2)}_{DK,2}[V_{nuc}] + \mathcal{E}^{(2)}_1[V_{ee}] \tag{2.66}$$

$$h^{(2)}_{DKee2,2} = h^{(2)}_{DKee1,2} - \{W_{nuc}, \{W_{ee}, E_p\}\} \tag{2.67}$$

$$h^{(2)}_{DKee3,2} = h^{(2)}_{DKee2,2} - [[W_{ee}, W_{nuc}], E_p]/2 \tag{2.68}$$

$$h^{(2)}_{DK,2} \quad = h^{(2)}_{DKee3,2} - \{W_{ee}, \{W_{ee}, E_p\}\}/2 \tag{2.69}$$

Finally, we note that the linearization approach which we used for V_{ee} is applicable to any

(scalar) potential ΔV. All correction terms which are small enough to be treated by the linearization approach presented above, appear in additive fashion in the corresponding Hamiltonians. For instance, to account for relativistic effects of some ΔV in the Hamiltonian $h^{(2)}_{DKee2,2}$ one may add the term $\mathcal{E}^{(2)}_1[\Delta V] - \{W_{nuc}, \{W_{\Delta V}, E_p\}\}$ to that Hamiltonian as long as both V_{ee} and ΔV are small compared to V_{nuc}.

2.1.5 Density-Fit Based Relativistic Expression for the Hartree Energy

Thus far we have considered a four-component density functional formalism and its reduction to a two-component picture by a DK transformation. Starting from the four-component DKS formulation we obtained several approximate DKS Hamiltonians which incorporate the relativistic contributions to the *ee* potential at various levels of accuracy. Next, we will discuss how these approximate DKS Hamiltonians can be related to approximate DF energy expressions. At the same time, we would like to take into account how the approximate two-component DKS Hamiltonians just introduced can be efficiently implemented in existing density functional computer codes which rely on the expansion of a two-component DKS one-electron wave functions in a finite set $\{\chi_i\}$ of (basis) functions. This two-component basis is related to a four-component basis $\{\chi^{(4)}_i\}$ by the picture change with transformation U, Eq. (2.15); see Eqs. (2.3) and (2.39):

$$\chi^{(4)}_i = U^\dagger B^\dagger \chi_i \tag{2.70}$$

We will invoke a further approximation which exploits the common separation of the *ee* interaction energy E_{ee}, Eq. (2.5), into the classical Coulomb energy E_H and the significantly smaller exchange-correlation energy E_{xc} [13]. Whereas the discussion of the preceding Section 2.1.4 was based on the general *ee* interaction, i.e. all of V_{ee} in the effective potential $V_{eff} = V_{nuc} + V_{ee}$, Eq. (2.9), in the following we will restrict the relativistic treatment to the Hartree term represented by the potential V_H in $V_{ee} = V_H + V_{xc}$, exploiting the fact that commonly $V_{xc} \ll V_H$ [13]. Thus, formally this additional approximation implies that V_{ee} is replaced by V_H in all approximate two-component DKS Hamiltonians of Section 2.1.4 and that the *xc* energy (V_{xc} potential) is added *a posteriori* to the relativistic energy expressions (Hamiltonians) in its unmodified non-relativistic form. Of course, for the approximate Hamiltonian $h^{(2)}_{DKnuc,2}$, Eq. (2.48) and the corresponding energy expression, this new strategy does not imply any further change because the expressions for the Hartree potential (E_H energy) and the *xc* potential (E_{xc} energy) were left unmodified in the full Hamiltonian (total energy expression) in nuclear field only DK (model DKnuc).

In the model DKnuc, only relativistic effects on the kinetic energy and the nuclear

attraction energy are accounted for. Hence, a suitable energy expression is:

$$E = T_{S,\,rel} + E_{ext,\,rel} + E_H + E_{xc} \tag{2.71}$$

The subscript *rel* shall indicates the relativistic approximation; thus, here *rel*="DKnuc,2". Compared to non-relativistic calculations, it suffices to modify the matrices of the kinetic energy $\mathbf{t}_S \to \mathbf{t}_{S,\,rel}$ and the nuclear attraction $\mathbf{v}_{nuc} \to \mathbf{v}_{nuc,\,rel}$ in the basis $\{\chi_i\}$ to get the proper energy:

$$T_{S,\,rel} + E_{ext,\,rel} = \mathrm{tr}[\mathbf{P}(\mathbf{t}_{S,\,rel} + \mathbf{v}_{nuc,\,rel})]\,. \tag{2.72}$$

Here, tr indicates the trace of an operator, and $\mathbf{P}$ is the density matrix [7]. The last expression is invariant to any unitary transformation; therefore, it holds in both the original four-component Dirac picture and in a two-component picture after applying a suitable DK transformation, as done here. It is this latter case which we are targeting with this energy expression, the case of the Schrödinger picture normally employed in calculations. In this picture the operators have a modified form and the density matrix $\mathbf{P} = (P_{ij})$ represents the two-component density [60]

$$\rho^{(2)}(\boldsymbol{r}) = \sum_{\varepsilon}^{occ} |\psi_\varepsilon^{(2)}(\boldsymbol{r})|^2 = \sum_{ij} P_{ji}\chi_i^\dagger(\boldsymbol{r})\chi_j(\boldsymbol{r}) \tag{2.73}$$

generated from the solutions $\psi_\varepsilon^{(2)}(\boldsymbol{r})$ of the two-component DKS problem. When this density is used to evaluate E_H and E_{xc}, one recovers the approximate two-component DKS total energy expression and, by variation of that, the Hamiltonian of Eq. (2.46).

To evaluate the Hartree energy E_H, Eq. (2.6), and the matrix elements of the corresponding potential V_H, Eq. (2.10), one needs four-center (two-electron) Coulomb integrals of the basis functions $\{\chi_i\}$. An alternative approach, sometimes referred to as "density fit" [59, 60] or as "resolution of identity" [80, 81], avoids this computational effort by representing the electron density $\rho = \rho^{(2)}$ with the help of an auxiliary basis $\{f_k\}$:

$$\rho(\boldsymbol{r}) \approx \bar{\rho}(\boldsymbol{r}) = \sum_k a_k f_k(\boldsymbol{r})\,. \tag{2.74}$$

For convenience, we introduce the short-hand notation for the Coulomb interaction energy of two densities:

$$[\rho_1||\rho_2] = \iint d^3\boldsymbol{r}\, d^3\boldsymbol{r}' \frac{\rho_1(\boldsymbol{r})\rho_2(\boldsymbol{r}')}{|\boldsymbol{r}-\boldsymbol{r}'|}\,. \tag{2.75}$$

Together with an auxiliary density basis set, it is common [59, 60] to approximate the

Hartree energy $E_H[\rho]$ as

$$\bar{E}_H[\rho,\{a_k\}] \equiv [\rho||\bar{\rho}] - \frac{1}{2}[\bar{\rho}||\bar{\rho}] = E_H[\rho] - \frac{1}{2}[\Delta\rho||\Delta\rho] \tag{2.76}$$

$$= \sum_{ijk} P_{ji}[ij||k]a_k - \frac{1}{2}\sum_{kl} a_k[k||l]a_l\,. \tag{2.77}$$

where $\Delta\rho = \rho - \bar{\rho}$, $[k||l] \equiv [f_k||f_l]$ and

$$[ij||k] = [\chi_i^\dagger\chi_j||f_k]\,. \tag{2.78}$$

For given a density ρ (or $\rho^{(2)}$), the expansion coefficients a_k are determined by minimizing the difference

$$E_H - \bar{E}_H = [\Delta\rho||\Delta\rho]/2 \geq 0, \tag{2.79}$$

cf. Eq. (2.76), between the exact and the approximate Hartree energies [60], i.e. by maximizing $\bar{E}_H$. This variation procedure is apparently equivalent to the best density fit with the Coulomb norm defined by Eq. (2.75). With this particular choice of the Coulomb norm, the two variational approaches become equivalent and ultimately one obtains a system of linear equations:

$$\sum_l [k||l]a_l = [\rho||k] = \sum_{ij} P_{ji}[ij||k]\,. \tag{2.80}$$

Here, we neglected the constraint of this minimization due to charge conservation, $N = \int \bar{\rho}(\boldsymbol{r})d^3\boldsymbol{r}$, to simplify the presentation. The approximate Hartree potential $\bar{V}_H$ which is obtained by varying the approximate energy $\bar{E}_H[\rho,\{a_k\}]$ is

$$\bar{V}_H(\boldsymbol{r}) = \frac{\delta\bar{E}_H}{\delta\rho} = \int d^3\boldsymbol{r}'\frac{\bar{\rho}(\boldsymbol{r}')}{|\boldsymbol{r}-\boldsymbol{r}'|} = \sum_k a_k F_k(\boldsymbol{r}) \tag{2.81}$$

where

$$F_k(\boldsymbol{r}) = \int d^3\boldsymbol{r}'\frac{f_k(\boldsymbol{r}')}{|\boldsymbol{r}-\boldsymbol{r}'|}\,. \tag{2.82}$$

One reason for the computational efficiency of this fitting function (FF) approach derives from the identity

$$[ij||k] = \langle i|F_k|j\rangle = \langle\chi_i|F_k|\chi_j\rangle \tag{2.83}$$

so that

$$\langle i|\bar{V}_H|j\rangle = \sum_k a_k[ij||k]\,. \tag{2.84}$$

Now we go beyond the non-relativistic approximation for E_H, Eq. (2.76), and define a relativistically corrected expression $\bar{E}_{H,rel}$ in line with the FF methodology. For this

purpose, we approximate the Hartree energy of a four-component density ρ by

$$\bar{E}_{H,\,rel}[\rho,\{a_k\}] = \sum_{ijk} P_{ji}[ij||k]_{rel}\, a_k - \frac{1}{2}\sum_{kl} a_k[k||l]a_l\,. \tag{2.85}$$

The subscript rel indicates the decoupling transformation U or, more rigorously, the relativistic model used (see below). The analogy of Eq. (2.85) and Eq. (2.76) is obvious. A similarly close analogy can be constructed for the three-index integrals $[ij||k]_{rel}$ which describe the Coulomb interaction of a product of four-component basis functions $\chi_i^{(4)}$ and $\chi_j^{(4)}$ with the partial density f_k, see Eqs. (2.70) and (2.78):

$$[ij||k]_{rel} \equiv [\chi_i^{(4)\dagger}\chi_j^{(4)}||k] = \langle\chi_i^{(4)}|F_k|\chi_j^{(4)}\rangle = \langle\chi_i|F_{rel,\,k}^{(2)}|\chi_j\rangle \equiv \langle i|F_{rel,\,k}^{(2)}|j\rangle \tag{2.86}$$

Thus, the term $[ij||k]_{rel}$ can be considered as matrix element of a two-component operator $F_{rel,\,k}^{(2)}$ with two-component basis functions χ_i and χ_j. The operator $F_{rel,\,k}^{(2)}$ is the DK-transform of the operator F_k, see Eqs. (2.49) and (2.50):

$$F_{rel,\,k}^{(2)} = BUF_kU^\dagger B^\dagger\,. \tag{2.87}$$

Again, by variation of the energy expression $\bar{E}_{H,\,rel}$, Eq. (2.85), one obtains the corresponding relativistic approximation $\bar{V}_{H,\,rel}$ of the Hartree potential which can be represented by the matrix

$$\langle i|\bar{V}_{H,\,rel}|j\rangle = \sum_k a_k[ij||k]_{rel}\,. \tag{2.88}$$

Depending on the decoupling transformation U, one is able to account for relativistic effects on the Hartree contribution to the ee interaction at various levels. After adding the xc contribution V_{xc} in untransformed form (see above), one arrives at the effective two-component model Hamiltonians $h_{rel,2}^{(2)}$ where rel = DKee1 or DKee2 for $U \equiv U_0$ or $U \equiv U_1[V_{nuc}]U_0$ according to Eqs. (2.49) and (2.50), respectively. Recall that in these approximate DKS Hamiltonians the relativistic corrections to the ee interaction are *linear* in V_{ee} by construction, just as $\bar{E}_{H,\,rel}[\rho,\{a_k\}]$, Eq. (2.85), is linear in the electron density ρ. The matrix elements of $F_{rel,\,k}^{(2)}$ for rel = DKee1 or DKee2 also arise in the transformation of the Hartree potential of the approximate density $\bar{\rho}$ to the space of the two-component DKS solutions:

$$\bar{V}_H[\rho] = \sum_k a_k F_k \rightarrow BU\bar{V}_HU^\dagger B^\dagger = \sum_k a_k F_{rel,\,k}^{(2)}\,. \tag{2.89}$$

For a given density ρ, the density expansion coefficients a_k are obtained by maximizing $\bar{E}_{H,\,rel}[\rho,\{a_k\}]$, Eq. (2.85), just as in the non-relativistic case. Thus, one has to solve a

relativistically adjusted system of linear equations, see Eq. (2.80):

$$\sum_l [k||l]a_l = \sum_{ij} P_{ji}[ij||k]_{rel} \tag{2.90}$$

Because the approximate DKS Hamiltonians $h^{(2)}_{DKee1,2}$, Eq. (2.49), and $h^{(2)}_{DKee2,2}$, Eq. (2.50), as well as the density expansion coefficients a_k rely on the corresponding DK-transformed matrices of $\bar{V}_H$ or equivalently on $F^{(2)}_{rel,\,k}$, only one set of three-index terms $[ij||k]_{rel}$ occurs in each case. Thus, the two-component relativistic models $h^{(2)}_{DKee1,2}$, Eq. (2.49), and $h^{(2)}_{DKee2,2}$, Eq. (2.50), where one transforms the Hartree potential to the picture of first or second order, respectively, at the DKnuc level, may be associated with energy expressions which can be used in two variational procedures: for obtaining the Hamiltonian as well as for determining the optimal density fit $\bar{\rho}$, i.e. for the best set of expansion coefficient a_k. Such a computational scheme where all unknown variables arise in a variationally consistent fashion from a single total energy functional is advantageous, e.g. when nuclear displacement derivatives (forces) are to be calculated.

The situation is different at the next level of approximation, DKee3, because there are two options to arrive at a practical computational approach based on the two DKS Hamiltonians $h^{(2)}_{DKee3,2}$, Eq. (2.51). In the first case, one distinguishes two variational problems: one is the variation of an approximate total energy functional that generates the approximate DKS Hamiltonian $h^{(2)}_{DKee3,2}$, and another for constructing the auxiliary two-component representation $\bar{\rho}$ of the four-component density ρ based on the minimization of the Coulomb self-energy $[\Delta\rho||\Delta\rho]/2$ of the density difference $\Delta\rho = \rho - \bar{\rho}$, Eq. (2.76). The first problem requires relativistically modified three-index terms $[ij||k]_{rel}$ with rel=DKee3 as they occur in the matrix representation of the Hamiltonian $h^{(2)}_{DKee3,2}$ and hence in the corresponding total energy approximation; see Eq. (2.57). On the other hand, in the determination of the density expansion coefficients a_k, different three-index terms $[ij||k]_{rel}$ with rel=DKee2 as naturally defined by the DK transformation of two-component orbitals in order to determine the density of four-component orbitals, see Eqs. (2.70) and (2.86), should be used.

An alternative approach, favored by us, preserves the stationarity condition of the approximate total energy expression also with respect to the density expansion coefficients a_k. Instead of minimizing the Coulomb self-energy $[\Delta\rho||\Delta\rho]/2$ of the density difference defined in terms of four-component orbitals, back-transformed with the DK transformation U, one can define the coefficients a_k by minimizing the difference $E_{H,\,rel} - \bar{E}_{H,\,rel}$ between the true Hartree energy functional and its approximation in the two-component picture; see Eq. (2.76). The functional $\bar{E}_{H,\,rel}$ and the energy difference $E_{H,\,rel} - \bar{E}_{H,\,rel}$ are defined by the three-index terms $[ij||k]_{rel}$ with rel=DKee3; no other types of three-index integrals

are required. However, because the numerical differences between the two types of three-center integrals $[ij||k]_{rel}$, with rel=DKee2 and rel=DKee3, are rather small, only minor differences between the two alternatives are expected; see the discussion at the end of Sections 2.1.4 and 2.3.2.

The subtle difference of the two procedures defining the expansion coefficients a_k merits a closer look. The coefficients a_k are arguably considered as expansion coefficients of the electron *density*. However, in the first place, these coefficients enter the *energy* definition, Eq. (2.85). In fact, the fitting approximation was introduced to construct a practical energy expression. The two approaches to obtaining the expansion coefficients depend on the answer to the question, what the target quantity of the fitting procedure is, the density or the energy. The question is irrelevant in the non-relativistic case where density fit and energy fit are fully equivalent, see discussion following Eq. (2.79). In the relativistic picture, the *density* fit evolves to a four-component density fit driven by the Coulomb norm minimization of the error in the four-component density; the Hartree energy defined by the Coulomb self-interaction of the density naturally evolves into corrected terms *due to* the self-interaction of the electron density. Of course, the latter term covers the Hartree energy itself, now corrected relativistically, and the contributions due to the picture change of other operators, as induced by the Hartree potential; such operators include the nuclear attraction potential and the kinetic energy. At variance with the non-relativistic case, the best density fit and the best energy fit differ in nature. The question which target quantity to fit is disputable just as much as the question which norm to use in a general fitting procedure.

In all cases discussed previously — non-relativistic, DKee1 and DKee2, the self-interaction energy of $\Delta\rho$ provides a clear minimum. In the case of DKee3, this term still dominates and one can expect a clear minimum which is modified by small relativistic corrections. However, we do not have a strict proof that the stationary condition results in a minimum nor was it the goal of this work to establish a proof that such a minimum exists.

Note that in the DKee3 case, in the expression $E_{H,rel} - \bar{E}_{H,rel}$ to be minimized only the term $\bar{E}_{H,rel}$ depends on a_k. Thus, in the end, the approximate total energy functional is used both for defining the Hamiltonian by variation with respect to the elements P_{ij} of the density matrix and for determining the density expansion by variation with respect to the coefficients a_k. In both procedures the same three-index matrix elements $[ij||k]_{rel}$ with rel=DKee3 (and only those) are required. The corresponding approximate total energy functional, which when varied with respect to ρ yields the Hamiltonian $h^{(2)}_{DKee3,2}$, Eq. (2.51), can be constructed as a linearization in the density difference $\Delta\rho$. For the case of a non-relativistic Hartree energy, this more general strategy is equivalent to the original formulation [59, 60]; see Eqs. (2.76) and (2.85).

Finally, as an example, we give a closed expression for the Hartree-potential related three-index terms $[ij||k]_{DKee3}$ that are required for the matrix representation of the two-component effective KS Hamiltonian $h^{(2)}_{DKee3,2}$, Eq. (2.51), and the corresponding energy functional. We exploit the linearized form of the Hartree-related part of this Hamiltonian. The first potential term $\mathcal{E}^{(2)}_1$, Eq. (2.36), is linear in V; thus the relevant Hartree contribution is $\mathcal{E}^{(2)}_1[\bar{V}_H] = \sum_k a_k \mathcal{E}^{(2)}_1[F_k]$. The transformation generator $W_H \equiv W[\bar{V}_H]$, Eq. (2.37), which appears in $\delta\mathcal{E}^{(2)}_2/\delta V$, is a linear combination of contributions due to the various potential terms F_k, just as in the approximate Hartree potential, Eq. (2.81): $W_H = \sum_k a_k W_{H;k}$. We collect all terms of $h^{(2)}_{DKee3,2}$, Eq. (2.51), that are related to the Hartree contribution arising from a charge component f_k of the auxiliary basis, and obtain the following explicit form of the relativistic three-center integrals:

$$\begin{aligned}[ij||k]_{DKee3} &= \langle i|\mathcal{E}^{(2)}_1[F_k]|j\rangle \\ &\quad - \langle i|W_{nuc}E_pW_{H;k} + W_{H;k}E_pW_{nuc} + \{\{W_{nuc}, W_{H;k}\}, E_p\}/2|j\rangle \end{aligned} \tag{2.91}$$

As already mentioned, partitioning of the effective Kohn–Sham potential V_{eff} is of no fundamental relevance for the DK transformation of the relativistic Kohn–Sham formalism. The effective potential V_{eff} enters the final expressions of the DK decoupling as a whole only. However, from a practical point of view, it is convenient to distinguish different contributions to V_{eff} when constructing efficient implementations of the formalism.

The linearization approach can be extended to the *xc* contributions along the same lines the corrections of the Hartree terms were made. Several approaches to represent the *xc* potential (and the *xc* energy) by an algebraic expression, an expansion series similar to Eq. (2.81), instead of the commonly used numerical quadrature were developed and successfully applied to molecular systems [82, 83, 84, 85, 86, 87, 88]. These methods avoid, sometimes completely, the expensive numerical quadrature, thus reducing the calculation of the *xc* contributions by as much as an order of magnitude [88]. Calculating the *xc* potential in a numerical way often limits the overall performance of a calculation (see Section 3.5). Moreover, once the Hartree terms and the *xc* terms are treated by a similar fitting technique the relativistic formalism presented above for the Hartree energy and the resulting potential may be applied to the corresponding *xc* terms in analogous fashion. Ultimately, there may be no need at all to distinguish the two *ee* contributions as far as the relativistic transformations are concerned.

To complete this section, we briefly summarize the current derivation of computationally practical two-component relativistic DF methods which incorporate relativistic effects due to the Hartree part of *ee* interaction. In the fully relativistic four-component Dirac picture, the Hartree energy E_H which is a bilinear functional of the four-density ρ con-

structed of four-component orbitals is replaced by an approximate functional $\bar{E}_H$ that is linear in ρ. The four-component orbitals are solutions of the DKS Hamiltonian in an effective field that comprises the approximate Hartree potential $\bar{V}_H$. A unitary rotation, here a suitable approximation of the "exact" DK transformation, is used to eliminate the small components of the DKS solutions and to bring the Hamiltonian into an approximately decoupled block-diagonal form. The form of the energy functional and the operators entering the DKS Hamiltonian change accordingly, and so does the form of the approximate Hartree potential $\bar{V}_H = \sum_k a_k F_k$. The latter form of the potential reflects the approximation $\bar{\rho} = \sum_k a_k f_k$ of the density ρ. Exploiting the linear structure of the approximate two-component DKS Hamiltonians discussed above, one can collect all those contributions of the matrix representation of the DKS Hamiltonian which are due to a single F_k into a three-index integral $[ij||k]_{rel}$. Of course, the exact form of these quantities depends on the specific two-component DKS Hamiltonian. For the approximations DKee1 and DKee2, these relativistic three-center integrals $[ij||k]_{rel}$ are equivalent to the matrix elements of the corresponding two-component DK transformed potential operators $F^{(2)}_{rel,\,k}$. Because the same operators $F^{(2)}_{rel,\,k}$ enter the equations defining the density expansions coefficients a_k, one arrives at a completely variational structure of the formalism where the total energy expression is stationary with respect to a_k. When the contributions due to a given potential term F_k do not combine into the DK transformed operator (e.g. in DKee3), one can still formulate a variational scheme if one defines the density fit in a different way, namely by maximizing the approximate relativistic Hartree functional $\bar{E}_{H,\,rel}$. This is consistent with the previous definition of the best fit where one minimizes the difference $E_H - \bar{E}_H = [\Delta\rho||\Delta\rho]/2$ which happens to be the self-interaction energy of the density difference $\Delta\rho$.

2.2 Implementation

2.2.1 Primitive Integrals. Integrals Based on the Momentum Representation

In this section, we discuss the basics of how to calculate the additional primitive integrals that arise in the implementation of the relativistic treatment of the *ee* interaction discussed above. This includes also details for evaluating *momentum integrals* as required by DKee implementation.

The program ParaGauss is a general purpose molecular DFT program designed to take full advantage of the parallel architecture of modern computers [20, 21]. A detailed description of the computational methods implemented in ParaGauss, and the internal

workflow of the program may be found in Refs. [77, 89, 90, 91]. There, one may find an introduction to the evaluation of standard integrals in ParaGauss [89, 90].

ParaGauss makes use of the common LCAO approach (*linear combination of atomic orbitals*) to represent the molecular orbitals [7, 6]. The LCAO approximation is based on the fact that one-electron molecular eigenfunctions may be accurately represented as a linear combination of atomic orbitals. The atomic orbitals, in turn, are represented by linear combinations of the so-called *primitive basis functions* which are given as simple analytic expressions; for this representation, one may achieve any desired accuracy, depending on the number and quality of such primitive functions. Alternative implementations may use the tabulated atomic eigenfunctions as a basis for the LCAO approach [7, 6]. Finally, some implementations, those targeting solids and surfaces in the first place, may go beyond LCAO approximation by introducing basis functions not centered on any atom, e.g. the plane waves [7, 6]. The program ParaGauss adopts the LCGTO-FF-DF method [59, 92, 60, 93] (*linear combination of Gaussian-type orbitals fitting-functions density-functional*) which exploits the advantages of Gaussian-type functions for the analytic evaluation of integrals [94, 95, 96, 97, 98, 99, 100, 101, 92, 102, 103, 104, 105]. Many other implementations of the LCAO method for solving the KS equation exist [106, 107, 108, 109, 110, 111, 112, 113, 114, 115, 116, 117]. Although Slater-type functions [7, 6] permit a more compact presentation of atomic eigenfunctions, many QM programs adopt Gaussian-type functions because the former do not allow simple analytical expressions and an efficient implementation of the complex integrals [118]. To build the Hartree energy functional in ParaGauss, one expands the density in an auxiliary basis set of so-called "fitting functions" (FF) [92, 102]. This auxiliary basis set is constructed similarly to the orbital basis from the Gaussian-type functions.

The atomic orbitals used in ParaGauss as basis functions are combinations of angular and radial dependent parts [119, 89]

$$\varphi(\boldsymbol{r};\, \boldsymbol{a}, l, m) = C^l_m(\boldsymbol{r} - \boldsymbol{a}) d_p(|\boldsymbol{r} - \boldsymbol{a}|). \tag{2.92}$$

This particular atomic basis function with electron coordinates $\boldsymbol{r}$ belongs to the angular momentum shell l of an atom at position $\boldsymbol{a}$. The angular dependent part $C^l_m(\boldsymbol{x}) = x^l C^l_m(\boldsymbol{x}/x)$ is a solid spherical harmonic [120, 95, 96]. The radial part d_p depends only on the distance $x = |\boldsymbol{r} - \boldsymbol{a}|$ from the center $\boldsymbol{a}$ and it is a linear combination of Gaussian-type functions

$$d_p(x) = \sum_q d^q_p \exp(-\alpha_q x^2). \tag{2.93}$$

The process of forming linear combinations of primitive exponentials is referred as basis

set *contraction*; in general, it reduces the essential degrees of freedom of the LCAO ansatz. One speaks of a *segmented contraction* scheme when the coefficients d_p^q are non-zero only for some range of the index q [7, 6]. The most general case without restrictions on the coefficients d_p^q is called a *general contraction* scheme [7, 6]; ParaGauss exploits the latter, more general scheme. In the auxiliary basis sets used to fit the density, some exponentials are pre-multiplied by a factor proportional to r^2 to improve the representation of partial densities generated by p orbitals.

The angular dependent part, the real spherical harmonic $C_m^l(\boldsymbol{r})$, may be expressed with the help of complex spherical harmonics $Y_{lm}(\boldsymbol{r}/r)$ [120, 95, 96]

$$C_0^l(\boldsymbol{r}) = r^l Y_{00}(\boldsymbol{r}/r) \tag{2.94}$$

$$C_m^l(\boldsymbol{r}) = r^l \frac{1}{\sqrt{2}} \left[(-1)^m Y_{lm}(\boldsymbol{r}/r) + Y_{l,-m}(\boldsymbol{r}/r)\right] \text{ for } m > 0 \tag{2.95}$$

$$C_m^l(\boldsymbol{r}) = r^l \frac{1}{\sqrt{2}i} \left[(-1)^m Y_{l,-m}(\boldsymbol{r}/r) - Y_{lm}(\boldsymbol{r}/r)\right] \text{ for } m < 0\,. \tag{2.96}$$

For the complex spherical harmonics, we adopt the phase conventions of Condon and Shortley [120, 121, 122].

Thus, any orbital function in ParaGauss may be written as a linear combination of normalized primitive Gaussian functions [119, 89], parametrized by

$$\chi(\boldsymbol{r};\, \alpha, \boldsymbol{a}, l, m) = N(\alpha, l) C_m^l(\boldsymbol{r} - \boldsymbol{a}) \exp\left(-\alpha(\boldsymbol{r} - \boldsymbol{a})^2\right) \tag{2.97}$$

with the normalization factor

$$N(\alpha, l) = \left(\frac{2\alpha}{\pi} \frac{(4\alpha)^l}{(2l-1)!!}\right)^{1/2}. \tag{2.98}$$

One of the important features of Gaussian functions which promoted their use in quantum chemistry is that the product of two Gaussian functions is again a Gaussian function [102]. Another feature, the easy differentiation of Gaussian functions, allows an alternative definition for the primitive Gaussian basis function [102, 119, 89]

$$\chi(\boldsymbol{r};\, \alpha, \boldsymbol{a}, l, m) = n(\alpha, l) C_m^l(\boldsymbol{\nabla}_a) \chi(\boldsymbol{r};\, \alpha, \boldsymbol{a}, 0, 0) \tag{2.99}$$

with the normalization factor

$$n(\alpha, l) = (\alpha^l (2l-1)!!)^{-1/2}\,. \tag{2.100}$$

One may think of the differential operators $C_m^l(\boldsymbol{\nabla}_a)$, a "gradient spherical harmonic", as

polynomials of degree l in three variables $\partial/\partial a_x$, $\partial/\partial a_y$, and $\partial/\partial a_z$; the coefficients of these polynomials should be then taken from the definitions of the solid spherical harmonics.

These basis functions are used to compute the matrix elements of the KS Hamiltonian, in a complete analogy to the Roothan equations of the HF formalism [7, 6]. At this stage, the advantages of Gaussian functions become apparent. Many of the matrix elements involving simple operators and Gaussian basis functions may be expressed in closed analytical form [102]. For example, the overlap of two s-type Gaussian functions $\chi_a = \chi(\boldsymbol{r};\, \alpha, \boldsymbol{a}, 00)$ and $\chi_b = \chi(\boldsymbol{r};\, \beta, \boldsymbol{b}, 00)$ is given by [102, 119, 89]

$$S(\alpha, \boldsymbol{a}, \beta, \boldsymbol{b}) := \langle \chi_a | \chi_b \rangle = \left(4 \frac{\alpha\beta}{\alpha+\beta} \right)^{3/4} \exp\left(-\frac{\alpha\beta}{\alpha+\beta} (\boldsymbol{a}-\boldsymbol{b})^2 \right) . \tag{2.101}$$

The general overlap matrix elements for any angular momentum indices may be derived from this equation with the help of "differential" form of a spherical Gaussian, Eq. (2.99). For any functions $\chi_a = \chi(\boldsymbol{r};\, \alpha, \boldsymbol{a}, l_a, m_a)$ and $\chi_b = \chi(\boldsymbol{r};\, \beta, \boldsymbol{b}, l_b, m_b)$ one has [102, 119, 89]

$$S(\alpha, \boldsymbol{a}, l_a, m_a, \beta, \boldsymbol{b}, l_b, m_b) = n(\alpha, l_a) n(\beta, l_b) C^{l_a}_{m_a}(\boldsymbol{\nabla}_a) C^{l_b}_{m_b}(\boldsymbol{\nabla}_b) S(\alpha, \boldsymbol{a}, \beta, \boldsymbol{b}) . \tag{2.102}$$

To unfold this expression, one uses the following rules [119, 89]

$$C^L_M(\boldsymbol{\nabla}) f(r^2/2) = C^L_M(\boldsymbol{r}) f^{(L)}(r^2/2) \tag{2.103}$$

$$C^L_M(\boldsymbol{\nabla})(f \cdot g) = \sum_{l=0}^{L} \sum_{m,m'} \epsilon^{LM}_{lmm'} [C^l_m(\boldsymbol{\nabla}) f] \cdot [C^{L-l}_{m'}(\boldsymbol{\nabla}) g] \tag{2.104}$$

$$C^l_m(\boldsymbol{\nabla}) C^L_M(\boldsymbol{r}) = (2l-1)!! \sum_{m'} \epsilon^{LM}_{lmm'} C^{L-l}_{m'}(\boldsymbol{r}). \tag{2.105}$$

These formulae give the action of a gradient spherical harmonic on a spherically symmetric functions f, a product of functions $f \cdot g$, and a spherical harmonic, respectively. The coefficients $\epsilon^{LM}_{lmm'}$ are vector coupling coefficients, usually pre-computed and made available in tabulated form [123, 119]. With the help of these three rules, closed expressions for practically any type of integral can be derived, starting from the corresponding expressions for spherically symmetric Gaussians [102, 119, 89].

To build up the KS matrix and the energy expression, primitive integrals of the basic participating operators in the primitive basis are required. For the traditional nonrelativistic KS problem, these matrix elements are $\langle \chi_a | p^2/2 | \chi_b \rangle$ with $\boldsymbol{p} = -i\boldsymbol{\nabla}$ for the kinetic energy, $\langle \chi_a | R_c^{-1} | \chi_b \rangle$ with $R_c = |\boldsymbol{r} - \boldsymbol{c}|$ for the Coulomb field of a (point) nucleus at location $\boldsymbol{c}$, and $\langle \chi_a | F_k(\boldsymbol{r} - \boldsymbol{c}) | \chi_b \rangle$ with $F_k = \int d^3\boldsymbol{r}'\, f_k(\boldsymbol{r}' - \boldsymbol{c}) / |\boldsymbol{r} - \boldsymbol{r}'|$ for the Coulomb field of the partial fit densities f_k [60]. Integrals of the xc potential, though also required, are evaluated differently, namely by numerical integration on a grid [60]. In a SR calculation

at the DKnuc level, in addition the operator $\boldsymbol{p}V_{nuc}\boldsymbol{p}$ occurs when one constructs the relativistically modified nuclear field; this operator is represented by primitive matrix elements $\langle\chi_a|\boldsymbol{p}R_c^{-1}\boldsymbol{p}|\chi_b\rangle$ [77]. Its SO counterpart $\boldsymbol{\sigma p}V_{nuc}\times\boldsymbol{p}$, another contributor to $\boldsymbol{\sigma p}V_{nuc}\boldsymbol{\sigma p}$, requires similar primitive integrals $\langle\chi_a|\boldsymbol{p}R_c^{-1}\times\boldsymbol{p}|\chi_b\rangle$ [77]. Both types of integrals are some combinations of the more general primitive integrals $\langle\chi_a|p_iR_c^{-1}p_j|\chi_b\rangle$, $i,j=1,2,3$. When one goes beyond the DKnuc approximation in a relativistic calculation (e.g. at the DKee1 level), matrix elements $\langle m|\boldsymbol{\sigma p}F_k\boldsymbol{\sigma p}|n\rangle$ of the Coulomb potential of the partial fit densities F_k are required for a consistent extension of the DKH approach to the Hartree potential which is represented as partial potential contributions of auxiliary basis basis functions [27]. If one does not invoke the auxiliary expansion of the density and the resulting representation of the potential, similar matrix elements of the local Hartree (and xc) potentials are required [124].

To minimize the number of the primitive integral types required at higher levels of relativistic approximation and to simplify expressions for them, we exploit the "resolution of identity" where one inserts the expression $\sum_m|m\rangle\langle m|\approx 1$ and computes the matrix of an operator product as a product of representation matrices [77]:

$$\langle m|\boldsymbol{\sigma p}F_k\boldsymbol{\sigma p}|n\rangle\approx\sum_{rs}\langle m|\boldsymbol{\sigma p}|r\rangle\langle r|F_k|s\rangle\langle s|\boldsymbol{\sigma p}|n\rangle. \tag{2.106}$$

In this way, only two kinds of integrals have to be computed for the r.h.s. of this equation, namely those of the Coulomb field of the partial densities $\langle r|F_k|s\rangle$, already mentioned, which are required already at the non-relativistic level, and a new but fairly simple integral of the operator $\boldsymbol{\sigma p}$. After explicit expansion of the $\boldsymbol{\sigma}$ matrices, the matrix representation of this latter operator (in spinor space) is expressed via matrix elements of the momentum operator $\boldsymbol{p}$ in orbital space. Hence, primitive two-center integrals of the dipole type $\langle\chi_a|\boldsymbol{p}|\chi_b\rangle$ are required.

The primitive matrix elements of the operator $\boldsymbol{p}$ for s-type Gaussian basis functions have the form

$$\boldsymbol{P}(\alpha,\boldsymbol{a},\beta,\boldsymbol{b})=\langle\chi_a|\boldsymbol{p}|\chi_b\rangle=-i\langle\chi_a|\boldsymbol{\nabla}|\chi_b\rangle \tag{2.107}$$

$$=i\boldsymbol{\nabla}_bS(\alpha,\boldsymbol{a},\beta,\boldsymbol{b})=2i\frac{\alpha\beta}{\alpha+\beta}(\boldsymbol{a}-\boldsymbol{b})S(\alpha,\boldsymbol{a},\beta,\boldsymbol{b})\,. \tag{2.108}$$

To obtain the last expression we used the identity $\boldsymbol{\nabla}\equiv\boldsymbol{\nabla}_r=-\boldsymbol{\nabla}_b$ when acting on a function of the argument $\boldsymbol{r}-\boldsymbol{b}$, and the differentiation rule of the spherically symmetric function $S\sim\exp[-\alpha\beta/(\alpha+\beta)(\boldsymbol{a}-\boldsymbol{b})^2]$. The matrix elements for basis function of arbitrary angular momenta l_a and l_b are derived from the above expression by double differentiation

of the product $\boldsymbol{v}S := (\boldsymbol{a} - \boldsymbol{b})S$:

$$\boldsymbol{P}(\alpha, \boldsymbol{a}, l_a, m_a, \beta, \boldsymbol{b}, l_b, m_b) \sim C^{l_a}_{m_a}(\boldsymbol{\nabla}_a) C^{l_b}_{m_b}(\boldsymbol{\nabla}_b)\{\boldsymbol{v}S\}. \tag{2.109}$$

Note that S is also a function of $\boldsymbol{v} = \boldsymbol{a} - \boldsymbol{b}$. For any function of $\boldsymbol{v}$, one has the operator identity $C^l_m(\boldsymbol{\nabla}_a) = -C^l_m(\boldsymbol{\nabla}_b)$, and one arrives at an expression where both differential operators have the same argument:

$$C^{l_a}_{m_a}(\boldsymbol{\nabla}) C^{l_b}_{m_b}(\boldsymbol{\nabla})\{F \cdot G\} \tag{2.110}$$

with $F = \boldsymbol{v}$ and $G = S$. This double differentiation of a product occurs with many integral types required for a typical calculation. Therefore, it was made available as a subroutine in ParaGauss. The input to such a subroutine should be the values of F and G, for a particular parameter set $(\alpha, \boldsymbol{a}, \beta, \boldsymbol{b})$, and all values of the (double) derivatives $C^{l_1}_{m_1}(\boldsymbol{\nabla}) C^{l_2}_{m_2}(\boldsymbol{\nabla}) F$ and $C^{l_1}_{m_1}(\boldsymbol{\nabla}) C^{l_2}_{m_2}(\boldsymbol{\nabla}) G$ for $l_1 \leq l_a$, $|m_1| \leq l_1$, $l_2 \leq l_b$, $|m_2| \leq l_2$ at the chosen set of parameters $(\alpha, \boldsymbol{a}, \beta, \boldsymbol{b})$.[1] Such a strategy is analogous to providing as input the *coefficients* of a Taylor expansion, instead of an supplying an *expression* which determines the *functional* dependence of F and G.

The derivatives of $\boldsymbol{v}$ are trivial

$$C^l_m(\boldsymbol{\nabla}_a) v_k = \begin{cases} v_k & \text{if } l = 0 \\ \delta_{mk} & \text{if } l = 1 \\ 0 & \text{otherwise} \end{cases} \tag{2.111}$$

In fact, C^0_0 is the identity, $C^1_m(\boldsymbol{\nabla}_a) = \partial/\partial a_m$, and all higher-order derivatives yield zero. In ParaGauss, a different indexing of vector components is often used to allow a uniform treatment together with the indexing of the component of C^1_m [90]. In that notation, the vector components (v_{-1}, v_0, v_{+1}) refer to the (v_y, v_z, v_x) in their usual meaning. [However, vector components and other quantities with the indexing (lm) are stored in the order $(0, \pm 1, \pm 2, ... \pm l)$, positive indices first.] The result of the double derivative $C^{l_a}_{m_a}(\boldsymbol{\nabla}_a) C^{l_b}_{m_b}(\boldsymbol{\nabla}_b)$ applied to $\boldsymbol{v}$ is an obvious extension of the case list above. The double derivatives of the overlap $C^{l_a}_{m_a}(\boldsymbol{\nabla}_a) C^{l_b}_{m_b}(\boldsymbol{\nabla}_b) S$ are overlap matrix elements which are required for almost any type of integrals and are employed in the evaluation of many types of integrals [119, 77, 89].

[1] For consistency, one may also consider the *value* of the functions F and G as result of "zeroth-order" differentiation, e.g. $C^0_0(\nabla) C^0_0(\nabla) F$.

2.2.2 Relativistic Transformations

The implementation of the DKH transformation follows the strategy for the SR variant [125] which later on was extended to a treatment of the nuclear SO interaction [77]. However, the DKH SO implementation was mostly rewritten to allow for a more uniform treatment of both types of DKH variants, that in the nuclear field only DKH (DKnuc) and the DKee models (Section 2.1.4). Another reason for rewriting this program sections is connected with the goal to improve the performance of the relativistic transformations via efficient computational routines for matrix algebra [126, 127, 128]. In fact, the whole DKH machinery is based on matrix manipulations including the very expensive ones like similarity transformations and matrix diagonalizations. From the new implementation, one could also expect a performance improvement for the construction of the KS Hamiltonian due to a reorganization of the matrix manipulations in momentum space. There is even room for further improvements, especially with regard to the symmetry properties of spinless operators; this question will be addressed in Section 3.6.

In the classic DKH approach, construction of a relativistically corrected Hamiltonian or a relativistic energy expression in algebraic from proceeds via the following steps [16].

Basis set orthogonalization. A typical quantum chemical computation starts from a non-orthogonal basis and explicitly deals with the overlap matrix S (which differs from a unit matrix). The so-called canonical orthogonalization [129], also used in ParaGauss for the DKH approach, involves a solution of the eigenvalue problem for the overlap matrix S. Furthermore, some matrices need to be adapted to an orthogonal representation by a similarity transformation.

Construction of the basis in momentum space. Most DK operators are best represented in momentum space, i.e. in a basis of plane-wave functions; for instance, the kinematic factors A_p, K_p and the relativistic (free-particle) kinetic energy E_p are diagonal in a momentum representation [16]. Relatively complex expressions of the DK Hamiltonian are easier to compute in momentum space. According to Hess and Buenker [130, 18], one may use the eigenvectors of the kinetic energy operator $p^2/2$ as basis for an approximate representation of momentum space, namely as finite basis analogue of plane waves. This concept lies at the very hart of the Douglas–Kroll–Hess (DKH) strategy. Because the kinematic factors and the relativistic kinetic energy expression are all functions of p^2, they are easily computed once the eigenvalues and eigenvectors of p^2 are known. This step involves solution of the eigenvalue problem for the kinetic energy $p^2/2$ after an orthogonalization transformation in the preceding step. The basis set rotation matrices made available in this step are further used to

transform other operators to a momentum space representation, e.g. the potential of the nuclei V_{nuc} as well as the SR and SO parts of $\boldsymbol{\sigma p} V_{nuc} \boldsymbol{\sigma p}$.

Construction of the relativistic operators in momentum space. This step comprises the actual implementation of the DK expressions for the Hamiltonian. The matrix algebra at this stage involves arithmetic operations with diagonal and full matrices as operands, but no eigenvalue problems. The computation time is comparable to that of the previous steps due to relative complexity of the DK expressions; it may be substantially reduced by reorganizing the expressions in a mathematically equivalent form which allows factorization and re-use of partial expressions.

Transformation back to real space. The relativistic Hamiltonian or the potential evaluated in momentum space is transformed back to real (orbital) space by another similarity transformation.

Matrix contraction. The accuracy of the approximate momentum space representation mediated by the eigenvectors of the operator p^2 in a finite basis strongly depends on the size and the flexibility of that basis. One way to ensure the accuracy of the relativistic transformations is to carry them out in the yet uncontracted Gaussian-type orbitals basis and contract the latter only afterwards to reduce the matrix size for the efficiency and stability of the SCF iteration process [130, 18].

If, as done in ParaGauss, one exploits the point group symmetry of the system then the total Hamiltonian and all related matrices are of block-diagonal from in the index of the irreducible representations ("irrep" for brevity) ([77], Chapter 3). In that case, the five steps just described have to be repeated for each symmetry (irrep) subblock, without any need for sharing any information between these tasks. This observation opens the possibility for splitting the whole tasks into smaller ones which can be processed in parallel on several processors [77].

An algorithm of the DKH transformation[2] as implemented in ParaGauss is illustrated by the pseudo-code shown in Algorithm 2.1. The input provided to the DKH procedure includes the matrix representations of the kinetic energy $\mathtt{T(i,j)} = \langle i \,|p^2/2|\, j\rangle$, the potential matrix $\mathtt{V(i,j)} = \langle i \,|V|\, j\rangle$, and the coupling potential terms $\mathtt{PVP(i,j)} = \langle i \,|\boldsymbol{\sigma p} V \boldsymbol{\sigma p}|\, j\rangle$ in the original non-orthogonal basis, and the overlap matrix `S`. The coupling matrix `PVP` contains, as presented here, both SR and SO contributions, may be, however, alternatively defined to contain only SR terms or only SO ones. On output the procedure provides the relativistic counterparts of the kinetic energy and potential, the matrices `TR` and `VR`, respectively. The preparations to the DKH transformation start from eigenvalue problem solution

[2] Implemented in `modules/reltrafo.f90` module. Some identifiers changed for readability

Algorithm 2.1: Pseudo-code of the DKH SO implementation in ParaGauss.

```
!! INPUT: overlap S, kinetic matrix T, potential V, coupling potential terms PVP
!! OUTPUT: relativistic kinetic energy TR, and potential VR
!!
!! STEP 1 : CANONICAL ORTHOGONALIZATION
                                        !! O(EV + 2MM)
call EigenSolver(S,s,Q)                 !! diagonalize overlap
QF = Q * s^{-1/2}                       !! orthogonal transformation matrix ...
QB = s^{1/2} * Q^†                      !! ... and reverse of that
T = QF^† * T * QF                       !! orthogonalize kinetic matrix
!! STEP 2 : CONSTRUCTING MOMENTUM SPACE BASIS
                                        !! O(EV + 7MM)
call EigenSolver(T,p2,U)                !! find p^2 eigenfunctions in orthogonal basis
UF = QF * U                             !! ... and now in the original basis
UB = U^† * QB                           !! ... and now the reverse transformation
V = UF^† * V * UF                       !! potential matrices to momentum space
PVP = UF^† * PVP * UF                   !! PVP contains SO and/or SR terms
!! STEP 3.1 : MOMENTUM SPACE COMPUTATIONS DKH(1)
                                        !! O(0MM)
call KineticFactors(p2,Ep,Ap,Kp)        !! compute diagonal matrices
AVA = Ap * V * Ap                       !! first-order DKH terms ...
ARVRA = (Ap * Kp) * PVP * (Kp * Ap)     !! including SO and/or SR potential terms
VR = AVA + ARVRA                        !! first-order DKH approximation
!! STEP 3.2 : MOMENTUM SPACE COMPUTATIONS DKH(2)
                                        !! O(2MM)
forall ( i=1:N, j=1:N )                 !! replace V_pp' by Ṽ_pp' = V_pp'/(E_p + E_p')
  AVA(i,j) = AVA(i,j) / (Ep(i) + Ep(j))
  ARVRA(i,j) = ARVRA(i,j) / (Ep(i) + Ep(j))
end forall
R2 = Kp^2 * p2                          !! put R^2 = K_p^2 p^2 between W matrices
RW = R2 * AVA - ARVRA                   !! in -1/2{2WE_pW - E_pW^2 - W^2E_p}
VR = VR + RW^† * (Ep/R2) * RW           !! add -WE_pW = -WR(E_p/R^2)RW
W2 = - RW^† * (1/R2) * RW               !! W^2 = WR(1/R^2)RW, RW^† = -WR
VR = VR - ( Ep * W2 + W2 * Ep )/2       !! add the rest of 2nd-order DKH
!! STEP 4: BACK TO REAL SPACE
                                        !! O(3MM)
VR = UB^† * VR * UB                     !! ... relativistic potential
TR = UB^† * (Ep - c^2) * UB             !! ... and rel. kin. energy w/o rest mass
```

for the overlap matrix `S`; its eigenvalues `s` and eigenvectors `Q` are used to construct orthogonalization transformation matrix `QF` and its reverse counterpart `QB = QF`$^{-1}$.The kinetic energy matrix `T` is then transformed to the orthogonal basis by similarity transformation (Step 1, Algorithm 2.1).

As the next step, the eigenvalues `p2` and the eigenvectors `U` of the kinetic matrix `T` are found. The eigenvector basis, an approximation to the "plane-wave" basis, is used to build the momentum representation of the potential terms `V` and `PVP` (Step 2, Alg. 2.1). In the current implementation the preparation steps 1 and 2 together make up the largest part of the whole transformation. The formal cost of the preparation steps is $O(2EV + 9MM)$ where MM denotes the cost of a matrix multiply and $EV \approx 20 - 100MM$ [131] denotes the cost of an eigenvalue problem solution.[3] To estimate approximately the operation count, we ignore all matrix multiplications involving diagonal matrices, e.g. the square root $s^{1/2}$ of the diagonalized overlap matrix s, and the kinetic factors E_p, A_p, K_p. Such operations are much less expensive than those involving multiplications of dense matrices. A similarity transformations requires two multiplications of (dense) matrices; construction of the transformation matrix to momentum space and of the backward transformation matrix requires one (dense) matrix multiplication each.

As next, the relativistic potential matrix `VR`, as given by the 1st order DKH expression $V_{rel} = AVA+ARVRA$ [$\mathcal{E}_1$ of Eq. (2.36)], is computed. This step is particularly cheap, since it does not require expensive dense matrix multiplications (Step 3.1, Alg. 2.1). Indeed, the matrix representations of V and $\boldsymbol{\sigma p} V \boldsymbol{\sigma p}$ need only to be multiplied by kinetic factors A_p and K_p, which are diagonal in momentum space. Further the program flow proceeds to the evaluation of the 2nd order DKH correction terms (Step 3.2, Alg. 2.1). The rotation generator W, Eq. (2.37), contains the factor $\boldsymbol{\sigma p}$ once, so is not possible to construct its matrix representation starting from the matrix representations of V (`V`) and $\boldsymbol{\sigma p} V \boldsymbol{\sigma p}$ (`PVP`) only; neither is it possible for R, Eq. (2.38). One circumvents this by slightly modifying the expressions for $\mathcal{E}_2$, Eq. (2.36), with the help of an identity $R^2 = (K\boldsymbol{\sigma p})^2 = K^2 p^2$:

$$\mathcal{E}_2 = -WE_pW - \frac{1}{2}\{W^2, E_p\} \tag{2.112}$$

$$= -WR(E_pR^{-2})RW - \frac{1}{2}\{WR(R^{-2})RW, E_p\} \tag{2.113}$$

$$= +\underline{RW}^{\dagger}(E_pR^{-2})\underline{RW} + \frac{1}{2}\{\underline{RW}^{\dagger}(R^{-2})\underline{RW}, E_p\} \tag{2.114}$$

[3] In fact, for our current needs, which are limited by the single-point SO runs, there is no need to separate the two first steps, canonical orthogonalization and diagonalization of kinetic energy matrix. One may solve a generalized eigenvalue problem for the kinetic energy matrix T with the metric S instead. The presented approach matches well the SR implementation which covers not only the single point calculations but also allows evaluation of the relativistic forces and, thus, efficient geometry optimization procedure.

In the the last equality, Eq. (2.114), the quantity $\underline{RW}$ appears repeatedly and may thus be re-used; this possibility is emphasized by underlining. Also note that $WR = -(RW)^\dagger$ as can be seen by comparing the two definitions:

$$RW = R^2(\tilde{AVA}) - AR\tilde{VRA} \tag{2.115}$$

$$WR = AR\tilde{VRA} - (\tilde{AVA})R^2 \tag{2.116}$$

R^2 is a diagonal matrix so that the evaluation of RW from the matrices $\tilde{AVA}$ and $AR\tilde{VRA}$ matrices is inexpensive. The savings due to the pre-evaluation of this intermediate quantity become apparent when one compares how, for instance, the quantity $WR(R^{-2})RW$ had been previously evaluated [125, 77]:

$$(AR\tilde{VRA})(\tilde{AVA}) + (\tilde{AVA})(AR\tilde{VRA}) \tag{2.117}$$

$$- (AR\tilde{VRA})(R^{-2})(AR\tilde{VRA}) - (\tilde{AVA})R^2(\tilde{AVA}) \tag{2.118}$$

Here, *four* multiplications of dense matrices are required. With the intermediate matrix quantity $\underline{RW}$ the final expression for $\mathcal{E}_2$, Eq. (2.114), requires only *two* multiplications of full matrices, disregarding for this purpose the effort of multiplications involving the diagonal matrices E_p and R^{-2}.

Alternatively, one may "factorize" the diagonal elements of E_p by sacrificing algebraic matrix operations. In such an approach, the matrix elements of $\mathcal{E}_2$ are obtained in element-wise fashion in a three-fold loop over all $i \leq j$, and k [125, 77]:

$$\mathcal{E}_2(i,j) = \mathcal{E}_2^*(j,i) = \frac{1}{2}\sum_k \{2E(k) + E(i) + E(j)\}\underline{RW}^*(k,i)R^{-2}(k)\underline{RW}(k,j)\,. \tag{2.119}$$

Although this is equivalent to Eq. (2.114), it does not follow the strategy of exploiting efficient implementations of matrix algebra operations. Still, this approach may be sufficiently efficient on vector computers. Note that, here as well, one may profit from pre-computing the matrix $\underline{RW}$.

Evaluation of the DKH Hamiltonian in the momentum space together with the last step, the back transformation of the relativistic matrices into real (orbital) space, formally takes only $O(5MM)$ operations, Alg. 2.1.

The pseudo-code of Alg. 2.1 is very close to the actual Fortran 90 implementation, even up to the operator notation for matrix operations. The operator interface to an efficient matrix arithmetics module is described in Appendix A. Two types of matrices are involved in the computations: diagonal matrices and full (dense) square matrices. The former are internally represented as one-dimensional arrays. The most demanding operations, which

determine the performance of the algorithm, are the subroutine calls for the eigenvalue problem and the general matrix multiplications. Both procedures require $O(N^3)$ floating point operations and work with $O(N^2)$ storage elements. The different scaling behavior of floating point operation number and memory references suggest algorithmic solutions which allow an efficient re-use of memory (caching) to minimize memory references as best strategy for a high performance implementations. For the matrix operations on most platforms, we use the library ATLAS [127], an efficient implementation of the basic linear algebra subroutine package BLAS L3 [126]. We solve the eigenvalue problem with the help of the library LAPACK [128] which refers to BLAS L3 for matrix arithmetics, ensuring high efficiency.

2.2.3 Relativistic Transformation of the Hartree Potential

Section 2.1.5 presented the formalism for incorporating relativistic effects of the screening Hartree (Coulomb) field into the DK approach. In particular, the DK transformation concept was combined with the so-called "fitting-function" approach to the Coulomb self-interaction energy of the electron density and the corresponding potential terms. In this section, we will discuss the relevant details of its implementation in ParaGauss.

The task of computing the relativistic corrections due to the Hartree terms of the fitted density $\bar{\rho}$ [Eq. (2.74)] is very closely related to the DKH transformation of the Hartree potential $\bar{V}_H$. The latter is a linear "contraction" of partial contributions due to the individual functions of the fit basis which represents the density $\bar{\rho}$. The number of such functions may be comparable to the size of the orbital basis, $20 - 50$ per atom and more; it is especially large for heavy elements. The coefficients of this contractions are adjusted in every SCF iteration until convergence is reached. One is faced with a choice between two alternatives.

For one, one carries out the DKH transformation of the whole (contracted) potential $\bar{V}_H = \sum_k a_k F_k$ during each SCF iteration. Alternatively, as preferred by us, one pre-calculates relativistic corrections due to each potential contribution F_k and contracts them every time a new set of coefficients a_k is available. In this latter strategy, one has a *number* of uniformly defined operators which have to be subjected independently to a DKH transformation; this number grows with the size of the system. This should be contrasted with a standard DKH implementation (DKnuc) where one has to transform only the nuclear attraction V_{nuc} and kinetic energy T. On a parallel computer one may achieve an efficient parallelization by dividing the workload among processors according to subranges of the index k of the fit function f_k or F_k, respectively. Nevertheless, for the overall performance, it is crucially important to implement efficiently the relativistic

transformation of a given partial contribution F_k. As an immediate consequence, one has to avoid the repetition of the same computational steps for consecutive contribution. For this reason, it is absolutely essential to rearrange the existing (standard) code for a DKH transformation so that it can be applied efficiently to the DKH transformation of FF contributions.

Another issue which makes the DKH transformation of a potential term F_k different from that of transforming the nuclear potential V_{nuc} is the way how the matrix elements of the relativistic coupling terms are presently evaluated. Whereas the coupling terms due to the nuclear potential $\boldsymbol{\sigma p} V_{nuc} \boldsymbol{\sigma p}$ are combined from four analytically derived contributions $\sum_{\mu\nu} \{\delta_{\mu\nu}, \sigma_\kappa \epsilon_{\mu\nu\kappa}\} \langle i|p_\mu V_{nuc} p_\nu|j\rangle$, $\kappa = 1, 2, 3$ corresponding to the scalar operator $\boldsymbol{p} V_{nuc} \boldsymbol{p}$ and three components of the vector operator $\boldsymbol{p} V_{nuc} \times \boldsymbol{p}$, we opted for an alternative strategy where the corresponding matrix elements of F_k are *algebraically* evaluated from the matrix representation $\langle i|F_k|j\rangle$ and the matrix representation of the bracketing operator $\langle i\,|\boldsymbol{\sigma p}|\,j\rangle$. For this purpose, we (twice) introduce the approximate resolution of the identity:

$$\langle i|\boldsymbol{\sigma p} F \boldsymbol{\sigma p}|j\rangle \approx \sum_{k,l} \langle i|\boldsymbol{\sigma p}|k\rangle \langle k|F|l\rangle \langle l|\boldsymbol{\sigma p}|j\rangle \tag{2.120}$$

Use of the resolution of the identity reduces the number of additional integral types to be computed and stored; however, at the same time, it increases the quality requirements on the basis set that is used to construct the matrix representations (see Section 2.3.4).

Moreover, the fact that the two-component operator $\boldsymbol{\sigma p}$ is not totally symmetric, requires one to treat simultaneously two coupled irreps. Even though $\boldsymbol{\sigma p}$ looks like a scalar, it is not. Loosely speaking, it is a contraction of the vector $\boldsymbol{p}$ and the pseudo-vector (axial vector) $\boldsymbol{\sigma}$ into a *pseudo-scalar*. A pseudo-scalar transforms as a true scalar quantity under all proper symmetry rotations (i.e. it is invariant) but it changes sign under improper rotations, among them the inversion. This feature of the two-component operator $\boldsymbol{\sigma p}$ is closely related to the parity balance requirement [78] between large and small components of four-spinors (see Section 3.3.4) and to the totally symmetric character of the four-component operator $\boldsymbol{\alpha p}$. Throughout the thesis, we adhered to the following particular choice of the parity operator P as expressed by the action on large and small components of a four-spinor [78]:

$$P : \psi^L \rightarrow \psi^L \text{ and } \psi^S \rightarrow -\psi^S \tag{2.121}$$

Here P designates the inversion of the spatial coordinate system. Instead of the sign change, one often employs an alternative choice of phases which entails additional factor i in the transformations above [76].

The appearance of the pseudo-scalar operator $\boldsymbol{\sigma p}$ forces one to choose different basis

sets for large and small components to achieve a numerically adequate description. This kinetic balance [132] between basis sets of large and small components can be (approximately) achieved by generating the basis set of the small components from that of the large component as follows [133]:

$$\psi^S \approx \boldsymbol{\sigma p}\psi^L/2c \tag{2.122}$$

In the program ParaGauss, basis sets for large and small components are constructed from two-spinors of two irreps $\tilde{\nu}$ and $\tilde{\nu}'$ which are coupled by the pseudo-scalar irrep $\mathcal{P}$: $(\tilde{\nu}') = \mathcal{P} \otimes (\tilde{\nu})$; see Section 3.3.4. The two-spinor bases for irreps $\tilde{\nu}$ and $\tilde{\nu}'$ are constructed from the atomic bases in standard fashion, without any further reference to the kinetic balance condition, simply by reduction of the direct product of orbital and spin state spaces. Therefore, it is natural that the basis set dimensions of coupled irreps differ in such an approach, $\dim \tilde{\nu} \neq \dim \tilde{\nu}'$, as is the case in general. The basis for one of the coupled irreps, say $\tilde{\nu}'$, may even be empty: $\dim \tilde{\nu}' = 0$. This happens normally only in atomic systems when the basis does not contain sufficiently high angular momentum functions. Of course, the coupling between irreps is mutual; if $(\tilde{\nu}') = \mathcal{P} \otimes (\tilde{\nu})$ then $(\tilde{\nu}) = \mathcal{P} \otimes (\tilde{\nu}')$ because $\mathcal{P}^2 = 1$. This coupling also defines selection rules for any pseudo-scalar operator.

The peculiarities presented above originate in the need to handle explicitly the momentum matrix representation $\boldsymbol{\sigma p}$. For the sake of simplicity, the two-component pseudo-scalar operator $\boldsymbol{\sigma p}$ should always be considered as (off-diagonal) block of the four-component *totally symmetric* operator $\boldsymbol{\alpha p}$ because the selection rules for totally symmetric operators are remarkably simple. Totally symmetric operators have non-zero matrix elements only between functions of the same irrep. In general, the matrix of a totally symmetric operator in a symmetrized basis reduces to block diagonal form comprising smaller matrices:

$$V = \bigoplus_{\tilde{\nu}} V^{(\tilde{\nu})} \tag{2.123}$$

Here, $V^{(\tilde{\nu})}$ denotes a single block which corresponds to irrep $\tilde{\nu}$. For four-spinors, it is convenient to specify the transformation properties $\tilde{\nu}$ by those of its large component. In this work, this convention will be assumed whenever the symmetry of a four-spinor is referred.

In the four-component picture, it is also useful to exploit the 2×2 block structure of matrices induced by the classification of large and small components. Specifying the subscripts LL, SS, SL, and LS, the block structure of matrices can be represented as

follows:

$$V = \begin{pmatrix} V_{LL} & V_{LS} \\ V_{SL} & V_{SS} \end{pmatrix} \tag{2.124}$$

This partitioning may, of course, be combined with the symmetry reduction, Eq. (2.123). Then each irreducible block $V^{(\tilde{\nu})}$ will additionally be separated into the blocks $V_{LL}^{(\tilde{\nu})}$, $V_{SS}^{(\tilde{\nu})}$, $V_{SL}^{(\tilde{\nu})}$, and $V_{LS}^{(\tilde{\nu})}$. Furthermore, for an even operator V only the LL- and SS-blocks are non-zero, and for an odd V only the SL- and LS-blocks.

With all this in mind, the trivial selection rules for the totally symmetric operator $\boldsymbol{\alpha p}$ which limit its matrix elements to those between *four-spinors* of the same irrep $\tilde{\nu}$,

$$\boldsymbol{\alpha p} = \bigoplus_{\tilde{\nu}} (\boldsymbol{\alpha p})^{(\tilde{\nu})}, \tag{2.125}$$

replace the non-trivial selection rules of $\boldsymbol{\sigma p}$. In addition, the matrix representation of the odd operator $\boldsymbol{\alpha p}$ is restricted to the off diagonal blocks $(\boldsymbol{\alpha p})_{LS}^{(\tilde{\nu})}$ and $(\boldsymbol{\alpha p})_{SL}^{(\tilde{\nu})}$; see Eq. (2.124).

Several cases of irrep coupling $(\tilde{\nu}') = \mathcal{P} \otimes (\tilde{\nu})$ by a pseudo-scalar $\mathcal{P}$ are discriminated in the code ParaGauss. According to the symmetry rules, the overall transformation of the potential contribution F_k may be separated into smaller tasks, similarly to a reduction of the eigenvalue problem to a set of smaller ones in the case of symmetry. Reduction of the eigenvalue problem allows one to treat symmetry-reduced matrices of different irreps independent of each other, cf. Eq. (2.123). However, the non-trivial symmetry relation of large and small components of a four-spinor sometimes makes it advantageous to treat *two* coupled symmetries in parallel.

One can distinguish three cases of pseudo-scalar coupling:

1. The case $\tilde{\nu} \equiv \tilde{\nu}'$. The spinor irreps for the large and small components of the four-spinor coincide. This implies that the dimensions of the bases for large and small components are equal. Hence, all matrices, e.g. the blocks of the even operator V, $V_{LL}^{(\tilde{\nu})}$ and $V_{SS}^{(\tilde{\nu})}$, and the blocks of the odd operator $\boldsymbol{\alpha p}$, $(\boldsymbol{\alpha p})_{LS}^{(\tilde{\nu})}$ and $(\boldsymbol{\alpha p})_{SL}^{(\tilde{\nu})}$, are all square matrices of the same dimensions. However, even if $\tilde{\nu} \equiv \tilde{\nu}'$, the irrep bases for the large and small components may still differ by a unitary transformation which brings the direct product basis of $\mathcal{P} \otimes (\tilde{\nu})$ into the canonical form of the irrep $\tilde{\nu}' \equiv \tilde{\nu}$ (see Section 3.3.4).

2. The case $\tilde{\nu} \neq \tilde{\nu}'$ and $\dim \tilde{\nu}' \neq 0$. The spinor irreps for the large and small components of the four-spinors of symmetry $\tilde{\nu}$ differ. The bases for the large and small components have different sizes which results in (square) matrix blocks $V_{LL}^{(\tilde{\nu})}$ and $V_{SS}^{(\tilde{\nu})}$ of different size and rectangular matrices $(\boldsymbol{\alpha p})_{LS}^{(\tilde{\nu})}$ and $(\boldsymbol{\alpha p})_{SL}^{(\tilde{\nu})}$.

3. The case $\tilde{\nu} \neq \tilde{\nu}'$ and $\dim \tilde{\nu}' = 0$. The spinor basis of symmetry $\tilde{\nu}'$ for the small components is empty. This case occurs in systems of high symmetry in cases of a relatively small orbital bases (with low maximum angular momentum). It is is a subcase of the previous case; however, it requires some special treatment because the matrices which formally involve small component functions vanish. With the matrix arithmetic and eigensolver routines properly extended to such "zero-sized" matrices, one is able to avoid a third branch of the code (see Appendix A).

As will be show in Section 3.3.4, careful construction of the small component *four-spinor* basis for irrep $\tilde{\nu}$ from the *two-spinor* basis of the coupled symmetry $\tilde{\nu}'$ may save the effort of maintaining the matrix representation of the four-diagonal operators (e.g. V) in the four-spinor basis. (Such an operator, which is diagonal in all four spinor components, is necessarily even and spin-free, i.e. it does not couple "up" and "down" components of neither large nor small components.) The procedure ensures that any four-diagonal totally symmetric operator, e.g. the matrix of the potential V, reduces to block form[4]

$$V = \bigoplus_{\tilde{\nu}} (V_{LL}^{(\tilde{\nu})} \oplus V_{SS}^{(\tilde{\nu})}) \tag{2.126}$$

where the SS and LL blocks of irreps $\tilde{\nu}$ and the corresponding irrep $\tilde{\nu}'$, coupled by a pseudo-scalar, are equal (Sec. 3.3.4):

$$V_{SS}^{(\tilde{\nu})} = V_{LL}^{(\tilde{\nu}')} \text{ and } V_{LL}^{(\tilde{\nu})} = V_{SS}^{(\tilde{\nu}')} \text{ for } (\tilde{\nu}') = \mathcal{P} \otimes (\tilde{\nu})\,. \tag{2.127}$$

This relation between the matrix elements does not hold for a general independent choice of large- and small-component bases. One can imagine a unitary transformation of the large-component basis of irrep $\tilde{\nu}$ (or just a random phase shift applied to each basis spinor) which will change the phases of $V_{LL}^{(\tilde{\nu})}$ but not those of $V_{SS}^{(\tilde{\nu}')}$, and, thus, the relation in Eq. (2.127) would not hold any more.

Because both matrices $V_{LL}^{(\tilde{\nu})}$ and $V_{SS}^{(\tilde{\nu})}$ (equal to $V_{SS}^{(\tilde{\nu}')}$ and $V_{LL}^{(\tilde{\nu}')}$ respectively) are needed in the DK transformation to obtain the two-component representation of V, it is advantageous to process irreps $\tilde{\nu}$ and $\tilde{\nu}'$ in parallel and re-use the quantities which otherwise would have to be stored or re-computed. Note that the potential matrix V discussed here is a matrix representation of one of the many auxiliary potential basis functions F_k, the potential of the partial fit density f_k to be DK-transformed. Therefore, any optimization gain is multiplied by the number of FF basis functions, hence may drastically reduce the total computing time.

[4] In Sections 3.2.4 and 3.3.3 it will be shown how to further reduce the matrix representation of *spin-free* operators.

Algorithm 2.2: Pseudo-code of the relativistic transformation of a potential contribution F_k.

```
!! INPUT: non-relativistic potentials F
!!   forward and backward transformations UF, UB
!!   kinetic factors, σp represented in momentum space by SP
!! OUTPUT: relativistic potential FR

!! LEVEL 1 : LOOP OVER IRREPS
do Irr1=1,N_IRREPS
  Irr2 = pseudoScalarCoupling(Irr1)   !! returns NO_IRREP in case Irr2 is empty
  if( Irr1 /= Irr2 )then
    call doTwoBlocks(Irr1,Irr2)       !! mark both as processed to skip afterwards
  else
    call doOneBlock(Irr1)
  endif
enddo
!! LEVEL 2: TWO-BLOCKS-AT-ONCE DKH(1)
SUBROUTINE doTwoBlocks(Irr1,Irr2)
!!  processes two blocks with irrep indices Irr1 and Irr2
!!  takes into account relation of LL/SS and Irr1/Irr2 blocks
!! STEP 1 : PREPARATIONS
!! composite indices XX and YY below will refer to LL and SS diagonal
!! blocks of matrices, indices XY and YX to the off-diagonal ones
!! it has to be assured that if X=L then Y=S and, reversed, if X=S then Y=L
do XX=LL,SS
  A(XX) = UB† (XX) * Ap(XX) * UF†(XX) !! diagonal blocks A_LL and A_SS to real space
enddo
do XY=LS,SL
  AR(XY) = Ap(XX) * Kp(XX) * SP(XY)   !! off-diagonal blocks (AR)_LS and (AR)_SL ...
  AR(XY) = UB†(XX) * AR(XY) * UF†(YY) !! ... transformed to real space
enddo
!! STEP 2 : FIT TRANSFORMATIONS
do k=1,N_FF                           !! for all fit functions
  F(LL) = readFromTape(Irr1,k)        !! use mapping LL ⇔ Irr1, SS ⇔ Irr2
  F(SS) = readFromTape(Irr2,k)        !! must handle NO_IRREP gracefully
  do XX=LL,SS
    FR(XX) = A(XX) * F(XX) * A† (XX)  !! compute A_LL F_LL A_LL + (AR)_LS F_SS (RA)_SL
           + AR(XY) * F(YY) * AR†(XY) !! ... and A_SS F_SS A_SS + (AR)_SL F_LL (RA)_LS
  enddo
  call writeToTape(Irr1,FR(LL))       !! output results
  call writeToTape(Irr2,FR(SS))       !! use mapping LL ⇔ Irr1, SS ⇔ Irr2
enddo
END SUBROUTINE
```

Common prerequisites for the consecutive transformations of all auxiliary potential basis functions F_k should be precomputed once and re-used later for all F_k. These prerequisites differ for the DKH transformation of first and second order. One clearly does not need to repeat the construction of the momentum space basis, i.e. the matrix U_f of the forward transformation to momentum space and the matrix $U_b = U_f^{-1}$ of the backward transformation to orbital space; they can be taken from the nuclear potential transformation procedure (Algorithm 2.1). Moreover, the bracketing matrices of the final expression for the transformed potential matrix $F_{rel,k}$ should be factorized and precomputed for re-use. As an example, we discuss the first-order DKH transformation of an auxiliary potential F_k at the DKee1 level [see Eq. (2.36)]:

$$\begin{aligned} F_{rel} &= U_b^\dagger (AF_{pw}A + ARF_{pw}RA)U_b \\ &= U_b^\dagger (AU_f^\dagger F_{orb} U_f A + ARU_f^\dagger F_{orb} U_f RA)U_b \\ &= A_{orb}^\dagger F_{orb} A_{orb} + (AR)_{orb} F_{orb} (RA)_{orb} \end{aligned} \tag{2.128}$$

Here, we have omitted the subscript k for easy readability. The indices *orb* and *pw* refer to the *orbital* and *plane-wave* (momentum) representations, respectively, of the operator F and the index *rel* identifies the *relativistically* transformed operator F. The following definitions were used for the "kinetic factors" in the orbital representation:

$$A_{orb} = U_f A U_b = U_b^{-1} A U_b \tag{2.129}$$

$$(RA)_{orb} = U_f RA U_b = U_b^{-1} RA U_b \tag{2.130}$$

$$(AR)_{orb} = (RA)_{orb}^\dagger \tag{2.131}$$

The last expression of Eqs. (2.128) is the usual definition of the first-order DK transformed operator F_{rel} where the operators are represented in orbital space instead of momentum space. In such a formulation, computing the relativistically corrected operator F_{rel} requires only four matrix multiplications. Note that one can avoid the transformation of F to the momentum space representation; its relativistic counterpart can be obtained directly from the orbital representation F_{orb}, see Eq. (2.128). Because of the more complex expressions involved in the DKee2 and DKee3 models, calculations in the momentum representation are unavoidable.

The four-component structure of the last expression in Eq. (2.128) is masqueraded by the designations used. If written explicitly, the essential difference between the first and second terms becomes apparent. Indeed the LL (upper left) block of the DK transformed

operator F_{rel} is made up of two contributions (subscript *orb* omitted)

$$\begin{aligned}(AFA)_{LL} &= A_{LL}F_{LL}A_{LL} \\ (ARFRA)_{LL} &= (AR)_{LS}F_{SS}(RA)_{SL}\,.\end{aligned} \tag{2.132}$$

To compute the first contribution, the representation of the operator F in the basis of the large components is required; for the second contribution, the representations of F in the small component basis and the "large-small" off-diagonal transition elements of the odd operator R or rather of AR are needed.

A careful reader will have noticed that we do not group odd operators R (or RA), which contain one instance of $\boldsymbol{\alpha p}$ ($\boldsymbol{\sigma p}$), into couples to render the resulting operators representable as a matrix — at variance with what we had done in the previous section for the DKnuc implementation. This difference goes back to the primitive matrix elements with which we start. For DKnuc, these were $\langle i\,|V|\,j\rangle$ and $\langle i\,|\boldsymbol{\sigma p}V\boldsymbol{\sigma p}|\,j\rangle$; for the DKee models and the contained fit transformation, the pertinent primitives are $\langle i\,|F_k|\,j\rangle$ and $\langle i\,|\boldsymbol{\alpha p}|\,j\rangle$, the latter being derived from $\langle i\,|\boldsymbol{\sigma p}|\,j\rangle$, of course. Thus, in the fit transformations, we *have* the possibility to build explicit matrix representations of operators, containing an odd number of the $\boldsymbol{\alpha p}$ ($\boldsymbol{\sigma p}$) instances.

The evaluation of the expression for the second-order DKH Hamiltonian — in fact, several flavors thereof (DKee2 and DKee3, Section 2.1.4) — was implemented in momentum space. Reverting back to orbital space works only for the model DKee1, but not for DKee2 and DKee3 where a large part of the calculation is performed via the momentum representation. In the following, we will discuss our computation strategy for the models DKee2 and DKee3. The second-order *ee* terms in Eq. (2.62) contributing to the DKee2 model Hamiltonian for a particular $W_{ee} = W_{ee}[F_k]$ are given by the lengthy expression

$$\mathcal{E}_2 = -W_{nuc}E_pW_{ee} - W_{ee}E_pW_{nuc} - W_{nuc}W_{ee}E_p - W_{ee}W_{nuc}E_p\,. \tag{2.133}$$

These terms may be evaluated in two steps:

$$X := W_{nuc}W_{ee}E_p + W_{nuc}E_pW_{ee} \tag{2.134}$$

$$\mathcal{E}_2 := -(X + X^\dagger)\,. \tag{2.135}$$

The first step involves expensive matrix multiplications, the second step is cheap. The second-order terms in the DKee3 model, Eq. (2.91), differ by an alternative definition of

X. Using a temporary quantity Y, one can write:

$$Y := W_{nuc} W_{ee} \tag{2.136}$$

$$X := \frac{1}{2}(Y + Y^\dagger) E_p + W_{nuc} E_p W_{ee} \,. \tag{2.137}$$

Again, as done in the implementation of the DKnuc variant, expressions which include products of two W operators are evaluated via RW (WR) intermediates:

$$W_{nuc} W_{ee} = (WR)_{nuc} R^{-2} (RW)_{ee} \tag{2.138}$$

with the help of the identity $R^{-2} = K_p^{-2} p^{-2}$ for diagonal matrices. The definition is similar to that in Section 2.2.2:

$$(WR)_{nuc} = AR\tilde{V}RA - (A\tilde{V}A)R^2 \tag{2.139}$$

$$(RW)_{ee} \;\; = R^2(A\tilde{F}A) - AR\tilde{F}RA \,. \tag{2.140}$$

The computation of the matrices $AR\tilde{F}RA$ and $AR\tilde{V}RA$ deserves a comment. In a true momentum space basis, the perturbation by the "scaling" operation expressed by the tilde [see Eq. (2.29)], is interchangeable with operators depending only on $\boldsymbol{p}$ or p^2.

$$\widetilde{ARVRA} \equiv AR\tilde{V}RA \tag{2.141}$$

However, this identity holds only *approximately* for the representation matrix $R(\boldsymbol{p}) = K_p \boldsymbol{\alpha p}$ in the *finite* basis of the eigenvectors of the operator p^2:

$$\widetilde{ARVRA} \approx AR\tilde{V}RA \tag{2.142}$$

Of two approximately equal matrices in the last equation, the former was chosen in the implementation; in other words, first the quantity $ARVRA$ is evaluated and the scaled, following Eq. (2.29).

The pseudo-code presented in Algorithm 2.2 shows the Fortran implementation of the DKH transformation of potential contributions F_k at the DKee1 level as implemented in the program ParaGauss. Much of the information computed during the DKnuc step where the nuclear potential is transformed, can be re-used here, e.g. the forward and backward transformation matrices and the kinetic factors. The first part of the code examines the given conditions and dispatches the execution to the appropriate branch (Level 1, Algorithm 2.2). Each particular branch is optimized for the specific case. Only one case is shown in the pseudo-code of Algorithm 2.2, namely the case of a symmetry where

the irreps coupled by the pseudo-scalar are distinct and, as a result, a fit transformation where two blocks are treated at once (DKH(1), Level 2). First, the orbital space operator representations of A_{LL}, A_{SS}, $(AR)_{LS}$ and $(AR)_{SL}$ are pre-evaluated (Step 1, Algorithm 2.2). The irrep coupling, discussed above, is taken into account. Then, for each fit function potential F_k, the matrix representations for irreps `Irr1` and `Irr2` are transformed to the relativistic picture according to Eqs. (2.132) and (2.128), (Step 2, Algorithm 2.2).

2.3 Applications

2.3.1 Computational Details

The various relativistic methods for a self-consistent two-component treatment of the SO interaction discussed in Section 2.1.4 were implemented in the parallel density functional program ParaGauss [21, 20], based on the LCGTO-FF-DF method (linear combination of Gaussian-type orbitals fitting-functions density functional) [60].

As mentioned before, the functional form of the exchange-correlation energy E_{xc} is in general different in non-relativistic and relativistic methods. Relativistic corrections to the xc functional often have very little influence on many molecular properties [30, 36, 61, 63]. To allow for easy comparison with earlier results on various diatomic molecules that accounted only for the self-consistent effect of the spin-orbit interaction due to the nuclear potential [26], we used standard non-relativistic xc approximations, namely the local density approximation (LDA) as suggested by Vosko, Wilk, and Nusair (VWN) [134] during the KS SCF iteration and, afterwards, evaluated the energy functional of the generalized gradient approximation (GGA) for the self-consistent LDA density. As GGA, we used the combination of Becke's exchange and Perdew's correlation functionals (BP) [135, 136]. Such a post-SCF approximation is very economical and usually sufficiently accurate.

Next, we describe the basis sets used for representing the Kohn–Sham orbitals and the relativistic transformations. In general, we use larger bases for the relativistic transformations of the integrals (uncontracted, higher angular momentum) than for describing the KS orbitals. In the relativistic transformations of the various DKee variants, higher angular momentum functions provide an improved representation of the resolution of identity, in particular for representing vector operators like $\boldsymbol{p}$ and $\boldsymbol{\sigma p}$ which locally couple angular momentum eigenfunctions according to the selection rule $L \rightarrow L \pm 1$. (For technical reasons it was not possible to eliminate completely these additional angular momentum basis functions during the SCF procedure, but we minimize the effect of these functions by contracting them during the SCF procedure as much as possible.)

For NO_2 we used a $(13s,8p,7d)$ basis set for each atom, contracted in generalized fashion

to [8*s*,7*p*,3*d*] [137]; the *s* and *p* contractions were taken in generalized form, employing atomic eigenvectors of VWN calculations. The *d*-type exponents were set equal to the (largest) exponents of the corresponding *p* set; in the SCF calculations, only the 2nd, 3rd, and 4th most diffuse *d* exponents were used in uncontracted fashion.

For the diatomics examined here, we used a series of four sequentially improved basis sets for the heavy elements Pb, Bi, and Tl, to judge accuracy and completeness of the basis sets, in particular with respect to the relativistic transformation. We started with smaller basis sets of "standard" quality (referred as *std*) for Pb, Bi, and Tl [138] of the size (20*s*,18*p*,12*d*,6*f*,6*g*). Available basis sets [138] of size (19*s*,16*p*,10*d*,5*f*) were augmented by one diffuse *s* exponent, one diffuse and one tight *p* exponent, two diffuse *d* exponents, and one diffuse *f* exponent. All added exponents were derived from the highest or lowest exponents of the original set in an even-tempered fashion. The set of *g*-type exponents was set equal to the set of *f*-type exponents, in analogy to the procedure described above for NO_2. The larger basis sets of the heavy atoms were well-tempered basis sets (*wtbs*, [139]): (28*s*,24*p*,18*d*,12*f*,12*g*) for Pb, Bi, and Tl. We augmented these *wtbs* basis sets in several ways. One extension (*wtbs+3c*) comprised the addition of three core exponents in each *L* shell: $\alpha_{-1/2} = \alpha_0^2/\alpha_{1/2}$, $\alpha_{1/2} = (\alpha_0\alpha_1)^{1/2}$, and $\alpha_{3/2} = (\alpha_1\alpha_2)^{1/2}$, where α_0, α_1, and α_2 are the three largest exponents of a shell. Another, even larger basis set (*wtbs+3c3v*) was constructed by extending the latter basis set in an analogous fashion by three valence exponents in each *L* shell, designated as $\alpha_{n-3/2}$, $\alpha_{n-1/2}$, and $\alpha_{n+1/2}$. In each case, the set of *g*-type exponents was identical to the set of *f*-type exponents. None of these heavy-element basis sets was contracted.

In the calculations on diatomics, we used the contracted basis sets (8*s*,4*p*,3*d*) → [4*s*,3*p*,2*d*] for H and (14*s*,9*p*,4*d*) → [5*s*,4*p*,2*d*] for O [140]. The basis set used for calculations of the orbital spectrum of the Hg atom was (21*s*,17*p*,12*d*,7*f*,4*g*) [141].

In the LCGTO-FF-DF method, the classical Coulomb contribution to the electron-electron interaction is evaluated with the help of a basis set representation of the electronic density [60], see Section 2.1.5, Eq. (2.74). The corresponding "auxiliary" basis sets were constructed from the corresponding orbital basis in a standard fashion [60] and augmented by even-tempered sets (factor 2.5) of five *p* exponents starting at 0.1 au and five *d* exponents starting at 0.2 au.

Grids for the numerical integration of the *xc* contributions were set up as combination of radial and angular grids [142]. The radial grids comprised 112 shells for Hg, 166 shells for Bi, 185 shells for Pb, 193 shells for Tl, 48 shells for O, and 44 shells for H. In each shell, a Lebedev angular grid [143] accurate up to angular momentum values $L = 23$ was used in the molecular calculations.

The interatomic distance of diatomics was optimized in a point-wise fashion. Typically,

$N = 5$ or 6 calculated total energy values were fitted with a polynomial of degree $N - 1$; the energy minimum was obtained from this polynomial representation. The harmonic vibrational frequency was derived by numerical differentiation using two additional total energy values at distances located symmetrically with respect to the equilibrium.

2.3.2 Spin-Orbit Splittings in the Hg Atom

As a first illustration of the relativistic corrections due to *ee* interactions, we considered the fine structure of the mercury atom, i.e. the SO splitting of the atomic shells with non-zero angular momentum. In Table 2.1 we present the spin-orbit splittings of the Hg atom, calculated with three models. DKnuc is the DK level introduced previously [26], with the DK transformation in the nuclear field only. The models DKee1 and DKee2, as defined in Sec. 2.1.4 by Eqs. (2.49, 2.50), take *ee* contributions into account; in the KS Hamiltonian, the untransformed Hartree potential V_H of DKnuc is replaced by its relativistic counterpart. As a reference, we use results of a fully relativistic four-component DKS calculation [144]. The relative errors of the models DKnuc, DKee1, and DKee2 with respect to the DKS results are designated as Δ_{nuc} and Δ_1, and Δ_2, respectively. Effects of the DKee3 approximation, Eq. (2.51), will be discussed later.

The errors Δ_{nuc} of the DKnuc results clearly demonstrate the limitation of this model. First of all, all SO splittings are overestimated, and the relative error increases with the value of the angular momentum. Starting from 1.6% for the $2p$ splitting, the error gradually increases with the principal quantum number to 2.2% for the $5p$ shell. For the d shells, the errors, ranging from 14% to 18% again increase with the principal quantum number. Finally, in the $4f$ shell, Δ_{nuc} acquires the ultimate value of 51%. The errors Δ_1 of the DKee1 results are much more uniform over the range of angular momenta and principal quantum number values, and are substantially smaller than the Δ_{nuc} values (Table 2.1). For instance, the error Δ_{nuc} of the $4f$ shell splitting is drastically reduced from 51% to –3.2%. The splittings of the d shells are reproduced with errors of –3.0 to –3.8% at the DKee1 level. Thus, most DKee1 values are considerably more accurate than the corresponding DKnuc values; the absolute accuracy of the p shell splitting is only slightly improved. The negative sign of the error Δ_1 in all cases is worth noting. Thus, in general, the first-order method DKee1 slightly underestimates the SO splittings, at variance with the clear overestimation at the DKnuc level. In addition, the accuracy of the $1s_{1/2}$ orbital energy increases by a factor of two, from –0.4% at the DKnuc level to –0.2% at DKee1 level. The errors Δ_2 of the DKee2 method are similar to those of the DKee1 variant. For the absolute energy of the $1s_{1/2}$ level and the SO splittings of the p levels, the errors Δ_2 are slightly smaller than Δ_1; on the other hand, errors Δ_2 of the d splittings are slightly larger.

Table 2.1: Energy of $1s_{1/2}$ orbital and spin-orbit splittings ΔSO of the p, d, and f shells of the Hg atom (in au). DKS — numerical DKS results[a], DKnuc — model without *ee*-corrections, DKee1 and DKee2 — models including first- and second-order *ee*-corrections due to V_H, respectively. Δ_{nuc}, Δ_1, and Δ_2 designate deviations of the models DKnuc, DKee1, and DKee2, respectively, from the corresponding full DKS results. For the number of digits displayed, results of the DKee3 approach are identical to DKee2 (compare Table 2.2).

	DKS	DKnuc	Δ_{nuc} [%]	DKee1	Δ_1 [%]	DKee2	Δ_2 [%]
$\varepsilon(1s_{1/2})$	–3047.5	–3033.8	–0.4	–3041.7	–0.2	–3043.7	–0.1
ΔSO							
2p	71.493	72.649	1.6	70.615	–1.2	70.712	–1.1
3p	15.831	16.110	1.8	15.630	–1.3	15.649	–1.1
4p	3.832	3.905	1.9	3.783	–1.3	3.788	–1.1
5p	0.679	0.694	2.2	0.671	–1.2	0.672	–1.1
3d	3.395	3.862	13.8	3.291	–3.1	3.281	–3.4
4d	0.714	0.820	14.8	0.687	–3.8	0.685	–4.1
5d	0.067	0.079	17.9	0.065	–3.0	0.065	–3.0
4f	0.154	0.233	51.3	0.149	–3.2	0.149	–3.2

a) Ref. [144].

Table 2.2: Contribution to the energy of the $1s_{1/2}$ level and the spin-orbit splittings of Hg at successive approximate levels normalized to the corresponding DKnuc value (in %). Column ΔDKee$n$, $n = 1, 2, 3$ shows the fractional corrections (in %) to the preceeding approximation: ΔDKee$n$ = 100 [DKee$n$ – DKee$(n-1)$]/DKnuc (DKee0 ≡ DKnuc).

	ΔDKee1	ΔDKee2	ΔDKee3
$\varepsilon(1s_{1/2})$	0.3	0.06	$2{\cdot}10^{-3}$
ΔSO			
2p	–2.8	0.14	$5{\cdot}10^{-3}$
3p	–3.0	0.12	$6{\cdot}10^{-3}$
4p	–3.2	0.12	$6{\cdot}10^{-3}$
5p	–3.4	0.12	$6{\cdot}10^{-3}$
3d	–16.8	–0.30	$3{\cdot}10^{-3}$
4d	–18.7	–0.40	$3{\cdot}10^{-3}$
5d	–20.8	–0.44	$4{\cdot}10^{-3}$
4f	–55.2	–0.01	$-1{\cdot}10^{-3}$

In Table 2.2 we collected data illustrating the relative importance of different *ee* contributions to the DK Hamiltonian. The columns ΔDKee1, ΔDKee2, and ΔDKee3 denote successive contributions due to the relativistic treatment of the Hartree term for the series of corresponding approximations, Eqs. (2.36). The largest effect is due to ΔDKee1: this term eliminates the main source of the DKnuc inaccuracy as just discussed. This term contributes ∼3% to the splittings of p shells, 17–21% to splittings of d shells, and 55% to the $4f$ shell splitting. Obviously, the second-order contribution ΔDKee2 is much less important than ΔDKee1: contributions to the splittings are 0.12–0.14% for p shells, 0.30–0.44% for d shells, and 0.01% for the $4f$ shell. The latter value likely should not be considered representative. The last column of Table 2.2, denoted as ΔDKee3, shows the difference of DKee2 and DKee3, not a further correction of DKee2. The values displayed in the last column are the relative difference (in percent) of two similar *second-order* models (see Section 2.1.4): the one derived as a linearized expansion of $\mathcal{E}_2^{(2)}[V_{nuc}+V_H]$ in V_H and the other derived by adding the Hartree term V_H, resulting from a second-order DK transformation in the nuclear field, to $h^{(2)}_{DKnuc,2}$. The quantity ΔDKee3 is several orders of magnitude smaller than the second-order correction ΔDKee2 itself; relative contributions range from -10^{-3} to $6\cdot 10^{-3}$% of the quantity of interest. Thus, at least at the present level of accuracy, there is apparently no difference between the two flavors of second-order corrections terms in $h^{(2)}_{DKee2,2}$ and $h^{(2)}_{DKee3,2}$ as described in Section 2.1.4. From the data presented in Table 2.2 we conclude that the most important *relativistic SO* contributions to the DK Hamiltonian of the Hartree term derives from the first-order potential term $\Delta\mathcal{E}_1^{(2)} := \mathcal{E}_1^{(2)}[V_H] - V_H$. Inclusion of the second-order potential contributions due to the Hartree term introduces changes that are smaller at least by an order of magnitude.

It is easy to rationalize the changes induced by a particular SO approximation and the relative importance of different contributions. The relativistic transformation in the nuclear field only (DKnuc) does not account for the screening effect of the *ee* repulsion on the SO interaction. Effectively, the SO field (that part of the whole field which does not commute with the spin) is overestimated if the screening due to *ee* interaction is completely ignored; this rationalizes the sign of Δ_{nuc} (Table 2.1). The overestimation is more pronounced for outer orbitals, for which the *ee* screening of the nuclear potential plays a more significant role, namely for orbitals with higher angular momentum or principal quantum number. The Hartree contribution to the SO field apparently eliminates the main error of the DKnuc level. In regions far from the nuclei, the nuclear attraction is partially compensated by the Hartree repulsion; the same obviously holds for the SO coupling field at the DKee1 level. Therefore, the errors Δ_1 of the model DKee1 (Table 2.1) are reduced and essentially independent of the spatial distribution of the orbital. The overcompensation by the Hartree term, reflected in the slightly underestimated splittings,

Table 2.3: EPR g-tensor shifts ($\times 10^{-5}$) of NO_2. Results of LDA (VWN) and GGA (BP) calculations in comparison with experiment.

	VWN		BP				
	DKnuc	DKee1	DKnuc	DKee1	ZORA[a]	UKS[b]	exp.[c]
xx	588	457	609	472	500	340	390
yy	–2051	–1573	–1977	–1514	–1600	–1123	–1130
zz	–91	–73	–90	–72	–60	–69	–30

a) ZORA SO, Refs. [150, 152], b) unrestricted Kohn–Sham calculation, perturbative treatment of an SO effective core potential, Ref. [47], c) Ref. [153]

likely is due to the fact that the (attractive) exchange potential has not been taken into account in the relativistic transformation.

2.3.3 Effects of Relativistic Contributions to *ee*-Interaction on the g-Tensor of NO_2

In this section we demonstrate effects of the newly derived relativistic models on a purely spin-orbit induced property, namely the g-tensor shifts of radicals. We will use the NO_2 radical as an example.

EPR spectroscopy is widely exploited to study systems with an unpaired electron, e.g. organic radicals, coordination compounds, and paramagnetic sites in solids. The interaction of the electron spin with the orbital movement (angular momentum) affects the resonance frequency of the spin-flip transition and thus results in a shift of the g-tensor from the corresponding isotropic value of a free electron. To properly reproduce the EPR parameters in a numerical simulation, one needs a model that describes SO interaction in an adequate fashion. We mention semiempirical models [145, 146] and HF-based *ab initio* models [147, 148, 149] as well as density functional methods [150, 151, 47, 152, 55]. In g-tensor calculations, the SO interaction often is introduced as a second perturbation, — along with the magnetic field. Our model, similarly to ZORA [150], provides a self-consistent treatment of SO interaction in a DF framework; therefore, the g-tensor is a first-order property in the magnetic field, fully determined by the ground-state orbital wavefunctions [55].

In Table 2.3, we collected various computational results for g-tensor eigenvalues of NO_2, obtained with both LDA (VWN) and GGA (BP) xc functionals. Only the difference with respect to the g-tensor value of a free electron is shown. This difference is of inherently relativistic nature and vanishes in the formal limit of infinite speed of light,

$c \rightarrow \infty$. These numbers are relatively sensitive to the approximations made for the SO treatment as demonstrated by a comparison of the DKnuc and DKee1 values. No changes in the significant digits were calculated when the alternative models DKee2 or DKee3 were applied.

At the BP/DKnuc level, the eigenvalue shifts (Δg_{xx}, Δg_{yy}, Δg_{zz}) = (609, –1977, –90), scaled by 10^5 for readability, are noticeably larger (by absolute value) than their experimental counterparts, (390, –1130, –30) (Table 2.3). At the DKee1 level, the absolute values of the shifts are reduced by about 30%, to (472, –1514, –72), bringing them significantly closer to experiment. Thus, the trend parallels our finding for the orbital SO splittings of the Hg atom (Section 2.3.2). LDA and GGA values differ by no more than 4% and therefore are not responsible for the remaining difference with experiment. Taking spin-polarization into account and extending the spin-orbit treatment to the *xc* potential probably improves the agreement with experiment.

The present DKee1 values are rather similar to the g-tensor shifts computed with the ZORA procedure, (500, –1600, –60) [150, 152] (Table 2.3). This holds in spite of the fact that the two models, ZORA and the improved DK method used in the present work, differ substantially not only in the underlying formalism, but also in the implementation. Our DK approach relies on an analytic evaluation of the Coulomb terms in a Gaussian-type basis set whereas the ZORA implementation uses Slater-type orbitals and a numerical integration which allows a uniform treatment of Coulomb and *xc* potential terms. On the other hand, our results differ notably from those of another DF based procedure [47], (340, –1123, –69) which agree better with experiment (Table 2.3). Malkina et al. include the SO interaction by perturbation theory after SCF convergence is achieved at the non-relativistic unrestricted DF level, exploiting gauge corrected IGLO orbitals for post-SCF g-tensor calculations; they explicitly deal with two-electron SO terms, whereas we aimed at including *ee* interaction consistently in our relativistic KS model.

For an extensive study of paramagnetic species using the implementation of SO interaction presented in this work, we refer to the recent work of Neyman et al. [55] where limitations and further improvements of the DK approach to g-tensor shifts are discussed in detail.

2.3.4 Spin-Orbit Effects on Properties of Diatomic Molecules

Finally, in our examination of spin-orbit effects related to Coulomb screening of the nuclear field, we present properties of the diatomic molecules TlH, PbO, Pb_2, Bi_2. All of these molecules contain elements of the sixth period which, due to their relatively high atomic numbers, are expected to exhibit relativistic effects including those of SO interaction. How

important SO effects are for the *structural* properties of molecules depends, among other things, on the atomic orbitals which participate in the bonding. The heavy elements selected here all bind essentially via their outer p orbitals, so that one may expect some changes between different approximations of the relativistic model. Our choice of diatomics was guided by the intention to compare directly with experimental and theoretical results of other investigations [154, 155, 26, 156].

Previous versions of the code ParaGauss allowed a treatment of SO interaction via the DK transformation of second order only in the nuclear potential (DKnuc) [26]. Now, we also include the classical Coulomb part of the *ee* interaction in that transformation (DKee1, DKee2, and DKee3), at least in an approximate way. For the diatomics just mentioned, we calculated the equilibrium geometry, the binding energy and the harmonic vibrational frequency at the LDA (VWN) and post-SCF GGA (BP) levels (see Tables 2.4, 2.5, and 2.6). For reference, we also provide results obtained with the SR variant of the DKnuc approach.

The results compiled in these tables show how the selected molecular properties depend on the quality of the orbital basis. We compare results of the methods DKnuc, DKee1, and DKee2 for the basis sets *std, wtbs, wtbs+3c, wtbs+3c3v* (see *Computational details*, Section 2.3.1). Data obtained with the DKee3 approach yield no differences to DKee2 results at the accuracy displayed. Thus these results are not shown in Tables 2.4–2.6. The basis set dependence is to a significant degree connected with the strategy to evaluate complex operators like $\boldsymbol{\sigma p} V \boldsymbol{\sigma p}$ via a matrix representation of the operators $\boldsymbol{p}$ (and $\boldsymbol{\sigma p}$). This procedure is convenient, but certainly not optimal; direct analytical evaluation of the corresponding integrals is preferable, but for the present work such more efficient treatment is not required. The DKnuc results for bond lengths and vibrational frequencies hardly change with the various basis sets; even the basis set dependence of the binding energies is small for this formalism. Scalar relativistic results are even less dependent on the basis set, as shown by a comparison of the results for the smallest (*std*) and a more flexible (*wtbs*) basis sets (see Tables 2.4, 2.5, and 2.6).

The results of the methods DKee1 and DKee2 depend noticeably more on the basis set. Bond lengths and harmonic vibrational frequencies are in general less sensitive than the binding energy. In fact, for these observables, relatively small changes occur when one switches from the smallest basis set *std* to the basis set *wtbs*; further extension of the latter basis set to *wtbs+3c3v* causes only minor changes (Tables 2.4 and 2.5). The situation is notably different for the binding energy (Table 2.6). Inspection of Table 2.6 supports the conclusion that the most flexible basis set *wtbs+3c3v* yields results that, at the level of accuracy reported, are close to convergence for all observables studied. Now, we discuss the various properties in detail.

Table 2.4: Bond lengths r_e (in Å) of the diatomic molecules determined with various SO approximations DKnuc, DKee1, and DKee2 (Sec. 2.1.4) using molecular orbital basis sets *std*, *wtbs*, *wtbs+3c*, and *wtbs+3c3v* of increasing accuracy (see Sec. 2.3.1). Also given are results of SR calculations, other calculations, and experiment.

		Bi_2		Pb_2		PbO		TlH	
		LDA	GGA	LDA	GGA	LDA	GGA	LDA	GGA
DKee2	*wtbs+3c3v*	2.639	2.687	2.892	2.971	1.911	1.939	1.867	1.899
	wtbs+3c	2.650	2.697	2.901	2.978	1.915	1.942	1.868	1.899
	wtbs	2.646	2.693	2.894	2.970	1.915	1.942	1.868	1.899
	std	2.610	2.654	2.835	2.904	1.913	1.941	1.856	1.886
DKee1	*wtbs+3c3v*	2.640	2.688	2.895	2.974	1.911	1.939	1.867	1.899
	wtbs+3c	2.651	2.698	2.903	2.980	1.915	1.943	1.869	1.900
	wtbs	2.649	2.697	2.900	2.977	1.915	1.943	1.869	1.900
	std	2.619	2.663	2.848	2.919	1.913	1.941	1.856	1.886
DKnuc	*wtbs+3c3v*	2.644	2.693	2.900	2.981	1.912	1.939	1.866	1.897
	wtbs+3c	2.655	2.703	2.909	2.988	1.915	1.943	1.866	1.897
	wtbs	2.655	2.703	2.909	2.988	1.915	1.943	1.866	1.897
	std	2.651	2.699	2.900	2.978	1.916	1.944	1.854	1.884
SR	*wtbs*	2.621	2.660	2.865	2.924	1.915	1.942	1.895	1.923
	std	2.617	2.658	2.858	2.917	1.916	1.942	1.882	1.910
ZORA[a]		2.637	2.685			1.910	1.937	1.868	1.900
BDF[b]			2.689		2.982		1.939		1.901
exp[c]			2.661		2.932		1.922		1.870

a) Ref. [154], b) Refs. [155, 156], c) Ref. [157]

Comparison of the Tables 2.4, 2.5, and 2.6 reveals that LDA and GGA results exhibit very similar changes if one compares results for any two of these four basis sets. In the following, we will discuss the quality of the various relativistic approximations using results for the most flexible basis set available, i.e. for basis set *wtbs+3c3v*.

The equilibrium bond lengths of the diatomics are hardly affected when the classical Coulomb part of the *ee* interaction is accounted for in the SO treatment; cf. DKnuc and DKee1 results in Table 2.4. The GGA distance at the DKee1 level is 0.005 Å shorter for Bi_2 than the DKnuc result; for Pb_2 the contraction is 0.007 Å. For PbO and TlH, the bond length hardly changes at all in this comparison. The results of the DKee1 and DKee2 models are to a large extent equivalent; the largest difference, a further contraction by 0.003 Å, occurs for Pb_2. DKee3 results (not shown in Table 2.4) agree with those obtained at the DKee2 level in all digits displayed.

The various SO models change the interatomic distances approximately by an order of

Table 2.5: Harmonic vibrational frequencies ω_e of various diatomic molecules (in cm^{-1}). Lay-out as in Table 2.4.

		Bi_2		Pb_2		PbO		TlH	
		LDA	GGA	LDA	GGA	LDA	GGA	LDA	GGA
DKee2	*wtbs+3c3v*	179	169	119	109	745	710	1388	1337
	wtbs+3c	182	172	119	108	740	705	1385	1336
	wtbs	182	173	118	110	740	703	1388	1335
	std	198	185	133	123	736	700	1411	1349
DKee1	*wtbs+3c3v*	179	169	119	109	745	711	1389	1339
	wtbs+3c	182	172	120	108	740	703	1385	1329
	wtbs	181	173	119	111	740	705	1392	1336
	std	194	182	131	120	735	701	1410	1348
DKnuc	*wtbs+3c3v*	179	167	119	107	744	710	1393	1331
	wtbs+3c	182	170	118	108	739	703	1399	1332
	wtbs	182	171	118	108	740	702	1392	1332
	std	184	171	120	109	733	696	1412	1350
SR	*wtbs*	202	193	138	130	751	715	1383	1326
	std	203	194	140	131	745	709	1396	1337
ZORA[a]		186	174			755	720	1390	1330
BDF[b]			171		107		716		1324
exp[c]			173		110		721		1391

a) Ref. [154], b) Refs. [155, 156], c) Ref. [157]

magnitude less than inclusion of the SO interaction itself. From the SR reference data of this work and a previous study [26], it follows that inclusion of SO interaction may change the distances by several hundreds of an angstrom; the largest effects occur again for Pb_2, namely a bond elongation by 0.04 or 0.06 Å for LDA and GGA, respectively. As often, LDA distances turn out somewhat shorter than GGA distance, calculated with the same method; differences (0.05 Å for Bi_2, 0.08 Å for Pb_2, 0.03 Å for PbO and TlH) are very similar for the various methods of approximation DKnuc, DKee1, and DKee2. In fact, in all cases studied, the experimental bond length [157] is bracketed by the LDA and GGA results (Table 2.4). It is gratifying to note that the present calculated results agree very well with those of previous accurate relativistic DF methods, namely those of ZORA SO [154] and a four-component treatment by the BDF program [155, 156].

Next, we discuss the harmonic vibrational frequencies of the set of test molecules (Table 2.5). Again, a flexible basis set is required for SO calculations to avoid artifacts due to the relativistic transformation procedure; frequencies change by up to 20 cm^{-1}; cf. *std* and *wtbs+3c3v* values. The absolute values of the SO effect, derived from a comparison of

Table 2.6: Binding energies D_e of various diatomic molecules (in eV). Lay-out as in Table 2.4.

		Bi_2		Pb_2		PbO		TlH	
		LDA	GGA	LDA	GGA	LDA	GGA	LDA	GGA
DKee2	*wtbs+3c3v*	2.92	2.19	1.60	1.24	5.41	4.65	2.40	2.17
	wtbs+3c	2.89	2.17	1.60	1.24	5.36	4.60	2.40	2.16
	wtbs	3.00	2.28	1.71	1.35	5.27	4.61	2.40	2.17
	std	4.37	3.73	2.65	2.27	5.43	4.67	2.56	2.37
DKee1	*wtbs+3c3v*	2.88	2.15	1.57	1.21	5.41	4.65	2.40	2.17
	wtbs+3c	2.85	2.13	1.57	1.21	5.36	4.60	2.39	2.16
	wtbs	2.90	2.18	1.61	1.26	5.37	4.61	2.40	2.17
	std	4.07	3.44	2.41	2.03	5.41	4.65	2.56	2.37
DKnuc	*wtbs+3c3v*	2.80	2.08	1.49	1.13	5.34	4.58	2.38	2.15
	wtbs+3c	2.75	2.04	1.48	1.13	5.29	4.53	2.38	2.15
	wtbs	2.76	2.04	1.48	1.13	5.29	4.53	2.38	2.15
	std	2.96	2.35	1.51	1.15	5.27	4.51	2.54	2.35
SR	*wtbs*	3.75	2.70	2.93	2.39	6.59	5.46	2.96	2.73
	std	3.77	2.72	2.96	2.41	6.55	5.43	2.98	2.76
ZORA[a]		2.83	1.98			5.25	4.15	2.39	2.10
BDF[b]			2.45		1.14		4.39		2.17
exp[c]			2.03		0.86		3.87		2.06

a) Ref. [154], b) Refs. [155, 156], c) Ref. [157]

vibrational frequencies determined at the SR and DKnuc levels with the *wtbs* basis set, range from a decrease of about 20 cm^{-1} for Bi_2 and Pb_2, via a moderate decrease by slightly more than 10 cm^{-1} for PbO, to an increase by less than 10 cm^{-1} for TlH. The effects of the improved SO models DKee1 and DKee2 follow a the different pattern, but are very small; compared to the DKnuc results, the DKee frequencies increase by about 2 cm^{-1} for Bi_2 and Pb_2, 1 cm^{-1} or less for PbO and 5–8 cm^{-1} for TlH, depending on the *xc* functional and the particular DKee model. The various DKee models are essentially equivalent for determining the vibrational frequencies of the selected diatomics. As often, LDA frequencies are larger than GGA values, by 5–10%, which is of the order of 10–60 cm^{-1} for the current set of molecules; the increments between different SO models are quite similar for LDA and GGA. Except for TlH, the LDA and GGA values bracket the experimental frequencies; both LDA and GGA underestimate the vibrational frequency for TlH. The frequencies agree well with those computed by ZORA and BDF calculations [154, 155, 156]; the largest deviation is below 15 cm^{-1} for the highest frequency (TlH).

Finally, we turn to a discussion of the binding energies, Table 2.6. This quantity is most sensitive to SO effects, i.e. even at the DKnuc level as already shown by a comparison of *std*

and *wtbs* results. This sensitivity increases notably when one goes to DKee1 and DKee2 results which clearly exhibit artifacts with the *std* basis set; the discrepancy is particularly large for Bi_2 and Pb_2, small for TlH, and essentially absent for PbO. In all cases, more flexible basis sets yield smaller binding energies. This deficiency may be interpreted as a basis set superposition effect of the relativistic transformation because the binding energies converge to smaller values with the more flexible basis sets *wtbs*, *wtbs+3c*, and *wtbs+3c3v*. In fact, the binding energies convergence to some extent with growing size of the basis set.

Compared to the SR results, SO binding energies at the DKnuc level (with the basis set *wtbs*) are lower by 0.6–1.5 eV. The SO effect on the binding energy is largest for Pb_2 where it approaches 1.3 eV at the GGA level or 1.5 eV at the LDA level. For Bi_2, this effect is 1.0 and 0.7 eV and for PbO 1.3 and 0.9 eV, with GGA or LDA, respectively; for TlH, the SO effect is about 0.6 eV irrespective of the *xc* functional. The absolute values of the binding energies — and in most cases, the SO induced changes — are larger for LDA than for GGA, in accordance with the known tendency of LDA to overestimate binding energies. The changes induced by the DKee1 model relative to the DKnuc energies are in general smaller and, as noted previously for the vibrational frequencies, they are largely independent of the *xc* functional. Furthermore, these changes have a sign opposite to that of the previously discussed SO effect, thus canceling partly the effect of DKnuc on the SR reference. For Bi_2, Pb_2, and PbO, differences between DKee1 and DKnuc results are about 0.08 eV, and for TlH about 0.02 eV. For Bi_2 and Pb_2, the binding energies decrease even further at the DKee2 level, by 0.04 and 0.03 eV, respectively; for PbO and TlH no further change occurs. The slight increase of DKee binding energies, relative to the values calculated at the DKnuc level, may again be interpreted as partial compensation ("screening") of the decrease induced by the SO terms when going from the SR treatment to the DKnuc level. The GGA results overestimate the experimental binding energies, even at the DKnuc level, by about 0.05 eV for Bi_2, 0.3 eV for Pb_2, 0.7 eV for PbO, and 0.1 eV for TlH. The DKee levels increase the binding energies slightly and thus enlarge the discrepancy with experiment even more. The DKee2 results (obtained with the basis set *wtbs+3c3v* in the GGA *xc* approximation) agree very well with those of previous accurate relativistic DF calculations, namely those obtained with ZORA [154] and a four-component treatment [155, 156].

Thus, with a suitable basis set, the binding energies of the DKee models are larger than at the DKnuc level, by about 0.1 eV for Pb_2, Bi_2, PbO, and less than 0.02 eV for TlH (Table 2.6). These effects normally reduce the interatomic distance by a rather small amount, with the largest effect, 0.007 Å, obtained for Pb_2 (Table 2.4).

In summary, the results of the models DKee1 and DKee2 agree essentially for the molecular properties investigated. Changes at the DKee3 level relative to the results of

DKee2 are not significant at the level of accuracy discussed here; therefore these results were not included in Tables 2.4, 2.5, and 2.6.

2.4 Conclusions

The Douglas–Kroll–Hess scheme of treating the Dirac–Kohn–Sham (DKS) problem of relativistic DFT was extended to account for spin-orbit (SO) interaction due to the classical Coulomb (Hartree) part of electron-electron interaction. This allows for a screening of the nuclear attraction field by the electron density. In particular, we discussed the implementation of various approximate schemes in combination with the density fitting technique ("resolution of identity"). We used several examples to illustrate the effect of the new type of corrections to the standard DKS treatment where the transformation to the two-component picture is restricted to the nuclear part of the effective one-electron potential: (*i*) the fine structure of the mercury atom, (*ii*) the g-tensor shift of the NO_2 radical, and (*iii*) structural and energetic properties of the diatomic molecules Bi_2, Pb_2, PbO, and TlH. We showed that replacing the hitherto employed unmodified Hartree term V_H by its relativistically corrected counterpart $\mathcal{E}_1[V_H]$ can substantially improve the accuracy of properties that inherently depend on the spin-orbit interaction, such as the spin-orbit splittings of heavy atoms and the g-tensor of molecules (even in molecules containing only light atoms). The SO interaction due to the Hartree potential affects the structural properties of the diatomics in a minor way only. In particular, a first-order approximate treatment is often sufficient. The corresponding second-order correction is much less important; the two flavors of second-order corrections introduced here lead to essentially the same results.

Chapter 3

Symmetry Treatment in Relativistic Electronic Structure Calculations of Molecules

Understanding symmetry in quantum chemistry tasks provides not only the power of adequate interpretation of basic interaction pattern but also allows a significant reduction of the computational expense. Symmetrized molecular orbitals used throughout in quantum chemistry proved to provide a basis for computational efficiency. There are several ways to generate symmetrized bases, e.g. the projection technique [158, 159], matrix diagonalization [160], algebraic approaches [161], and the method of generator orbitals [162, 163]. In relativistic quantum chemistry where one is not able to separate spin coordinates from space coordinates, orbitals evolve to spin-orbitals (spinors) or, in a fully relativistic description, to four-spinors (bi-spinors); concomitantly, the computational cost often increases drastically. It is therefore imperative for an efficient implementation of a quantum chemistry method to fully exploit the symmetry of the system under investigation. Indeed, much effort was spent to construct symmetrized bases for double group representations as required for relativistic electronic structure problems [164, 165, 166, 167, 168, 169].

Some methods for constructing symmetrized basis functions rely on tabulated standard group-theoretical information, e.g. characters, matrices of irreducible representations (irreps), as for instance the standard projection operator technique [158]. Other methods specifically try to avoid such a dependence [160]. A good compromise, from our point of view, is to generate all group theoretical information starting with the group definition (e.g. via its generators), thus avoiding the need of much tabulated data like group multiplication tables, irrep matrices, Clebsch-Gordan (CG) coefficients. In this spirit, a method is preferable which allows a clear algorithm and is easily implemented in the form of a computer program. One of the most successful tools for constructing and analyzing rotation

groups is the algebra of quaternions [76] which is formal enough to be implemented in a program. However, it permits only to build the group elements from group generators and to construct multiplication tables and class operators. To proceed to the transformation matrices of irreps, irrep bases, and CG coefficients, the eigenfunction method (EFM) [170] fulfills the requirements for implementation as a program [171]. The basic idea of EFM is to find symmetry functions as eigenfunctions of some symmetry related operators; hence, it is a natural choice for generating symmetrized basis functions. The method was also successfully applied to obtain consistent irrep matrices and CG coefficients for subgroup chains [172].

One of the advantages of using symmetrized basis functions is that one is able to exploit selection rules for symmetric operators. Totally symmetric operators are of particular importance; the (KS) Hamiltonian is an obvious example. However, invariance under all group operations is not the only characteristic which may be used to treat operator representations efficiently in symmetrized bases. Coupling orbital and spinor components is another example: operators diagonal in the spinor components should be treated differently from those which couple spinor components. There may also be a difference in how even and odd operators are treated in a four-component formalism (see Section 2.2.3).

In this chapter, we describe that part of the ParaGauss code which deals with symmetry and the underlying algorithms: group parametrization by quaternions (Section 3.1), the EFM formalism (Section 3.2), and issues of symmetry adaption specific to orbitals, two- and four-spinors (see Sections 3.3.1, 3.3.3, and 3.3.4, respectively). In Section 3.5 we illustrate the advantages of symmetry adapted basis functions for solving the relativistic (DKH) KS problem, specifically for building the representation of the *xc* potential by numerical integration over symmetrized two-spinor basis functions, a task which may become a bottleneck of the calculation if symmetry is not fully exploited.

3.1 Quaternion parametrization

The first step on the way to exploit the symmetry of molecular system is to provide access to the full group-theoretical information, in either tabulated or re-computed form. For this purpose, a single module in ParaGauss collects the generators of all pertinent (74 in total) point groups. Next, group multiplication tables, classes and coset decompositions are constructed to establish all pertinent group-theoretical information. These operations rely on the parametrization of the group elements by quaternionic numbers. An excellent review of the properties of quaternions and their usage in group theory can be found in Ref. [76].

There exists a homomorphism between any group of proper rotations and the algebra

of quaternions of the type $\pm q(\phi\boldsymbol{n})$: $q(\phi\boldsymbol{n}) = (\lambda, \boldsymbol{\Lambda}) = (\cos(\phi/2), \boldsymbol{n}\sin(\phi/2))$ where ϕ is the rotation angle and $\boldsymbol{n} = n_x\mathbf{i} + n_y\mathbf{j} + n_z\mathbf{k}$ expanded in the basis of unit quaternions $\mathbf{i}$, $\mathbf{j}$, and $\mathbf{k}$ defines the rotation axis. The quaternionic product of two parametrized rotations readily yields the parameters of the resulting composite rotation. This permits one to construct all elements starting with the group generators. The group multiplication table is easily obtained as well. The ambiguity regarding the sign is not a deficiency of the parametrization; rather, it is a key aspect with regard to projective representations (see below) that are required for the symmetrization of spinor wavefunctions. For example, quaternionic parameters of rotations that differ by an angle 2π have opposite signs: $q((\phi + 2\pi)\boldsymbol{n}) = -q(\phi\boldsymbol{n})$. This is exactly the familiar behavior of spinors or projective (double valued) representations [173].

To define a projective representation, one starts with the assumption that application of a symmetry operation $g_k = g_i g_j$ to a wavefunction is different from that of applying g_j and g_i in this sequence. The postulates of quantum theory indeed allow a phase factor $\eta(i, j)$:

$$\hat{g}_i\hat{g}_j\varphi(\boldsymbol{r}) = \eta(i, j)\hat{g}_k\varphi(\boldsymbol{r}). \tag{3.1}$$

Here, the notation $\hat{g}_i$ was adopted to distinguish an operator acting on a spinor wavefunction them from the corresponding group element g_i. A standardized set of phase factors $\eta(i, j)$, which, by a careful choice of phases of the operators $\hat{g}_i$, $\hat{g}_j$, and $\hat{g}_k$, may be reduced to the values ± 1, forms the projective factor system of the group under investigation [76]. To distinguish representations with the trivial factor system $\eta(i, j) = 1$ and those with non-trivial ones one refers to them as "vector" and "projective" representations, respectively. Another very convenient feature of the quaternion parametrization is that the projective factors $\eta(i, j)$ are given by the signs of products $q_i q_j = \pm q_k$, once the quaternionic parameters have been fixed in some fashion for all rotations g_i, g_j and g_k [76].

For the full rotation group $SO(3)$, a standard parametrization may be chosen by the following simple rules. The parameter space $\{\phi\boldsymbol{n},\, 0 \leq \phi \leq \pi\}$ of all rotations is geometrically equivalent to a ball of radius π. For all rotations "inside" the ball, i.e. rotations by angle $\phi < \pi$ (so-called *regular* rotations) one adopts the standard quaternionic parameters $(\cos(\phi/2), \boldsymbol{n}\sin(\phi/2))$. The restriction $\phi < \pi$ ensures that for the real part of this quaternion one has $\lambda = \cos(\phi/2) > 0$. Now, one is left with the task to select the standard quaternionic parameters for rotations which correspond to points on the surface of the ball $\phi = \pi$. Rotations by π, called *binary* rotations, are bilateral, i.e. their axis may be either $\boldsymbol{n}$ or $-\boldsymbol{n}$; the resulting operations are equivalent. To provide a unique parameter set $\{\phi\boldsymbol{n}\}$ for binary rotations, one separates the surface of the parametric ball into positive and negative "hemispheres" $\aleph$ and $\bar{\aleph}$ such that if the sphere point $\boldsymbol{n}$ belongs to hemisphere $\aleph$ then the opposite point is automatically assigned to another hemisphere $\bar{\aleph}$. There are

many choices for such partitions. Probably the simplest one is given by

$$\aleph = \begin{cases} \text{all } \boldsymbol{n} \text{ with } n_z > 0 \\ \text{all } \boldsymbol{n} \text{ with } n_z = 0 \text{ and } n_x > 0 \\ \boldsymbol{n} = (0, 1, 0) \end{cases} \tag{3.2}$$

However, for applications to point groups and to point group chains, alternative partitions prove to be more useful [76, 174]. The standard quaternionic parameters for binary rotations are chosen to be $(0, \boldsymbol{n})$ with $\boldsymbol{n} \in \aleph$. In summary, the rules to chose standard quaternionic parameters for a particular sphere partitioning into hemispheres $\aleph$ and $\bar{\aleph}$ are:

$$(\lambda, \boldsymbol{\Lambda}) = \begin{cases} (\cos(\phi/2), \boldsymbol{n}\sin(\phi/2)) & \text{for } \phi < \pi \\ (0, \boldsymbol{n}) \text{ with } \boldsymbol{n} \in \aleph & \text{for } \phi = \pi \end{cases} \tag{3.3}$$

Note, that the real part of the standard quaternionic parameters is non-negative: $\lambda \geq 0$. According to these rules, the identity corresponds to the real unitary quaternion $q(E) = (1, \mathbf{0})$.

The product of two "standard" quaternions, however, may not comply to the rules above. For instance, the square of any binary rotation C_2 (in quaternionic parametrization) yields $q(\pi)^2 = q(2\pi) = -1$, i.e. the negative of the quaternionic unity. The real part of the resulting quaternion, $(-1, \mathbf{0})$, is negative so that it does not belong to the standard set. On the other hand, in the group algebra we have the identity $C_2^2 = E$, parameterized by $q(E) = +1$. Thus, by comparing the results of the group algebra and the quaternion algebra, we obtain that, for any binary rotation C_2, the projective factor $\eta(C_2, C_2) = -1$. Similarly, one obtains the complete projective factor table of a group.

The four quaternion components may be augmented by a fifth parameter which acquires the values 1 or -1 to represent proper and improper rotations, respectively; for the composition of two symmetry operations, these fifth parameters are to be multiplied. In this way, improper rotations are treated in ParaGauss.

We have showed how the quaternionic parametrization can be used to construct all group elements from the group generators, the group multiplication table, and the projective factor system of the group. At this stage, the decomposition of the group into classes and cosets may be achieved. Also, based on the quaternionic rotation parameters, simple expressions of the rotation matrices in the space of angular momentum eigenfunctions (and in three-dimensional vector space as a special case) are readily available for integer and half integer angular momentum values. These matrices can be used to construct other matrix group representations. The basic group-theoretical information is then used in the EFM to generate matrices of irreducible representations (irreps) and to classify accordingly any set of functions.

3.2 The Eigenfunction Method

The key idea of the EFM is to classify objects that transform into each other by symmetry with the help of an eigenvalue problem into "symmetry types", so-called "irreducible representations". The idea is quite familiar in quantum mechanics where eigenvalues of an operator (observable) are often used to identify quantum states. For example, the eigenvalues of an operator pair (l^2, l_z) uniquely identify the rotational symmetry character of states of any spherically symmetric problem. In this particular case of symmetry operators, observables are often referred to as integrals (invariants) of motion or "good" quantum numbers. Note that (i) one actually needs two operators to fully determine the rotational behavior of a function because the eigenvalue of l^2 only assigns the function to a (in general) degenerate subspace of otherwise indistinguishable functions and (ii) these two operators must commute so that they can be simultaneously diagonalized. In the following, we will follow the programme of Chen [170] as implemented in ParaGauss by Mayer [77] and we will construct so-called "class operators", to be used in the EFM. In fact, for any point group, a class operator can be chosen whose eigenvalues uniquely define the basic symmetry character of a function, i.e. its irrep and thus the corresponding "symmetry label". Furthermore, class operators of a (properly chosen) chain of subgroups form a *complete set of commuting symmetry operators* determining *all* symmetry related quantum numbers in a function space.

3.2.1 Basic Concepts of the Eigenfunction Method: Atomic Orbitals in C_{4v} Symmetry

We will illustrate the basic idea of the EFM method by way of an example before we describe the method in detail.

Consider an atom in a ligand field of C_{4v} symmetry. The group C_{4v} consists of 8 elements: identity E, four-fold rotations in either direction, C_4^+ and C_4^-, around the z-axis, the binary rotation C_2 around z-axis, and two groups of reflections (σ_{v1}, σ_{v2}) and (σ_{d1}, σ_{d2}) with mutually orthogonal mirror planes. The properties of s, p, and d functions, atomic eigenfunctions in a spherically symmetric field, will be analyzed in the lower C_{4v} symmetry. It is natural to classify the atomic functions according to their behavior with respect to the operations of the group C_{4v}. For instance, the s function is invariant under any operation. In C_{4v}, this also holds for the function p_z, in spite of the fact that it represents a quite different distribution in space. Application of C_4^+ and C_4^- to the two

other p functions, p_x and p_y, transforms them into each other:

$$\begin{aligned} C_4^+ &: \; p_x \to p_y \text{ and } p_y \to -p_x \\ C_4^- &: \; p_x \to -p_y \text{ and } p_y \to p_x. \end{aligned} \tag{3.4}$$

Here, we adopted the active picture of symmetry transformations [76] in which a transformation of a function, more precisely of its graph, is performed similarly to rotating a solid object. Application of the reflections $\sigma_{v1} \equiv \sigma_{xz}$ and $\sigma_{v2} \equiv \sigma_{yz}$ changes the sign of the functions p_y and p_x, respectively; they do not lead to a mutual "coupling":

$$\begin{aligned} \sigma_{v1} &: \; p_x \to p_x \text{ and } p_y \to -p_y \\ \sigma_{v2} &: \; p_x \to -p_x \text{ and } p_y \to p_y. \end{aligned} \tag{3.5}$$

In C_{4v} symmetry, the d functions d_{zx} and d_{zy} behave similarly to the functions p_x and p_y as can be seen from the analogy $d_{zx} \sim p_z p_x$ and $d_{zy} \sim p_z p_y$. Results of applying symmetry operations to d_{z^2}, $d_{x^2-y^2}$, and d_{xy} are obtained in similar fashion.

Looking ahead to conjugate or "similar" elements, i.e. elements which belong to the same class, we now consider the result of applying an operator constructed as a sum of such "similar" symmetry operations:

$$\begin{aligned} \mathcal{C}_1 &:= C_4^+ + C_4^- \\ \mathcal{C}_2 &:= \sigma_{v1} + \sigma_{v2}. \end{aligned} \tag{3.6}$$

The result of such composite operators is taken as sum of the results of the individual contributors. When applied to the atomic trial functions discussed above, the "class" operators $\mathcal{C}_1$ and $\mathcal{C}_2$ yield just multiples of those functions. Thus, all these atomic functions are *simultaneous* eigenfunctions of both class operators. The corresponding eigenvalues were collected in Table 3.1. The atom-centered trial functions were augmented by one two-electron function $p_x(1)p_y(2) - p_y(1)p_x(2)$ to show a symmetry behavior (irreducible representation) not yet covered by the rest. Inspection of this table reveals a one-to-one correspondence of the symmetry behavior of the function (indicated by the C_{4v} irrep label) and the pair of eigenvalues of the class operators $\mathcal{C}_1$ and $\mathcal{C}_2$. In fact, these eigenvalues may be used to *define* the labels of the irreps.

By convention, symmetrized functions (of one-dimensional irreps) which are not changed by a rotation along the principal symmetry axis are labeled with the letter a. Such functions may be identified by the eigenvalue 2 of the operator $\mathcal{C}_1$. The totally symmetric irrep is always assigned the label a_1; the other function with eigenvalue 2 is called a_2. One-dimensional irreps with eigenvalue -2 of the class operator $\mathcal{C}_1$ are assigned the label b,

Table 3.1: Atomic functions as eigenfunctions and the corresponding eigenvalues of the class operators $\mathcal{C}_1 = C_4^+ + C_4^-$ and $\mathcal{C}_2 = \sigma_{v1} + \sigma_{v2}$ of C_{4v} as well as of the class operator $\mathcal{C}_3 = \sigma_{v1}$ of the subgroup C_s (see text).

	C_{4v}			C_s	
	$\mathcal{C}_1$	$\mathcal{C}_2$	Irrep	$\mathcal{C}_3$	Irrep
s, p_z, d_{z^2}	2	2	a_1	1	a'
p_x, d_{zx}	0	0	e	1	a'
p_y, d_{zy}				–1	a''
$d_{x^2-y^2}$	–2	2	b_1	1	a'
d_{xy}	–2	–2	b_2	–1	a''
$p_x(1)p_y(2) - p_y(1)p_x(2)$	2	–2	a_2	–1	a''

again with the subscript depending on behavior under further symmetry operation classes. The two-dimensional irrep is, by convention, labeled as e.

Careful inspection of Table 3.1 reveals the limitation of our choice of the eigenvalues of $\mathcal{C}_1$ and $\mathcal{C}_2$ as symmetry identifiers. These class operators, or rather their eigenvalues, do not distinguish the *partners* within an irrep e.g. p_x and p_y. This is a principal restriction which one is not able to circumvent by another choice of C_{4v} classes when building the class operators. For fundamental reasons, one can not distinguish between p_x and p_y on the base of their characteristics in C_{4v}.[1] In fact, as the class operators identify only spaces but not basis functions in them, the equivalence of partners goes beyond the fact that one cannot distinguish between them; in fact, any two orthogonal combinations of partners are equally well suited as "basis functions", e.g. the pair $p_x \pm p_y$.

This degeneracy issue is often met in physical problems. Degenerate states (i.e. states of the same energy) in a system of high symmetry are split by a field of a lower symmetry. Thus, it is natural to classify the atomic orbitals further by their symmetry behavior in a system of lower symmetry — in addition to the irrep classification performed for C_{4v}. Symmetry properties in subduced groups provide criteria for distinguishing irrep partners of the starting group. There are several possibilities to chose a subgroup of C_{4v}. Consider the groups C_s and C_4; both have only one-dimensional irreps. The major difference is that the irreps of C_s are real and those of C_4 (as for any axial group) are complex [174]. Thus, from a practical point of view, one should prefer C_s.

The group C_s comprises two elements: the identity E, and a reflection σ. Let us select the group element σ_{v1} of C_{4v} as generator of the subgroup C_s. This mirror operation forms a class of C_s on its own and is the only candidate for a class operator. The atomic

[1] This statement holds as long as there is no sufficient reason to prefer, for instance, σ_{v1} to σ_{v2} — which would amount to a lowering of the symmetry.

trial functions we had chosen are again eigenfunctions of $\mathcal{C}_3 = \sigma_{v1}$; the corresponding eigenvalues are also listed in Table 3.1. Note that the functions p_x and p_y, degenerate in C_{4v}, are eigenfunctions of $\mathcal{C}_3$ with different eigenvalues 1 and –1, respectively. This reflects the irrep subduction $(e) \rightarrow (a') \oplus (a'')$ in the subgroup chain $C_{4v} \supset C_s$. For higher symmetries, irrep subduction may sometimes lead to a situation where a subduced multi-dimensional group irrep contains multiple instances of a subgroup irrep. This introduces an ambiguity for the classification of eigenfunctions which, however, can be avoided by choosing a canonical subgroup chain [170, Section 3.3.3].

In practice, one can avoid the simultaneous diagonalization of two class operators of C_{4v}, $\mathcal{C}_1$ and $\mathcal{C}_2$. For this purpose, one introduces an operator which is a linear combination of them, e.g. $\mathcal{C}_{12} := 2\mathcal{C}_1 + \mathcal{C}_2$. The eigenvalues λ_{12} of this operator are linear combinations of the eigenvalues λ_1 and λ_2 of $\mathcal{C}_1$ and $\mathcal{C}_2$ according to $\lambda_{12} = 2\lambda_1 + \lambda_2$. Due to the one-to-one correspondence between eigenvalues of λ_{12} and pairs (λ_1, λ_2), one can use the former instead of the latter to classify the irreps. The coefficients of such linear combinations are not unique; the only requirement is to avoid any accidental degeneracy which would destroy the one-to-one correspondence.

The eigenvalues of $\mathcal{C}_{12}$ and $\mathcal{C}_3$ form a complete set of *symmetry-related* quantum numbers. These quantum numbers may be interpreted either as irrep labels and, in the case of multi-dimensional irreps, as labels of partner functions, or as irrep labels in a group chain subduced from the original group. The remaining degeneracy, e.g. between p_x and d_{zx} (see Table 3.1) will be lifted by the ligand field, i.e. the Hamiltonian H which assigns different energy eigenvalues ϵ to them. The term "lifting the degeneracy" should be understood as "forming linear combinations with well defined quantum numbers". For example, the ligand field of C_{4v} symmetry will mix p_x and d_{zx} into two functions with different eigenvalues; a Hamiltonian of spherical symmetry will leave the functions unchanged, but still, their eigenvalues for p and d functions will in general differ. If we started from a different set of trial functions, e.g. from the complex functions $p_\pm = p_x \pm \mathrm{i}p_y$, we would also have combined them in linear fashion to produce proper eigenfunctions of $\mathcal{C}_3 = \sigma_{v1}$.

We implicitly assumed that it is possible to find simultaneous eigenfunctions of H and the pair of class operators $(\mathcal{C}_{12}, \mathcal{C}_3)$. Only mutually commuting operators may be diagonalized simultaneously. This requirement is indeed fulfilled for Hamiltonians H of C_{4v} symmetry or higher. A formal requirement that H commutes with any symmetry operation in C_{4v} automatically implies that the commutators of H and $(\mathcal{C}_{12}, \mathcal{C}_3)$ vanish because the latter are linear combinations of C_{4v} elements.

Now, the set of operators $(H, \mathcal{C}_{12}, \mathcal{C}_3)$ with eigenvalues $(\epsilon, \lambda_{12}, \lambda_3)$ form a complete set of quantum numbers for our system: ϵ is interpreted as energy and $(\lambda_{12}, \lambda_3)$ as symmetry-related quantum numbers. The corresponding eigenfunctions are, in general, linear com-

binations of the trial functions chosen as atomic basis.

3.2.2 Theory of the Eigenfunction Method

In the previous section, the basic concepts of the EFM method were illustrated with the symmetry classification of atomic basis functions. An advantage of the EFM method is that it is equally well applicable to any set of objects which are transformed into each other under symmetry operations. This set of objects may be a closed subset of atom-centered basis functions, as in the example above, atomic displacement vectors (forces), or any derived quantities like products of basis functions or matrix elements of some operator. To emphasize this generality, one often refers to a linear space $\mathcal{L}$ with symmetry operations of some group G defined as linear transformations on it. A linear space is an *invariant* space if the result of any symmetry operation applied to its elements belong to that space as well.

The formal theory of the EFM method is developed by exploring an abstract linear space, the so-called group algebra space $\mathcal{L}_G$ of a group G [170, Sections 2.6.2 and 2.6.3]. This is a linear space where the elements of G are considered as basis vectors and the application of the group operators to those vectors is derived from the group multiplication table. Thus, in practice, the group elements are not only allowed to by multiplied by each other according to the group multiplication rules, but also to form any linear combination with arbitrary coefficients. For example, the operators $\mathcal{C}_{12} = 2(C_4^+ + C_4^-) + \sigma_{v1} + \sigma_{v2}$ and $\mathcal{C}_3 = \sigma_{v1}$ (Section 3.2.1) are two specific elements of the group space (or, more exactly of the group algebra). Note that one is talking about an algebra if multiplications of the elements are defined. Without emphasis on multiplications one may consider any algebra space as a linear space. By reference to the group multiplication table and simple arithmetics, one may easily check that $[\mathcal{C}_{12}, \mathcal{C}_3] = 0$.

A general element of the group algebra,

$$g = \sum_{i=1}^{|G|} x_i g_i \in \mathcal{L}_G,\ x_i \in \mathbb{C}, \tag{3.7}$$

can be interpreted either as a vector or as an operator in the group algebra space, depending on the context. For example, when considering "matrix elements" $D_{ab}(g) \equiv \langle a|g|b\rangle$ of some group (or algebra) element g defined by

$$gb = \sum_{a \in G} a D_{ab}(g)\,, \tag{3.8}$$

the bra and ket vectors $\langle a|$ and $|b\rangle$ should be considered as elements of $\mathcal{L}_G$ and g as

an operator acting on $|b\rangle$. The group algebra space $\mathcal{L}_G$ carries the so-called "regular representation" of the group. For any group element g, the representation matrices of the regular representation are the matrices $D(g)$ build of matrix elements $D_{ab}(g)$ of g in the basis $a, b \in G$; for each b, there is only one non-zero element $D_{ab}(g)$ equal to 1, namely that for which $a = gb$ [170, Section 2.6.1]. The regular representation comprises all irreps [170, Section 3.9] and, in the EFM, via its reduction the complete irrep information is generated [170, Section 3.9].

Class operators of the group G are elements $C_i = \sum_k g_k$, $g_k \in \mathcal{C}_i$ of the group algebra which represent the sum of all elements of class $\mathcal{C}_i$, $i = 1, \ldots N$; N is the number of classes in the group. Recall that N is also the number of irreps [170, Section 3.2]. Class operators have following important properties: they commute with all group operations,

$$[C_i, g] = 0 \ \ \forall g \in G \tag{3.9}$$

and thus can be viewed as "integrals of motion", constant in the space of symmetry equivalent functions [175]. Consequently, they commute with any element of $\mathcal{L}_G$, thus also among each other:

$$[C_i, C_j] = 0. \tag{3.10}$$

This is a necessary attribute of a set of properties (or operators) which are to be defined (or diagonalized) simultaneously. The set of class operators is closed under multiplication

$$C_i C_j = \sum_k c_{ij}^k C_k \tag{3.11}$$

with integer c_{ij}^k [170, Section 3.1.1] and thus also forms an algebra, to be referred to as $\mathcal{L}_C$. One can formally prove that the chosen set of "motion invariants" is complete by showing that any group algebra operator $A \in \mathcal{L}_G$ commuting with all group elements, $[A, g] = 0$, $\forall g$, is necessarily a class operator or a linear combination thereof, $A \in \mathcal{L}_C$ [170, Section 3.1.1]. Class operators are either Hermitean operators or can be used to construct Hermitean operators [170, Section 3.2.4]. For an ambivalent group where inverse group elements belong to the same class, one has: $C_i^\dagger = C_i$. In a non-ambivalent group, one uses the following combinations instead, $C_i + C_{i'}$ and $i(C_i - C_{i'})$, which are always Hermitean with $C_{i'} := C_i^\dagger$.

The complete set of N class operators $(C_1, \ldots C_N)$ corresponding to N group classes is a *complete set of commuting operators* (CSCO) in the *class space* $\mathcal{L}_C$; we refer to it as CSCO-I of the group G [170, Section 3.2]. The CSCO-I set may actually be reduced (in a non-unique way) to less than N class operators (cf. Section 3.2.1 where we used only two

class operators $\mathcal{C}_1$ and $\mathcal{C}_2$); it may be even linearly combined into a *single* operator

$$\begin{aligned} C &= \sum_i \alpha_i C_i \\ \lambda^{(\nu)} &= \sum_i \alpha_i \lambda_i^{(\nu)} \end{aligned} \tag{3.12}$$

with some coefficients α_i analogous to what we did when we constructed $\mathcal{C}_{12}$ from $\mathcal{C}_1$ and $\mathcal{C}_2$ in Section 3.2.1. The purpose of such linear combination is to avoid the task of simultaneous diagonalization of several operators in practical applications; a single operator is diagonalized instead. The only requirement on the coefficients α_i is that the resulting operator affords a one-to-one correspondence between $\lambda^{(\nu)}$, $\nu \leq N$, and the N-tuples of eigenvalues $(\lambda_1^{(\nu)}, \ldots, \lambda_N^{(\nu)})$. Class operators C_i for which the corresponding coefficient α_i is taken equal to zero are not required in the definition the CSCO-I operator C. The CSCO-I for 74 point groups, as used in ParaGauss, are specified in Appendix B. While not unique, different CSCO-I sets are nevertheless equivalent in the sense that they have identical eigenvectors in the class space $\mathcal{L}_C$,

$$Q^{(\nu)} = \sum_{i=1}^{N} q_i^{(\nu)} C_i \tag{3.13}$$

$$CQ^{(\nu)} = \lambda^{(\nu)} Q^{(\nu)}. \tag{3.14}$$

The eigenvectors $Q^{(\nu)}$ as algebra elements form a set of idempotent projection operators,

$$Q^{(\nu)} Q^{(\mu)} = \delta_{\nu\mu} \eta_\nu Q^{(\nu)} \tag{3.15}$$

$$P^{(\nu)} P^{(\mu)} = \delta_{\nu\mu} P^{(\nu)}, \tag{3.16}$$

where $P^{(\nu)} = \eta_\nu^{-1} Q^{(\nu)}$ and η_ν are suitable factors. Therefore, one can represent a CSCO-I operator in spectral form as

$$C = \sum_{\nu=1}^{N} \lambda^{(\nu)} P^{(\nu)}. \tag{3.17}$$

The class space $\mathcal{L}_C$ is just a subspace, an N-dimensional hyperplane, in the larger $|G|$-dimensional group space $\mathcal{L}_G$. N eigenfunctions of CSCO-I in the N-dimensional class space $\mathcal{L}_C$ are uniquely identified by their CSCO-I eigenvalues $\lambda^{(\nu)}$, $\nu = 1 \ldots N$. Only these N eigenvalues appear if CSCO-I is applied to a larger $|G|$-dimensional group space $\mathcal{L}_G$ [170, Section 3.3]. Thus, in $\mathcal{L}_G$ CSCO-I is degenerate; it is not a *complete* set of commuting operators in the group space $\mathcal{L}_G$. However, (degenerate) eigenvalues of CSCO-I define the major symmetry "quantum number" of its eigenfunctions in $\mathcal{L}_G$, namely the irrep label. In

fact, by solving the eigenvalue problem for CSCO-I and *any* group representation space $\mathcal{L}$ (not limited to $\mathcal{L}_G$), one divides this space into subspaces $\mathcal{L}_{(\nu)}$ that correspond to distinct eigenvalues $\lambda^{(\nu)}$ of N inequivalent group irreps,

$$\mathcal{L} = \bigoplus_{\nu=1}^{N} \mathcal{L}_{(\nu)}, \tag{3.18}$$

such that

$$C\mathcal{L}_{(\nu)} = \lambda^{(\nu)}\mathcal{L}_{(\nu)}. \tag{3.19}$$

In general, subspaces corresponding to a particular eigenvalue $\lambda^{(\nu)}$ may be still be reducible into several irreducible subspaces:

$$\mathcal{L}_{(\nu)} = \bigoplus_{\epsilon} \mathcal{L}_{(\epsilon,\nu)}. \tag{3.20}$$

In general, this is the case for $\mathcal{L}_G$ (but not $\mathcal{L}_C$). The regular representation in the basis of $\mathcal{L}_G$ is known to contain h_ν instances of each h_ν-dimensional irrep [170, Section 3.9]. Another example occurs when one analyzes the symmetry properties of atomic f functions in the group C_{4v}, following the procedure of Section 3.2.1; in the manifold of seven f functions, there are two independent subspaces of irrep character e.

Thus far, we described a way how to separate an arbitrary invariant representation space of G into subspaces corresponding to inequivalent irreps by solving the eigenvalue problem for CSCO-I. However, an essential degeneracy exists within the subspaces corresponding to *multidimensional* irreps. Indeed, for any function $\psi_\epsilon^{(\nu)} \in \mathcal{L}_{(\nu)}$ one may find h_ν symmetry equivalent functions making up a basis of $\{G\psi_\epsilon^{(\nu)}\}$ and called *irrep partners*; the dimension of irrep ν is h_ν. However, the particular choice and grouping of partners is not defined by CSCO-I. A tedious iterative procedure of collecting the bases of $\{G\psi_\epsilon^{(\nu)}\}$ into $\mathcal{L}_{(\epsilon,\nu)}$ with a subsequent Schur orthogonalization [170] of the different $\mathcal{L}_{(\epsilon,\nu)}$ is feasible, but certainly not an elegant solution. Even if applied, the resulting partners may not be consistent for different irreducible subspaces $\mathcal{L}_{(\epsilon,\nu)}$ of the same symmetry; in other words, irrep matrices within each irreducible space will be similar, but not necessarily equal.

To classify the partners of multidimensional irreps uniquely and uniformly over the whole subspace $\mathcal{L}_{(\nu)}$, one has to lift their inherent degeneracy. This usually happens as a consequence of symmetry reduction. The behavior in lower symmetries naturally discriminates otherwise equivalent partners of an irreducible subspace. It is exactly this behavior which correlates the corresponding partners in different irreducible subspaces. As an example, we refer to Section 3.2.1, where we lowered the symmetry from C_{4v} to C_s to discriminate the partner functions p_x and p_y as well as d_{zx} and d_{zy}. Otherwise, in an

automatized procedure, one might arrive at the partner functions p_x and p_y in one subspace, but orthogonal linear combinations of d_{zx} and d_{zy} in the other subspace, hence one would have lost the distinct phase relationship among the partner functions of different subspaces. Thus, to avoid such an undesirable situation, subgroups and subgroup chains come into play.

We saw already that class operators of the group, conveniently combined in CSCO-I, define a particular symmetry class of any function. Subgroups $G(s_i) \subset G$ subdivide the classes further according to the behavior in the lower symmetries. A fully distinctive classification is achieved by taking a *canonical* subgroup chain

$$G \supset G(s_1) \supset \ldots G(s_n) \tag{3.21}$$

which is constructed in such a way that irreps of each member of the chain split into a sum containing no more than one instance of the irreps of the subsequent member of the chain. The last member of the chain must be an abelian group with one-dimensional irreps. These conditions assure an unambiguous classification of all partners of irreducible subspaces of G. ParaGauss follows the canonical chains suggested by Altmann and Herzig; [174] see Figure B.2 in Appendix B.

The class operators of a subgroup $G(s_1)$ may easily be added to the CSCO-I of G because the classes $C(s_1)$ of the subgroup $G(s_1)$ (as elements of the group algebra G) commute with all class operators C of the group G, Eq. (3.9), and, thus, with CSCO-I of G. This argument holds for any subsequent pair $G(s_i) \supset G(s_{i+1})$ of the subgroup chain. Thus, the CSCO-I operator C of G commutes with all CSCO-I operators $C(s_i)$ of any subgroup $G(s_i)$ from the group chain; therefore, all of them may be diagonalized simultaneously. The joint CSCO-I sets $(C, C(s))$ of the group and the subgroup chain is referred to as CSCO-II of the group G. Here $C(s)$ is a shorthand notation for the union of all CSCO-I operators $(C(s_1), \ldots, C(s_n))$ of subgroups or, in practical applications, a linear combination of them, similar to Eq. (3.12). The pair $(\mathcal{C}_{12}, \mathcal{C}_3)$, which forms a CSCO-II for C_{4v}, was used in Section 3.2.1 to fully characterize the symmetry properties of the atomic functions.

The eigenvalues of the CSCO-II $(\lambda^{(\nu)}, \kappa^{(\mu)})$ marked by indices (ν, μ) form a complete set of symmetry related quantum numbers. The first index ν labels the irrep and the second μ labels the partner functions of the irrep. Any remaining "degeneracy" of a set of functions of the same symmetry (ν, μ) has to be lifted by an operator of a different nature, e.g. the Hamiltonian H which was used in Section 3.2.1 to label the independent subspaces by their energy eigenvalues. With the introduction of the Hamiltonian H, a certain partitioning of the independent irrep subspaces, Eq. (3.20), is established, namely that based on the

energy eigenvalues ϵ:

$$\mathcal{L} = \bigoplus_{\nu} \mathcal{L}_{(\nu)} \tag{3.22}$$

$$\mathcal{L}_{(\nu)} = \bigoplus_{\mu} \mathcal{L}_{(\nu,\mu)} \tag{3.23}$$

$$\mathcal{L}_{(\nu,\mu)} = \bigoplus_{\epsilon} \mathcal{L}_{(\epsilon,\nu,\mu)} \tag{3.24}$$

Assuming that there are no accidental degeneracies, the linear space $\mathcal{L}_{(\epsilon,\nu,\mu)}$ is one-dimensional with eigenfunction $\psi_\epsilon^{(\nu\mu)}$ as the only basis function. The symmetry of the Hamiltonian H expressed by its commutation properties,

$$[H, G] = [H, C] = [H, C(s)] = 0. \tag{3.25}$$

assures that the three operators $(H, C, C(s))$ can be simultaneously diagonalized. The CSCO-II of the group together with the Hamiltonian H forms the CSCO of the common quantum-mechanical problem of finding the eigenvalues and the corresponding eigenvectors in a system $(H, C, C(s))$ with a certain (spatial) symmetry.

However, when one considers only the group-theoretical problem of constructing a CSCO for a group representation space $\mathcal{L}_G$, a different operator takes on the role of the Hamiltonian H. It may be shown [170] that the CSCO-II of the *intrinsic* group, which is anti-isomorphic to G [170, Section 3.7], together with the CSCO-II of G form a CSCO of the group space $\mathcal{L}_G$ [170, 77]. The union of the CSCO-II operators of the group G and its intrinsic isomorphism is called CSCO-III of the group [170]. The reduction of the regular representation with help of the CSCO-III operator is used in ParaGauss to obtain the canonical irrep matrices [77]; later on, they are required to obtain, for instance, the CG coefficients [77].

3.2.3 The Eigenfunction Method for Double Groups

Let us now discuss some issues specific to projective (double valued) representations of a group which are relevant for the symmetrization of spinor wavefunctions. Spinors emerge as mathematical representation of particles with half-integer intrinsic angular momentum (spin), e.g. electrons. In general, a particle with spin J (integer or half-integer) is represented by $2J + 1$ probability amplitudes ψ^σ, $\sigma = -J \ldots J$ that describe the measurement of finding the particle in one of the $2J+1$ selected states; for brevity, these states normally are chosen to have well-defined angular momentum projection on the z-axis, $M = -J \ldots J$. In this basis, the matrix representation of J_z is a diagonal matrix with the correspond-

ing eigenvalues M on the diagonal. An electron is characterized by spin $J = 1/2$; the corresponding wavefunction has two components. From angular momentum theory it is known that a rotation $\phi\boldsymbol{n}$ transforms the components of a wavefunction, characterized by an integer angular momentum L, according to [76]

$$\phi\boldsymbol{n} \to \exp(-\mathrm{i}\phi\boldsymbol{n}\boldsymbol{L}) \to \begin{pmatrix} e^{+\mathrm{i}\phi L} & & \\ & \ddots & \\ & & e^{-\mathrm{i}\phi L} \end{pmatrix}. \tag{3.26}$$

The matrix on the right-hand side is the representation of a rotation by ϕ around the z-axis in the basis which we have chosen above. Thus, a full turn, $\phi = 2\pi$, generates an identity transformation $\psi^\sigma \to \psi^\sigma$, due to the Euler relation $e^{2\pi i} = 1$.

The half-integer spin of electrons entails an essential difference. Similarly to Eq. (3.26), the transformation of the two spinor components corresponding under a rotation $\phi\boldsymbol{n}$ is given by [76]

$$\phi\boldsymbol{n} \to \exp(-\mathrm{i}\phi\boldsymbol{n}\mathbf{s}) \to \begin{pmatrix} e^{+\mathrm{i}\phi/2} & \\ & e^{-\mathrm{i}\phi/2} \end{pmatrix}. \tag{3.27}$$

Again, the rightmost matrix is the representation of rotation by ϕ around the z-axis in the basis of s_z eigenfunctions. The essential difference is connected to the fact that projections of spin $\boldsymbol{s} = \boldsymbol{\sigma}/2$ take on the half-integer values $\pm 1/2$. Thus, because of the identity $e^{\pi i} = -1$, a full turn induces a sign change, $\psi^\sigma \to -\psi^\sigma$. This mismatch requires one to treat spinors by projective representations. In Section 3.1, we considered the product of two binary rotations by π; that product is an identity operation from the group-theoretical point of view, but a phase change when this product is applied to a spinor.

As described in Section 3.1, projective representations are formally defined by the multiplication rules of linear operators $\hat{g}_i$, $\hat{g}_j$, and $\hat{g}_k$ which represent the action of the group elements g_i, g_j, and g_k when applied to spinors:

$$\begin{aligned} g_i g_j &= g_k \\ \hat{g}_i \hat{g}_j &= \eta(i,j)\hat{g}_k. \end{aligned} \tag{3.28}$$

Here, the projective factors $\eta(i,j)$ will acquire values 1 or -1 for some choice of phases for $\hat{g}_i$, $\hat{g}_j$, and $\hat{g}_k$ [76]. One may declare positive and negative elements of the operator algebra as elements of some abstract covering group $\tilde{G} = \{g_i, \tilde{g}_i;\ i = 1 \ldots |G|\}$, also called *double group*; the elements g_i and $\tilde{g}_i$ of the double group $\tilde{G}$ correspond to the operators $\hat{g}_i$, $-\hat{g}_i$, respectively. Then one may proceed to analyze the class structure of the double group, construct class operators, CSCO, irreps etc. However, in this approach, one ignores

the fact that actually not all elements of the operator representation of the double-sized group $\tilde{G}$ are linearly independent. Furthermore, double group representations cover the true vector representations of the group G; it would be less elaborate if one could obtain the vector irreps of $\tilde{G}$ directly from those of G.

With projective representations in mind, it is advantageous to consider operator representations of the double group $\tilde{G}$ with projective multiplications rules, Eq. (3.28), an approach which explicitly accounts for the linear dependence of the operators representing g and $\tilde{g}$. To illustrate the difference between the group algebra and the operator algebra, consider $g + \tilde{g}$ which is a *non-empty* group algebra element, but for the operators one has $\hat{g} + \hat{\tilde{g}} = \hat{g} - \hat{g} = 0$. For this reason, class operators of the double group which contain both g and $\tilde{g}$ vanish (see below).

Let us examine the class structure of the double group $\tilde{G}$ and compare it to the class structure of G. Here, we adopted the following notation:

- $\mathcal{C}(g)$: a class of G which contains the conjugates of g; it is an element of the *group* algebra G and never empty.
- $C(g)$: a class *operator* of G which corresponds to $\mathcal{C}(g)$; it is an element of the *operator* algebra G and may be zero.
- $\tilde{\mathcal{C}}(g)$: a class of $\tilde{G}$ which contains conjugates of g; it is an element of the *group* algebra $\tilde{G}$ and never empty.
- $\tilde{C}(g)$: a class *operator* of $\tilde{G}$ which corresponds to $\tilde{\mathcal{C}}(g)$; it is an element of the *operator* algebra $\tilde{G}$ and may be zero.
- g and $\tilde{g}$: corresponding elements of the double group $\tilde{G}$; element g is at the same time an element of G.
- regular g: in point groups a proper rotation by an angle $\phi \neq \pi$. For such g, $\mathcal{C}(g)$ is called *regular*.
- irregular g: the opposite of above, i.e. either a binary rotation by π, a reflection, or inversion. For such g, $\mathcal{C}(g)$ is called *irregular*.

The class structures of the group G and and the corresponding double group $\tilde{G}$ are closely related. In this discussion, we use the following notation. If $\mathcal{C}(g)$ designates a class of G which contains the conjugates of the regular element g, then $\tilde{\mathcal{C}}(g)$ and $\tilde{\mathcal{C}}(\tilde{g})$ are two distinct classes of the double group $\tilde{G}$ and one has $\mathcal{C}(g) = \tilde{\mathcal{C}}(g)$. The double group classes $\tilde{\mathcal{C}}(g)$ and $\tilde{\mathcal{C}}(\tilde{g})$ for an irregular group element g (i.e. a binary rotation, a reflection, or inversion) coincide and thus include conjugates of both g and $\tilde{g}$. Therefore,

the corresponding class *operators* are either linearly dependent for a regular g, $\tilde{C}(g) = -\tilde{C}(\tilde{g}) = C(g)$, or they vanish for an irregular g, $\tilde{C}(g) \equiv \tilde{C}(\tilde{g}) = 0$. Hence, there are only $r \leq N$ linearly independent class operators, r being the number of regular classes of G and N being the total number of classes of G. When applying the EFM method to an operator algebra of r linearly independent class operators, one obtains r eigenvectors with r eigenvalues corresponding to the r projective irreps of G. In analogy to the case of a "simple" group, the projective CSCO-I is constructed from the projective class operators of G; see Appendix B. Furthermore, class operators of a subgroup chain are added to construct a CSCO-II and the class operators of an intrinsic subgroup chain are added to construct a CSCO-III [77, 170].

3.2.4 CSCO in orbital and spinor spaces

Next, we will construct a complete set of commuting operators in orbital and spinor spaces and compare them in the light of a typical computational problem of quantum chemistry. As mentioned above, the choice of a CSCO is not unique. One may actually start from any given group operator set and extend it to completeness. We start with the group CSCO $(C, C(s))$ whose eigenvalues (ν, μ) uniquely identify the symmetry of states (irrep and irrep partner) and add the non-relativistic Hamiltonian H which will separate different energy levels of the same irrep. We arrive at a complete set of state quantum numbers in orbital space, defined as eigenvalues (ε, ν, μ) of

$$(H, C, C(s)). \tag{3.29}$$

Similarly, for the spinor space and a Hamiltonian $\tilde{H}$ that includes spin-orbit interaction, we may use the CSCO

$$(\tilde{H}, \tilde{C}, \tilde{C}(s)) \tag{3.30}$$

with eigenvalues $(\tilde{\varepsilon}, \tilde{\nu}, \tilde{\mu})$. However, in the last case, we may also use the spin-free totally symmetric (scalar relativistic) Hamiltonian H instead of the Hamiltonian $\tilde{H}$ which includes spin-coupling to build another CSCO

$$(H, \tilde{C}, \tilde{C}(s)) \tag{3.31}$$

in the spinor space. The spin-free Hamiltonian H exhibits energy levels which are degenerate with respect to the spin orientations, but the pair of projective symmetry operators $(\tilde{C}, \tilde{C}(s))$ with eigenvalues $(\tilde{\nu}, \tilde{\mu})$ provide the means to distinguish them. As an analogy, consider the angular dependence of atomic spinors where the eigenvalues of (L^2, J^2, J_z) *uniquely* identify the symmetry properties of any function ψ^{LJM} such that

$L^2\psi^{LJM} = L(L+1)\psi^{LJM}$, $J^2\psi^{LJM} = J(J+1)\psi^{LJM}$, and $J_z\psi^{LJM} = M\psi^{LJM}$. However, the spin-free operator L^2 is degenerate with respect to the spin projections, but it is complemented by the pair (J^2, J_z). On the other hand, L^2 is required to build a CSCO for the angular-only functions, because it discriminates the manifolds such as $p_{3/2}$ and $d_{3/2}$.

However, a CSCO $(H, C, C(s))$ in orbital space is not a CSCO in spinor space. The eigenvalues of this set are obviously degenerate with regard to the spin orientations because all operators of the set including $(C, C(s))$ act on the orbital (spatial) components only, and, hence, are spin-free. By appending the operator $\boldsymbol{\sigma n}$ for any direction $\boldsymbol{n}$ or just σ_z, we introduce an explicit dependence on spin and arrive at a complete set

$$(H, C, C(s), \sigma_z). \tag{3.32}$$

This last set is always implicitly used in any spin-polarized non-relativistic calculation — and also in any spin-restricted calculation where the degeneracy with respect to σ_z is factored out. Two sets of quantum numbers, $(C, C(s), \sigma_z)$ and $(\tilde{C}, \tilde{C}(s))$, of a spinor space CSCO are independent of a particular Hamiltonian H. These sets can be used interchangeably as they are fully equivalent.

The special case of a spin-free operator C as class operator in the set

$$(C, \tilde{C}, \tilde{C}(s)), \tag{3.33}$$

[see Eq. (3.31)] is of particular interest when dealing with other spin-free operators. In the angular momentum theory, this set corresponds to the set of quantum numbers (L^2, J^2, J_z), introduced above, which is essential for L-S coupling. Similarly to the latter, but defined for any point group, the set $(C, \tilde{C}, \tilde{C}(s))$ identifies spinors with well-defined projective irrep labels and well-defined vector irrep labels. C and $\tilde{C}$ commute and thus may simultaneously be diagonalized. The set of operators may now be augmented by the spin-free Hamiltonian H (which also commutes with C) to distinguish levels within the eigenspaces of $(C, \tilde{C}, \tilde{C}(s))$ and to transform this set into a CSCO of the system:

$$(H, C, \tilde{C}, \tilde{C}(s)) \tag{3.34}$$

The spin-free character of H makes this combination with C possible. The spin-coupling Hamiltonian $\tilde{H}$ is neither invariant under pure "orbital rotations" C, $[\tilde{H}, C] \neq 0$, nor under pure "spin rotations", $[\tilde{H}, \boldsymbol{\sigma}] \neq 0$; therefore, it cannot be used in a CSCO in combination with either C or σ_z.

The eigenvectors of $(C, \tilde{C}, \tilde{C}(s))$ with eigenvalues $(\nu, \tilde{\nu}, \tilde{\mu})$ form a suitable basis for representing the totally symmetric spin-free Hamiltonian H or the spin-coupling Hamiltonian

$\tilde{H}$ in matrix form. The commutation properties require the matrices to be diagonal in $\tilde{\nu}$ and $\tilde{\mu}$ and degenerate with respect to $\tilde{\mu}$:

$$\langle \psi_n^{(\tilde{\nu}\tilde{\mu})} | \tilde{H} | \psi_m^{(\tilde{\nu}'\tilde{\mu}')} \rangle = \tilde{H}_{nm}^{(\tilde{\nu})} \delta_{\tilde{\nu}\tilde{\nu}'} \delta_{\tilde{\mu}\tilde{\mu}'}. \tag{3.35}$$

In addition, the matrix of a spin-free operator H (or any other spin-free operator) must be diagonal in ν:

$$\langle \psi_n^{(\nu\tilde{\nu}\tilde{\mu})} | H | \psi_m^{(\nu'\tilde{\nu}'\tilde{\mu}')} \rangle = H_{nm}^{(\nu,\tilde{\nu})} \delta_{\nu\nu'} \delta_{\tilde{\nu}\tilde{\nu}'} \delta_{\tilde{\mu}\tilde{\mu}'}. \tag{3.36}$$

A procedure to construct spinor bases with the well-defined quantum numbers $(C, \tilde{C}, \tilde{C}(s))$ using CG coefficients will be presented in the following sections.

3.3 Symmetry Adapted Functions

3.3.1 Symmetrized Molecular Orbitals

Now, we will describe how molecular orbitals are symmetrized, using the information established by the EFM. The code ParaGauss is designed to perform molecular computations at the non-relativistic level on the one hand and with inclusion of spin-obit interaction on the other hand. With regard to symmetry and the basis functions needed, scalar relativistic calculations do not differ from the non-relativistic and thus do not represent a special case as far as this aspect is concerned. In short, it is necessary that one is able to establish symmetrized molecular orbitals as well as symmetrized molecular spinors. We will discuss possible ways to do so for both cases and we will relate the two types of symmetrization procedures to each other. The ultimate goal is to create an algorithm that reduces the computational costs to the minimum consistent with the symmetry properties of the operators involved.

The concept of a "*unique*" atom is used throughout the program to designate a representative of set of *symmetry-equivalent* atoms of a molecule. The positions $\boldsymbol{a}_i$ of equivalent atoms form a set $\{\boldsymbol{a}_i,\ i = 1...N_a\}$ of objects which are permuted among each other under the symmetry operations; thus, they form the basis of some group representation. As each $\boldsymbol{a}_i$ is a vector, all permutations of $\{\boldsymbol{a}_i\}$ may be easily obtained once the transformation properties of vectors (or equivalently, of spherical harmonics with $L = 1$) are known for a given group. These properties may be computed from the quaternion parametrization of the symmetry elements. In practice, all equivalent $\boldsymbol{a}_i$ are generated from the position of the "*unique*" atom provided in the input by applying symmetry operations. Only one of the coset representative of the "little group" $G(\boldsymbol{a_i})$ — the subgroup of G which leaves $\boldsymbol{a}_i$ invariant — needs to be applied to the initial $\boldsymbol{a}_i$ to obtain the rest. The constructed

group representation $\langle \boldsymbol{a}_i \,|G|\, \boldsymbol{a}_j \rangle$ in the basis of the set $\{\boldsymbol{a}_i\}$ becomes the input for the EFM routine which generates eigenvectors of "symmetrized positions", i.e. bases for irreducible representations of G.

$$\text{EFM:} \quad \langle \boldsymbol{a}_i \,|G|\, \boldsymbol{a}_j \rangle \rightarrow a_i^{(\nu\mu)\kappa} \tag{3.37}$$

Here and in the following discussion, the superscripts of symmetry adapted solutions denote the particular vector, e.g. its symmetry type, and subscripts run over vector components. The eigenvectors $a_i^{(\nu\mu)\kappa}$, $i = 1...N_a$ are labeled by (ν, μ) which indicates the symmetry of the solution, namely irrep ν and the partner μ; κ labels eventually multiple instances of that symmetry. These eigenvectors later will be coupled with spherical harmonics to distributed molecular orbitals. Note that here we consider $\boldsymbol{a}_i$ as a formal solid object so that the representation under investigation comprises $N_a = |G|/|G(\boldsymbol{a}_i)|$ permuting points and not the $3N_a$ mutually transforming vector components. In fact, one might have obtained the same result by investigating a representation of the group G in the algebra space of the factor group $G/G(\boldsymbol{a}_i)$, [170, Section 1.8] operating directly with cosets instead of a particular set of vectors $\{\boldsymbol{a}_i\}$. Even though there may be several "*unique*" atoms in a molecule, the symmetry types of the sets $\{\boldsymbol{a}_i\}$ are obviously limited by the number of the possible subgroups $G(\boldsymbol{a}_i) \subset G$.

Another prerequisite for the construction of symmetrized molecular orbitals is the symmetrization of the spherical harmonics. Here, the differences between orbitals and spinors have to be looked at more closely. It is natural to use atomic reference orbitals or at least basis functions of the same spherical symmetry for the construction of molecular orbitals. However, the types of functions that appear in the non-relativistic atomic model and in the spin-orbit model differ: these are the spherical harmonics Y_{jm} in the non-relativistic case and the two-spinors Ω_{jm} in the spin-orbit case. Both types are eigenfunctions of the angular momentum operator and their transformation properties (for both integer and half-integer angular momentum values) are assumed to be known as functions of the quaternion (rotation) parameters. The EFM may be applied to reduce bases of vector (integer j) as well as projective (half-integer j) representations. However, we first restrict ourselves to spherical harmonics of integer j keeping in mind that a similar procedure applies also for spherical spinors of half-integer j.

In fact, in ParaGauss real spherical harmonics C_{jm} are used instead of the complex harmonics Y_{jm}. The former are simple combinations of the latter; nevertheless, the transformation properties of C_{jm} differ slightly from those of Y_{jm}. Once a group representation in the space of $\{C_{jm},\ m = -j \ldots j\}$ is constructed, it is used by the EFM procedure to generate irrep bases.

$$\text{EFM:} \quad \langle C_{jm_1} \,|G|\, C_{jm_2} \rangle \rightarrow y_{jm}^{(\nu\mu)\kappa} \tag{3.38}$$

The CSCO eigenfunctions $y_{jm}^{(\nu\mu)\kappa}$, $m = -j \ldots j$, where the labels have the same meaning as above in Eq. (3.37) are symmetrized spherical harmonics. As indicated above, such symmetrized "atomic" orbitals will be now coupled with the symmetrized "positions vectors" to yield molecular orbitals.

Now, the central observation is: the function space generated by the atomic orbitals $|jm\boldsymbol{a}_i\rangle := \chi_{jm}(\boldsymbol{r}-\boldsymbol{a}_i)$ of some angular momentum j centered on every symmetry equivalent atom $\boldsymbol{a}_i$ of set $\{\boldsymbol{a}_i\}$ is a direct product of two vector spaces: the position vector space and the orbital space of a particular j-shell. The symmetrization in this product space is conveniently carried out with the help of the Clebsch-Gordan coefficients $c^{(\nu\mu)\kappa}_{(\nu_1\mu_1)(\nu_2\mu_2)}$ which govern the reduction of the product of the two participating irreps, specifically the κ-instance of irrep ν in the product of irreps ν_1 and ν_2: $(\nu_1)\otimes(\nu_2) = \bigoplus_{\nu\kappa}(\nu)_\kappa$. Expressed literally, molecular orbitals originating from j-shell orbitals of a "*unique*" atom a read:

$$|\nu\mu, kaj\rangle := \sum_{i=1}^{N_a} |\nu\mu, k\boldsymbol{a}_i j\rangle := \sum_{i=1}^{N_a}\sum_{m=-j}^{+j} d_{ai\,jm}^{(\nu\mu)k}\,|jm\boldsymbol{a}_i\rangle \tag{3.39}$$

Here, k represents the combined index $(\kappa, \nu_1, \nu_2, \kappa_1, \kappa_2)$ of multiple instances of the (ν, μ) symmetry. The coefficients $d_{ai\,jm}^{(\nu\mu)k}$ are evaluated as

$$d_{ai\,jm}^{(\nu\mu)\kappa\nu_1\nu_2\kappa_1\kappa_2} = \sum_{\mu_1\mu_2} c^{(\nu\mu)\kappa}_{(\nu_1\mu_1)(\nu_2\mu_2)} a_i^{(\nu_1\mu_1)\kappa_1} y_{jm}^{(\nu_2\mu_2)\kappa_2} \tag{3.40}$$

The indices ν_1 and ν_2 of the factors are not good "quantum numbers" for our purpose, so we simply subsume them into the multiplicity index k. In fact, once the quantum numbers (ν_1, ν_2) are recognized as unessential, the flexibility of the EFM allows an alternative approach to symmetrized molecular orbitals: provided the transformation properties of the position vectors $\{\boldsymbol{a}_i\}$ and the spherical harmonics $\{C_{jm}\}$ are known, one may skip the separate symmetrizations of $\{\boldsymbol{a}_i\}$ and $\{C_{jm}\}$ and *first* construct a representation of the product space which then is reduced by the EFM. Actually, this strategy would be quite similar to the work done when one computes the Clebsch-Gordan coefficients; therefore, we ignore this alternative.

Now that the symmetrized molecular orbitals have been constructed, the basis representation of any totally symmetric operator V is a block-diagonal matrix with respect to irrep index ν and partner μ:

$$\langle\nu\mu, k|V|\nu'\mu', k'\rangle = \langle\nu, k||V||\nu, k'\rangle\delta_{\nu\nu'}\delta_{\mu\mu'}. \tag{3.41}$$

Only the reduced matrix elements $V^{(\nu)}(k, k') := \langle\nu, k||V||\nu, k'\rangle$ need to be computed, stored, and processed. Because the matrix elements are independent of the partner in-

dex μ the following equation for "average over partners" holds:

$$\langle \nu\mu, k|V|\nu\mu, k'\rangle = \frac{1}{h_\nu}\sum_{\mu'}\langle \nu\mu', k|V|\nu\mu', k'\rangle \tag{3.42}$$

To rationalize this, note that any symmetry transformation g applied to a matrix element of the operator $V(\boldsymbol{r})$ can be expressed via the matrix elements of $V(g^{-1}\boldsymbol{r}) \equiv V(\boldsymbol{r})$; on the other hand, g applied to the basis function gives a linear combination of irrep partners

$$g|\nu\mu, k\rangle = \sum_{\mu'}|\nu\mu', k\rangle D^{(\nu)}_{\mu'\mu}(g)\,. \tag{3.43}$$

Selection rules, Eq. (3.41), and the unitarity of representation matrices $D^{(\nu)}(g)$ immediately gives the "average over partners" rule, Eq. (3.42). The real value of Eq. (3.42) lies in the following: the "average" may be evaluated for the symmetry "irreducible" part $\tilde{V}(\boldsymbol{r})$ of the totally symmetric operator $V = \sum_{g\in G}\tilde{V}(g^{-1}\boldsymbol{r})$. In the case of numerical integration of the exchange-correlation potential V_{xc} over a grid of points, this allows a substantial reduction of the number of integration points in space to the symmetry inequivalent subset of them.

The symmetry of the position vectors (or, better, the distance vectors) is used to reduce the number of primitive integrals needed to construct symmetry-adapted matrix elements $\langle \nu\mu, kaj|V|\nu\mu, k'bj'\rangle$ of some totally symmetric operator V. Leaving out non-pertinent indices k, k', j, and j', the symmetrized matrix element may be expressed as:

$$\langle \nu\mu, a|V|\nu\mu, b\rangle = \frac{1}{h_\nu}\sum_{\mu\, ik}\langle \nu\mu, \boldsymbol{a}_i|V|\nu\mu, \boldsymbol{b}_k\rangle \tag{3.44}$$

$$= \frac{N_a}{h_\nu}\sum_{\mu\, k}\langle \nu\mu, \boldsymbol{a}_1|V|\nu\mu, \boldsymbol{b}_k\rangle \tag{3.45}$$

$$= \frac{N_a N(1,k)}{h_\nu}\sum_{\mu\, k}{}'\langle \nu\mu, \boldsymbol{a}_1|V|\nu\mu, \boldsymbol{b}_k\rangle \tag{3.46}$$

First, the "average over partners" rule, Eq. (3.42), was invoked and the basis functions were separated as sums over "one-center" contributions, Eq. (3.39). Then, the integral was restricted to the "irreducible" part of it: only the contribution of $\boldsymbol{a}_1$ of the N_a symmetry-equivalent atoms of type a was factorized; at last, the sum Σ' over k was limited to one of the $N(1,k)$ atoms of type b generated by the "little group" $G(\boldsymbol{a}_1)$ which leaves $\boldsymbol{a}_1$ invariant [176].

3.3.2 Pseudo 2D Representations

Non-ambivalent groups, e.g. (abelian) cyclic groups of higher orders C_n, $n \geq 3$ or some polyhedral groups (e.g. T), are characterized by pairs of complex conjugate one-dimensional irreps ${}^1E(g) = {}^2E(g)^*$, $g \in G$. The corresponding irrep bases generated from spherical harmonics are, in general, complex functions, complex-conjugate for the conjugate irreps. However, in the absence of a magnetic field, the molecular Hamiltonian is invariant with respect to time reversal or, equivalently, with respect to complex conjugation of the orbital wavefunctions. Hence, all energy levels are doubly degenerate. This degeneracy allows us to combine complex *eigenfunctions* into real functions, which are still eigenfunctions of the original Hamiltonian. With due caution, one may perform a similar procedure for the *basis functions* at the early stages to avoid calculations in the domain of complex numbers. This is done by introducing so-called *pseudo-2D* irreps, which can be made real. A pseudo-2D representation is obtained by a unitary rotation of the joint bases of the two conjugate irreps. If the functions a and a^* are bases of the irreps ${}^1E$ and ${}^2E$, respectively, then the basis (b_{re}, b_{im}) is real:

$$\begin{pmatrix} b_{re} \\ b_{im} \end{pmatrix} = \frac{1}{\sqrt{2}} \begin{pmatrix} 1 & 1 \\ -\mathrm{i} & \mathrm{i} \end{pmatrix} \begin{pmatrix} a \\ a^* \end{pmatrix} = \sqrt{2} \begin{pmatrix} \mathcal{R}(a) \\ \mathcal{I}(a) \end{pmatrix} \tag{3.47}$$

$\mathcal{R}$ and $\mathcal{I}$ designate real and imaginary parts. However, because the functions b_{re} and b_{im} are both combinations of functions of two irreps, matrix elements of a totally symmetric operator are, in general, nonzero between them. In the original basis of size n, the matrix representation of a totally symmetric operator contains two $n \times n$ complex matrices, one being the conjugate of the other. In the pseudo-2D basis the corresponding matrix representation is a $2n \times 2n$ matrix built of n 2×2-blocks.[2] Each 2×2 block may be obtained from its diagonal representation in the (a, a^*) basis with the pair of complex conjugate values (c, c^*) on the diagonal by applying the similarity transformation form Eq. (3.47):

$$\begin{pmatrix} c & \\ & c^* \end{pmatrix} \rightarrow \frac{1}{2} \begin{pmatrix} c + c^* & \mathrm{i}(c - c^*) \\ -\mathrm{i}(c - c^*) & c + c^* \end{pmatrix} = \begin{pmatrix} \mathcal{R}(c) & -\mathcal{I}(c) \\ \mathcal{I}(c) & \mathcal{R}(c) \end{pmatrix} \tag{3.48}$$

Another efficient approach to work with pseudo-2D bases (and other, e.g. spinor, bases exhibiting time-reversal symmetry) would be a quaternion transformation [177].

A similar procedure is also used in ParaGauss to render irrep bases and irrep matrices real for other (higher) symmetries in cases where canonical irrep matrices are complex-valued. This situation occurs if the canonical subgroup chain contains a non-ambivalent

[2] Or, equivalently, of 4 $n \times n$ blocks. Then c and c^* in the equations below should be considered as $n \times n$ matrices.

group, which happens rather frequently. However, for higher symmetries where complex-conjugate (time reversal) partners belong to the same irrep and the transformation does not mix *irreps*, there is no need for a specific treatment of the resulting matrix representations. The real-valued basis is still irreducible and all symmetry selection rules apply without any changes. An alternative way to arrive at real irrep bases is to choose a subgroup chain different from the canonical one.

3.3.3 Symmetrized Molecular Spinors

One possible procedure for creating symmetrized molecular spinors is analogous to that just described for orbitals. Starting from position vectors and atomic *spinors* Ω_{jm} with half-integer (j, m) and proceeding along the same lines, one arrives at $|\tilde{\nu}\tilde{\mu}, kaj\rangle$ which are now two-component complex spinors constructed from the j-shells of atoms $\boldsymbol{a}_i$. We use $(\tilde{\nu}, \tilde{\mu})$ here to denote projective irreps and partners, respectively. CG coefficients $c^{(\tilde{\nu}\tilde{\mu})\kappa}_{(\nu_1\mu_1)(\tilde{\nu}_2\tilde{\mu}_2)}$ for products of vector and projective irreps are required to couple position vectors and (half-integer) angular momentum functions. Just as in the case of orbitals, any totally symmetric operator is diagonal in the irrep index $\tilde{\nu}$ (now projective) and partner index $\tilde{\mu}$. However, there are important differences between spinors and orbitals which have great consequences for the computational savings achieved by symmetrization. First, matrix elements of operators are in general complex-valued. Second, for the point groups, there are normally less projective irreps than vector irreps; thus, there are less independent blocks and they are on average of higher dimensions which reduces the computational savings. Finally, introducing spin coordinates already in the eigenfunctions Ω_{jm} of $\boldsymbol{j}^2 = (\boldsymbol{l} + \boldsymbol{s})^2$ effectively doubles the size of the basis. For a treatment of spin-orbit interaction, such doubling of the size of the basis by the spin components is unavoidable, in principle. However, only the spin-orbit operator couples spin components and hence by its nature requires a double-sized spinor basis from the very beginning. Spin-free operators (i.e. operators diagonal in the spin components) are naturally represented in an orbital basis of normal size. Therefore, in the following, we will present a procedure to construct a symmetrized spinor basis which allows us to exploit directly the spin-free character of such operators as the nuclear attraction V_{nuc}, the kinetic energy $p^2/2$, the Hartree potential V_H and the exchange-correlation potential V_{xc}, all of which are used throughout in (normal) quantum chemistry calculations.

The spin of an electron, parametrized as a column vector $u \in \mathbb{C}^2$, forms a projective representation $SU(2)$ of the full rotation group $SO(3)$. This is the same representation as the two-dimensional basis $D^{(1/2)}$ of angular momentum eigenfunctions with $j = 1/2$. Even when restricted to a finite point group G, we will refer to the spin rotation representation

$SU(2) \downarrow G \equiv D^{(1/2)} \downarrow G$ as $D^{(1/2)}$ or, later on, as (σ) to emphasize its spin origin.

Eigenfunctions of half-integer angular momentum j in spherical symmetry may be considered as irrep bases of the reduced direct product:

$$D^{(l)} \otimes D^{(1/2)} \rightarrow D^{(l-1/2)} \oplus D^{(l+1/2)}. \tag{3.49}$$

($D^{(j)}$ denotes an irrep carried by angular momentum eigenfunctions of eigenvalue j, $D^{(-1/2)}$ is a placeholder.) In angular momentum theory, this procedure is usually referred as LS coupling [122]. The same obviously holds for representations $D^{(j)}$ subduced to the finite point group G; however, that does not imply the irreducibility of $D^{(j)}$. Thus, instead of a reduction of a given basis of eigenfunctions of half-integer j, one might follow the standard two-step procedure, *direct product* $\rightarrow$ *reduction*, for the pure spinor and pure orbital bases.

The view of molecular spinor space as a direct product of three items — (i) orbital momentum eigenfunctions, (ii) different spin states, (iii) localization on a particular atom —, opens the possibility to couple them in various ways. To discuss different coupling schemes, we introduce the following notations for the symmetry-related quantum numbers of different spaces:

- $\bar{L}$ shall designate the symmetry-related atomic quantum numbers. It corresponds to the orbital angular momentum (l, l_z) in the spherically symmetric case and to the irrep and partner indices (ν, μ) of symmetrized spherical harmonics $y_{jm}^{(\nu\mu)\kappa}$, Eq. (3.38), in the case of point groups.

- $\bar{S}$ shall designate the spin state quantum numbers. It corresponds to the spin variables (s, s_z) in the spherically symmetric case. The spin rotation representation $D^{(1/2)}$ of $SO(3)$ subduced to point group G is an *irreducible* two-dimensional representation $D^{(1/2)} \downarrow G$ for point groups of interest. Two irrep partners are, thus, also interpreted as two spin states (Kramer's partners).

- $\bar{J}$ shall designate spinor state quantum numbers. It corresponds to total angular momentum (j, j_z) in the spherically symmetric case and to projective irrep and partner indices $(\tilde{\nu}, \tilde{\mu})$ in the case of point groups.

- $\bar{K}$ shall designate "rotational" or position vector quantum numbers. It corresponds to (ν, μ) of the symmetrized position vectors $a_i^{(\nu\mu)\kappa}$, Eq. (3.37). It is specific for molecular systems and has no counterpart in the angular momentum theory.

In the case of spherical symmetry, one commonly couples $\bar{L}$ and $\bar{S}$ to obtain eigenfunctions of the total angular momentum $\bar{J}$. With a slight generalization one may use an analogous terminology for any group G. In Section 3.3.1, we showed how to construct

symmetrized molecular orbitals by coupling $\bar{L}$ and $\bar{K}$, the symmetrized spherical harmonics and the symmetrized position vectors, respectively. We also mentioned that similar to $\bar{L}\bar{K}$ coupling one may use $\bar{J}\bar{K}$ coupling to produce symmetrized molecular spinors. The latter procedure may be implemented as $(\bar{L}\bar{S})\bar{K}$ coupling or even as $\bar{J}\bar{K}$ coupling if $\bar{J}$ eigenfunctions are given *a priory*. However, one can proceed via an alternative route to symmetrized molecular spinors, e.g. by $(\bar{K}\bar{S})\bar{L}$ coupling. We claim, however, that $(\bar{L}\bar{K})\bar{S}$ is a superior coupling scheme in cases where one wants to exploit the symmetry of the spin-free operators to full extent.

Recall that in cases without spin-orbit interaction $\bar{L}\bar{K}$ coupling leads to symmetrized molecular orbitals (Section 3.3.1). After subsequent coupling with spin $\bar{S}$, one obtains symmetrized spinors with well defined quantum numbers $\bar{L}\bar{K}$ which characterize the symmetry of the spatial components of the spinors. Because spin-free operators do not operate on spin components, their matrix representations will be diagonal in the coupled $\bar{L}\bar{K}$ quantum numbers (see Section 3.2.4 and below). With a proper choice of phases, those matrix elements will be equal to their counterparts in the non-relativistic case and, consequently, are necessarily real.

Suppose $\{|\nu\mu\rangle, \mu = 1...h_\nu\}$ is a set of molecular orbitals of (ν, μ) which refer to the coupled $\bar{L}\bar{K}$ labels, characterizing the symmetry of the product functions; the specific values of the quantum numbers $\bar{L}$ and $\bar{K}$ are irrelevant in the current context. If one now takes possible spin states $\{|\alpha\rangle := u^\alpha \in \mathbb{C}^2, \alpha = 1...2\}$ transforming as $D^{(1/2)}$ in G and examines the product space, one finds (e.g. with an EFM-based strategy) symmetrized spinors:

$$|\nu\tilde{\nu}\tilde{\mu}\rangle = \sum_{\mu\alpha} c^{(\tilde{\nu}\tilde{\mu})}_{(\nu\mu)(\sigma\alpha)} |\alpha\rangle|\nu\mu\rangle \tag{3.50}$$

Here, we use σ to denote the spin representation $D^{(1/2)}$; the quantities $c^{(\tilde{\nu}\tilde{\mu})}_{(\nu\mu)(\sigma\alpha)}$ are CG coefficients of $(\nu) \otimes (\sigma) \rightarrow \bigoplus(\tilde{\nu})$. We will keep the index ν in $|\nu\tilde{\nu}\tilde{\mu}\rangle$ because we will see that this is a good quantum number for our purposes. One should pay attention to the following aspects: (i) we did not yet clarify the question of the reducibility of $D^{(1/2)}$, (ii) there is no index of multiple instances of the same $(\tilde{\nu}, \tilde{\mu})$ in CG coefficients. The two-dimensional representation $D^{(1/2)}$ is irreducible for most point groups [174]. Exceptions are the abelian groups C_n, C_{nh}, and S_n where it necessarily reduces to two different one-dimensional complex-conjugate irreps. In C_1 and C_i with a certain gauge, the representation $D^{(1/2)}$ reduces to the two instances of a trivial unity irrep. On the other hand, the product of a vector and a projective irrep does not contain multiple instances of any other projective irrep [174]. With this in mind, there is no need for a multiplicity index of the CG coefficients, even if $D^{(1/2)}$ is reducible. C_1 is the special case; there, one may introduce Kramer's conjugation (equivalent to time reversal [177]) to establish a relation

between different spin states that build an "irrep".

The matrix representation of a totally symmetric spin-free operator V is diagonal in the spin coordinates, $\langle\alpha|V|\beta\rangle = V\delta_{\alpha\beta}$; therefore, in the $|\nu\tilde{\nu}\tilde{\mu}\rangle$ basis one has:

$$\langle\nu\tilde{\nu}\tilde{\mu}|V|\nu'\tilde{\nu}\tilde{\mu}\rangle = \sum_{\mu\mu'}\sum_{\alpha} c^{(\tilde{\nu}\tilde{\mu})*}_{(\nu\mu)(\sigma\alpha)} c^{(\tilde{\nu}\tilde{\mu})}_{(\nu'\mu')(\sigma\alpha)} \langle\nu\mu|V|\nu'\mu'\rangle \tag{3.51}$$

$$= \delta_{\nu\nu'}\sum_{\mu\alpha}\left|c^{(\tilde{\nu}\tilde{\mu})}_{(\nu\mu)(\sigma\alpha)}\right|^2 \langle\nu\mu|V|\nu\mu\rangle \tag{3.52}$$

$$= \delta_{\nu\nu'}\langle\nu||V||\nu\rangle \tag{3.53}$$

Here, we used the symmetry properties of V, in particular, the block-diagonal structure of the matrix representation in the symmetry indices (ν,μ) and the fact that the matrix elements are independent of μ. We also employed the orthonormalization condition of the CG coefficients $\sum_{\mu\alpha} c^{(\tilde{\nu}\tilde{\mu})*}_{(\nu\mu)(\sigma\alpha)} c^{(\tilde{\nu}'\tilde{\mu}')}_{(\nu\mu)(\sigma\alpha)} = \delta_{\tilde{\nu}\tilde{\nu}'}\delta_{\tilde{\mu}\tilde{\mu}'}$ [170, Section 3.16]. The quantity $\langle\nu||V||\nu\rangle$ denotes the symmetry-reduced matrix representation of V in the orbital basis of symmetry ν, i.e. exactly the same representation which appeared in the non-relativistic case, Section 3.3.1.

This finding was presented in Section 3.2.4 as the result of a possible choice of $(V, C, \tilde{C}, \tilde{C}(s))$ (with a spin-free operator V) as CSCO of the spinor space. The commuting operators V and C have common eigenvectors. Thus, in *any* basis of eigenvectors of C the matrix elements of V vanish between subspaces which correspond to different eigenvalues of C.[3] These eigenvalues label the vector irreps in the EFM theory.

With such spinor basis, the symmetry-reduced matrix representation of V is block-diagonal in both irrep indices $\tilde{\nu}$ *and* ν, the latter being the orbital symmetry where the spinors originate from. Last but not least, there are no accidental phase shifts, so that $V^{(\nu\tilde{\nu})}(k,k') = V^{(\nu)}(k,k')$. For example, V is represented by a real matrix, because the orbital basis was chosen to render $V^{(\nu)}(k,k')$ real. Phase shifts do not occur because we used the same (CG) coefficients for all subspaces $\{|\nu\mu,k\rangle,\ \mu = 1...h_\nu\}$ of different k to generate spinors. Independent reduction of each product space $\{u^\alpha\}\otimes\{|\nu\mu,k\rangle\}$ allows more freedom for the choice of phases. In other words, the sole fact that $(V, C, \tilde{C}, \tilde{C}(s))$ is a CSCO is not enough for making any statement about the phases of the matrix elements of V in the basis of $(C, \tilde{C}, \tilde{C}(s))$ eigenfunctions.

General symmetry considerations would only suggest a block structure for the matrix representation of the totally symmetric V with respect to the total spinor symmetry $\tilde{\nu}$: $V = \bigoplus_{\tilde{\nu}} V^{(\tilde{\nu})}$. Our specific choice of a basis ensures that each $V^{(\tilde{\nu})}$ is still block-diagonal in the other quantum number ν: $V^{(\tilde{\nu})} = \bigoplus'_{\nu} V^{(\nu)}$ where summation runs over such ν that

[3] Of course, the opposite also holds: matrix elements of C vanish between different eigenspaces of V.

$(\nu) \otimes (\sigma) \ni (\tilde{\nu})$.

As an example, let us consider the case of C_{4v}. In Figure 3.1, we present a schematic decomposition of a totally symmetric operator represented in a spinor basis which was constructed in the manner proposed above [Eq. (3.50)] using C_{4v} symmetry as an example. The block decomposition of the matrix representation depicted in Figure 3.1 illustrates the selection rules for the matrix elements based on the symmetry of the basis functions. The block decomposition of the *reduced* matrix elements is depicted in Figure 3.1: the trivial dependence of the matrix elements on the partner indices μ and μ' corresponding to the factor $\delta_{\mu\mu'}$ in Eq. (3.41) is omitted. Only the shaded blocks of the matrix representation in Figure 3.1 are non-zero for symmetry reasons; therefore, only these matrix elements need to be evaluated and stored. For a general totally-symmetric operator (including spin coupling ones), the matrix representation reduces to two independent blocks represented by the two large light-grey squares. This is, for example, the block structure of a Hamiltonian that includes spin-orbit interaction. For an operator which does not couple spin components, further restriction on the block structure apply: only the subblocks which are also diagonal in the vector irrep indices (labels) differ from zero. These subblocks are exactly the same as those which appear in the block-reduction of the same operator in the *orbital* basis without resorting to spinors and projective symmetries (double groups). They are of the same dimensions determined by the size of the orbital basis and are filled with the same (real) values. Therefore, the two instances of the e-subblocks (depicted as hatched squares), one belonging to the $e_{1/2}$ block, the other to the $e_{3/2}$ block, — are necessarily identical. In fact, both originate from the same orbital basis of e symmetry by coupling with the spin coordinates in different fashion: $(e) \otimes (\sigma) \to (e_{1/2}) \oplus (e_{3/2})$ (σ, as always, denotes the spin functions).

3.3.4 Symmetrized Molecular Four-Spinors

The implementation of the relativistic counterpart of the Coulomb self-interaction (Section 2.1.4) requires a representation of some operators in four-component space. Here, we briefly discuss the essential issues of how one constructs and symmetry adapts four-spinor bases for representing operators of the DKS Hamiltonian.

The DKH transformation of the DKS Hamiltonian $h = \boldsymbol{\alpha p}c + \beta c^2 + V$ involves computing matrix elements of some operators in the momentum space (Section 2.1.2). As an example, we examine the product $AK\boldsymbol{\alpha p}V\boldsymbol{\alpha p}KA$ where A and K are some functions of p^2; this operator is a part of the DKH Hamiltonian [Eqs. (2.35) and (2.36)]. Following the strategy of Hess (Section 2.2.2) the matrix elements of such an operator product are

Figure 3.1: Layout of a *reduced* operator representation in the spinor basis with well-defined spatial symmetry quantum numbers. C_{4v} symmetry is chosen as an example: a_1, a_2, b_1, b_2, and e are the vector irrep labels; $e_{1/2}$ and $e_{3/2}$ are the projective irrep labels. Blocks with an irrep label inside represent basis function/spinor indices of that symmetry. Spinor basis functions are constructed from the corresponding symmetrized orbital functions. The representation of a generic totally symmetric operator reduces to two non-zero blocks, diagonal in the projective irreps $e_{1/2}$ and $e_{3/2}$. Spin-free operators are additionally restricted to the subblocks diagonal in vector irreps. Moreover, the two hatched subblock instances originating from the same *orbital* basis e are identical. The pattern corresponding to selection rules with respect to partners of multi-dimensional irreps is not shown.

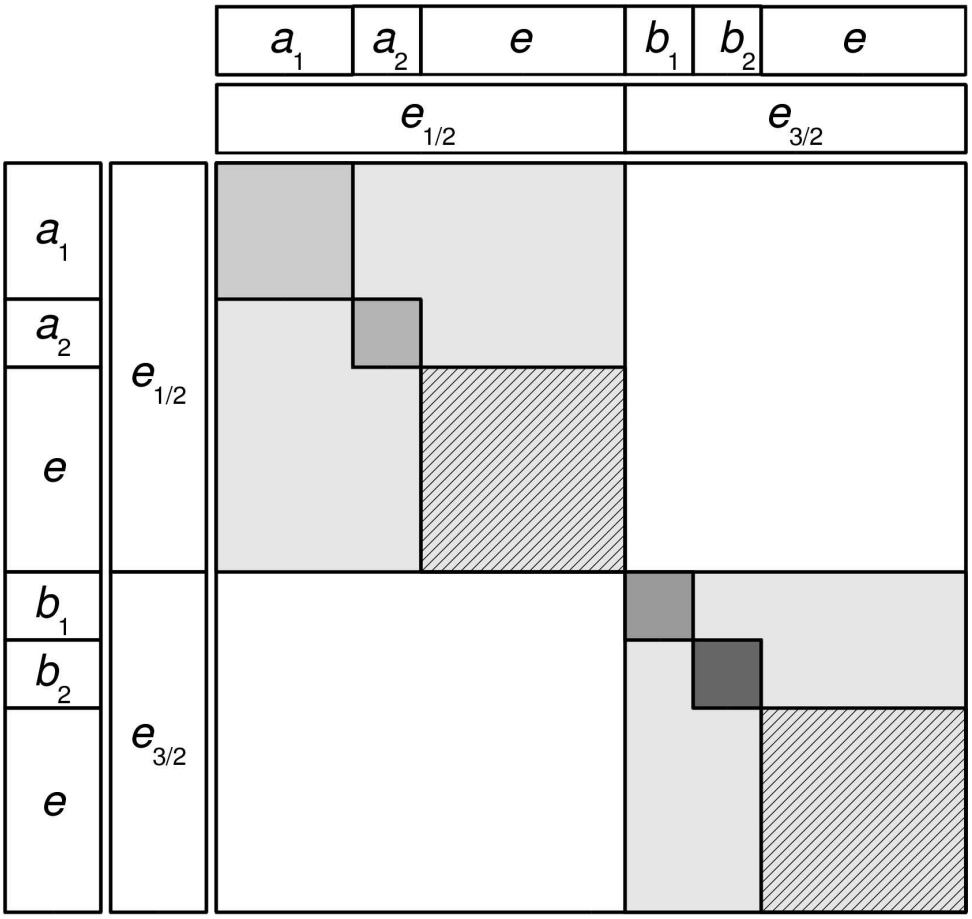

evaluated by invoking the resolution of the identity:

$$\langle p\,|AK\boldsymbol{\alpha p}V\boldsymbol{\alpha p}KA|\,q\rangle \approx \sum_{p'q'} \langle p\,|AK|\,p'\rangle\,\langle p'\,|\boldsymbol{\alpha p}V\boldsymbol{\alpha p}|\,q'\rangle\,\langle q'\,|KA|\,q\rangle\,. \tag{3.54}$$

For a basis functions $|p\rangle$ represented as a linear combination of Gaussian-type functions, it is possible to evaluate the expression $\langle p'\,|\boldsymbol{\alpha p}V\boldsymbol{\alpha p}|\,q'\rangle$ directly (analytically) for some potentials V, e.g. for the Coulomb $1/r$. Alternatively, one invokes once again the resolution of identity and constructs the "matrix of a product" as a "product of matrices"; this procedure implies a basis representation of the primitive operators $\boldsymbol{\alpha p}$ and V. We have implemented the first alternative for the nuclear attraction potential and the second alternative for the Hartree potential in ParaGauss.

A matrix representation of the odd operator $\boldsymbol{\alpha p}$ implicitly introduces small components into the calculations. For example, $\boldsymbol{\alpha p}$ is used for the evaluation of the relativistic counterpart of the fitted contribution F_{rel} [cp. Eq. (2.128)]:

$$F_{rel} \approx F_{LL} + \ldots (\boldsymbol{\alpha p})_{LS} F_{SS} (\boldsymbol{\alpha p})_{SL} \ldots \tag{3.55}$$

where L and S denote the large and small components, respectively. This notation brings out the block structure of the relevant operators in terms of large and small components of four-spinors. Note that only totally symmetric operators (in the sense of a "double group") enter the last equation. For example, the $\boldsymbol{\alpha p}$ operator can be viewed as a scalar product of two vectors (see related discussion in Section 2.2.3).

There is obviously "more symmetry" in the potential V than just the spatial symmetry when its four-component structure is considered. As a totally symmetric operator, V commutes with all symmetry transformations: $[V, g] = 0$, $\forall g \in G$. Moreover, as a four-component operator $V = V(\boldsymbol{r})\delta_{\alpha\beta}$ is diagonal in the four components, $\alpha, \beta = 1 \ldots 4$, with a single function on the diagonal. That is V is a spin-free operator, $[V, \boldsymbol{\sigma}] = 0$,[4] and at the same time, V commutes with the "charge conjugation" operation

$$\gamma_5 = \mathrm{i}\gamma_0\gamma_1\gamma_2\gamma_3 = \begin{pmatrix} 0 & 1 \\ 1 & 0 \end{pmatrix} \tag{3.56}$$

which permutes large and small components (here, standard notations are used for $\gamma_0 = \beta$, $\boldsymbol{\gamma} = \beta\boldsymbol{\alpha}$ [78]):

$$[V, \gamma_5] = 0 \tag{3.57}$$

Stated differently, the blocks V_{LL} and V_{SS} of the four-component operator V are *func-*

[4] In a true four-component notation one has $[V, \boldsymbol{\Sigma}] = 0$ where $\boldsymbol{\Sigma} = \gamma_5\boldsymbol{\alpha} = \left(\begin{smallmatrix} \boldsymbol{\sigma} & 0 \\ 0 & \boldsymbol{\sigma} \end{smallmatrix}\right)$.

tionally equivalent (yet, the latter interpretation is not universal: for the *odd* operator $\boldsymbol{\alpha p}$ "charge conjugation" invariance also holds, $[\boldsymbol{\alpha p}, \gamma_5] = 0$). However, if the bases for large and small components were chosen independently, the *matrices* V_{LL} and V_{SS} would not be related in any simple way. There are some considerations in favor of a particular choice of the small component basis, which are based on "kinetic balance" arguments [178]. These arguments rely on the fact that small components ψ_S and large components ψ_L are approximately related by

$$\psi_S \approx \gamma_5 \boldsymbol{\sigma p} \psi_L / 2c \tag{3.58}$$

(see Section 2.2.3). Here, we explicitly introduce the "charge conjugation" γ_5 to swap large and small components. One implication of this "kinetic balance" relation is that the *spatial* parts of large and small components exhibit opposite parity because of the factor $\boldsymbol{p}$ which is a real vector. Of course, a four-spinor as a whole can have only one parity, if any. Therefore, symmetrized basis functions for "electronic" and "positronic" subspaces must be constructed such that this parity difference is accounted for. No other "kinetic balance" restrictions will be adopted here for construction of large- and small-component bases, except these pure symmetry considerations.

Any small-component four-spinor transforms as a plain two-component spinor under all proper rotations, but differs by a sign under improper rotations. To account for this behavior, we explicitly introduce the pseudo-scalar $\mathcal{P}$ in their definition (cp. Section 2.2.3):

$$\psi_L = \begin{pmatrix} \psi \\ 0 \end{pmatrix}, \quad \psi_S = \begin{pmatrix} 0 \\ \mathcal{P}\psi \end{pmatrix} \tag{3.59}$$

Here, ψ is a plain two-spinor, e.g. an eigenfunctions of half-integer angular momentum j in the case of an atom. In compact form, the relation of the two basis functions may be expressed by

$$\begin{aligned} \psi_S &= \gamma_5 \mathcal{P} \psi_L \\ \psi_L &= \gamma_5 \mathcal{P} \psi_S \end{aligned} \tag{3.60}$$

This is a kind of "kinetic balance" relation to be compared with Eq. (3.58). Note that $\gamma_5^2 = 1$ and $\mathcal{P}^2 = 1$.

Different transformation properties, in this case by a pseudo-scalar $\mathcal{P}$, imply a change of the irrep involved. If the spinors $\{\psi_L^{(\tilde{\nu}\tilde{\mu})} \sim \psi^{(\tilde{\nu}\tilde{\mu})} : \tilde{\mu} = 1 \ldots h_{\tilde{\nu}}\}$ form a basis of an irrep $\tilde{\nu}$, then the set of spinors $\{\psi_S^{(\tilde{\nu}'\tilde{\mu})} \sim \mathcal{P}\psi^{(\tilde{\nu}\tilde{\mu})} : \tilde{\mu} = 1 \ldots h_{\tilde{\nu}}\}$ is a small-component basis of irreducible representation $\tilde{\nu}'$ (cp. Section 2.2.3). The symbol "$\sim$" reads "transforms as", however the irrep matrices associated with the basis $\{\mathcal{P}\psi^{(\tilde{\nu}\tilde{\mu})}\}$ are not necessarily in standard form chosen for $\tilde{\nu}'$ irrep. Therefore, one needs to apply a (unitary) similarity

transformation U which maps $\psi_S^{(\tilde{\nu}'\tilde{\mu})}$ to $\psi_S^{(\tilde{\nu}'\tilde{\mu}')}$ with a different choice of partners:

$$\psi_S^{(\tilde{\nu}'\tilde{\mu}')} = \sum_{\tilde{\mu}} U_{\tilde{\mu}'\tilde{\mu}} \psi_S^{(\tilde{\nu}'\tilde{\mu})} = \gamma_5 \mathcal{P} \sum_{\tilde{\mu}} U_{\tilde{\mu}'\tilde{\mu}} \psi_L^{(\tilde{\nu}\tilde{\mu})} \tag{3.61}$$

The elements of the unitary matrix U are in fact CG coefficients of the irrep product $(\tilde{\nu})\otimes(\mathcal{P}) = (\tilde{\nu}')$, the conjugate matrix $U^\dagger$ corresponds to the irrep product $(\tilde{\nu}')\otimes(\mathcal{P}) = (\tilde{\nu})$:

$$U_{\tilde{\mu}'\tilde{\mu}} := c^{(\tilde{\nu}'\tilde{\mu}')}_{(\tilde{\nu}\ \tilde{\mu})(\mathcal{P})} = c^{(\tilde{\nu}\ \tilde{\mu})*}_{(\tilde{\nu}'\tilde{\mu}')(\mathcal{P})} \tag{3.62}$$

The inverse transformation $\psi_S^{(\tilde{\nu}'\tilde{\mu}')} \rightarrow \psi_L^{(\tilde{\nu}\tilde{\mu})}$ is obtained similar to Eq. (3.61) by replacing U with $U^\dagger$; by just interchanging subscripts L and S without changing the irrep indices [see Eq. (3.60)], two complementary transformations may be obtained: $\psi_S^{(\tilde{\nu}\tilde{\mu})} \rightarrow \psi_L^{(\tilde{\nu}'\tilde{\mu}')}$ and $\psi_L^{(\tilde{\nu}'\tilde{\mu}')} \rightarrow \psi_S^{(\tilde{\nu}\tilde{\mu})}$.

With two basis functions $\psi_{L_1}^{(\tilde{\nu}\tilde{\mu})}$ and $\psi_{L_2}^{(\tilde{\nu}'\tilde{\mu}')}$ of a large-component basis, the following selection rule holds for the matrix elements of the operator V:

$$\langle \psi_{L_1}^{(\tilde{\nu}\tilde{\mu})} | V | \psi_{L_2}^{(\tilde{\nu}'\tilde{\mu}')} \rangle = V^{(\tilde{\nu})}(L_1, L_2) \delta_{\tilde{\nu}\tilde{\nu}'} \delta_{\tilde{\mu}\tilde{\mu}'} \tag{3.63}$$

where $V^{(\tilde{\nu})}(L_1, L_2)$ is an element of the symmetry reduced matrix of operator V, specifically, of its $V_{LL}^{(\tilde{\nu})}$ block. For the corresponding small-component functions $\psi_{S_1}^{(\tilde{\nu}'\tilde{\mu}')}$ and $\psi_{S_2}^{(\tilde{\nu}'\tilde{\mu}')}$, Eq. (3.61), we only need to investigate the case of the same irrep and and partner indices of the bra- and ket-functions due to selection rules as in Eq. (3.63):

$$\begin{aligned} V^{(\tilde{\nu}')}(S_1, S_2) &:= \langle \psi_{S_1}^{(\tilde{\nu}'\tilde{\mu}')} | V | \psi_{S_2}^{(\tilde{\nu}'\tilde{\mu}')} \rangle \\ &= \sum_{\tilde{\mu}_1\tilde{\mu}_2} U^*_{\tilde{\mu}'\tilde{\mu}_1} U_{\tilde{\mu}'\tilde{\mu}_2} \langle \psi_{L_1}^{(\tilde{\nu}\tilde{\mu}_1)} | \mathcal{P}\gamma_5^\dagger V \gamma_5 \mathcal{P} | \psi_{L_2}^{(\tilde{\nu}\tilde{\mu}_2)} \rangle \\ &= (UU^\dagger)_{\tilde{\mu}'\tilde{\mu}'} V^{(\tilde{\nu})}(L_1, L_2) \\ &= V^{(\tilde{\nu})}(L_1, L_2). \end{aligned} \tag{3.64}$$

Here, we used the identity $\mathcal{P}\gamma_5^\dagger V \gamma_5 \mathcal{P} = V$ which holds because γ_5 is self-adjoint: $\gamma_5^\dagger = \gamma_5$; it commutes with V, $[V, \gamma_5] = 0$, because of its "charge conjugation" invariance, Eq. (3.57). Note again that $\gamma_5^2 = 1$. Additionally, we used the fact that the pseudo-scalar $\mathcal{P}$ commutes with V and also yields unity if squared, $\mathcal{P}V\mathcal{P} = V$. Furthermore, we used the selection rules of Eq. (3.63) and the unitarity of the CG matrix U. The only property of operator V that was used to prove Eq. (3.64) was its "charge conjugation" invariance. For a *general* operator V, not necessarily even and spin-free, but commuting with γ_5 the above holds too. Additionally, there is a similar relation for the matrix representation of the odd part

of V: $V^{(\tilde{\nu}')}(S_1, L_2) = V^{(\tilde{\nu})}(L_1, S_2)$[5] in the basis constructed according to Eq. (3.61).

In summary, if the basis set was chosen according to Eq. (3.61), one has $V^{(\tilde{\nu}')}(S_1, S_2) = V^{(\tilde{\nu})}(L_1, L_2)$ and $V^{(\tilde{\nu}')}(S_1, L_2) = V^{(\tilde{\nu})}(L_1, S_2)$ or, equivalently,

$$V_{SS}^{(\tilde{\nu}')} = V_{LL}^{(\tilde{\nu})} \tag{3.65}$$

$$V_{SL}^{(\tilde{\nu}')} = V_{LS}^{(\tilde{\nu})} \tag{3.66}$$

between the corresponding blocks of irrep $\tilde{\nu}'$ and the *coupled* irrep $\tilde{\nu}$: $(\tilde{\nu}) \otimes (\mathcal{P}) = (\tilde{\nu}')$. This relation was used in Section 2.2.3 where two coupled irreps were processed at the same time for optimal performance and memory requirements.

The reader who wonders why one should apply transformation U if it always enters the final expressions in the combination $UU^\dagger = 1$ should recall that we considered only matrix elements which are diagonal in partner index $\tilde{\mu}$ as allowed by the symmetry selection rules. Selection rules are not immediately applicable if the partners within different subspaces, e.g. $\{\psi_L^{(\tilde{\nu}\tilde{\mu})}\}$ and $\{\psi_S^{(\tilde{\nu}\tilde{\mu}')}\}$, were not chosen consistently.

The odd operator $\boldsymbol{\alpha p}$ is also "charge conjugation" invariant. As is always the case for a totally symmetric operator, the blocks LS and SL of $\boldsymbol{\alpha p}$ need to be computed and stored only for pairs of four-spinors which exhibit the same symmetry $\psi_L^{(\tilde{\nu}\tilde{\mu})}$ and $\psi_S^{(\tilde{\nu}\tilde{\mu})}$. In the corresponding two-component picture, the pseudo-vector character of $\boldsymbol{\sigma}$ in $\boldsymbol{\sigma p}$ is canceled by the pseudoscalar $\mathcal{P}$ which is due to the small-component function $\psi_S^{(\tilde{\nu}\tilde{\mu})}$.

3.4 Implementation

3.4.1 Symmetrization Coefficients

In ParaGauss, a module is implemented to construct symmetry adapted functions of LCAO-type, starting with spherical harmonics, for orbitals, spinors, and four-spinors. Any symmetry-adapted function

$$|\nu\mu, k\rangle = \sum_q^Q d_q^{(\nu\mu)k} |q\rangle \quad \nu \le N,\ \mu \le h_\nu,\ k \le K_\nu \tag{3.67}$$

is internally represented as a set of indexed coefficients $d_q^{(\nu\mu)k}$ of its expansion in the basis $\{|q\rangle,\ q \le Q\}$. The indices of such coefficients include the symmetry indices (irrep ν and partner μ), index q of the original representation basis $|q\rangle$, and, eventually, index k which identifies one of $K_\nu \ge 0$ functions of the same symmetry. The coefficients $d_q^{(\nu\mu)k}$

[5] Not to be confused with $V^{(\tilde{\nu})}(S_1, L_2)^* = V^{(\tilde{\nu})}(L_2, S_1)$ for the SL and LS blocks of the *same* irrep which holds for any Hermitean V in any basis.

may be organized as a set of one-dimensional Fortran arrays $d^{(\nu\mu)k}(1:Q)$[6] with array elements $d^{(\nu\mu)k}(q)$, two-dimensional arrays (matrices) $d^{(\nu)k}(1{:}Q, 1{:}h_\nu)$ with array (matrix) elements $d^{(\nu)k}(q,\mu)$, or even three-dimensional arrays $d^{(\nu)}(1:Q, 1:h_\nu, 1:K_\nu)$ with array elements $d^{(\nu)}(q,\mu,k)$. Note that array bounds h_ν and K_ν depend on ν so that adding a forth dimension $\nu \le N$ to the array is not straightforward. However, if a unique mapping $(\nu\mu k) \leftrightarrow p$ of multiple indices onto a single one is established in some way, all the coefficients fit into a single square matrix $d(1{:}Q, 1{:}Q)$ with elements $d(q,p) = d_q^{(\nu\mu)k}$. (In some cases, e.g. when only functions of totally symmetric type are considered, the ranges of q and p may differ, rendering the matrix rectangular.)

The symmetrization procedure is a unitary transformation of the original, unsymmetrized basis. The unsymmetrized basis and thus the resulting symmetrized basis may be either orthogonal or non-orthogonal. The symmetrization procedure should be distinguished from the orthogonalization, although it enforces partial orthogonality according to the symmetry selection rules. The unitary matrix $u(q,p)$ for the symmetrization of the basis,

$$\{|\psi_q\rangle\} \rightarrow \bigoplus_{\nu\kappa}(\nu) = \bigoplus_{\nu\kappa}\{u_q^{(\nu\mu)\kappa},\ \ \mu \le h_\nu\}, \tag{3.68}$$

is a square matrix with the combined index $p = (\nu\mu\kappa)$ which in addition to the symmetry indices $(\nu\mu)$ comprises a counter κ for the instance of ν. The matrix elements $u_q^{(\nu\mu)\kappa}$ fit the layout of the structures described above for symmetrized functions. In fact, the expansion coefficients of the symmetrized functions may be considered as elements of (unitary) matrix implementing the symmetrizing transformation.

The original (unsymmetrized) representation basis $|q\rangle$ may actually be indexed by a combined index $q = (im)$ (i.e. a multiple index), to account for the underlying direct product representation of the basis: $|q\rangle = |i\rangle|m\rangle$. To construct coefficients of the symmetrized LCAO orbitals, Eqs. (3.39), (3.40), we considered direct products of position vectors $\{\boldsymbol{a}_i\}$ of a symmetry equivalent set of atoms a and spherical harmonics $\{C_{jm}\}$ with angular momentum j, Section 3.3.1. Taking all symmetry equivalent atom types a and all angular momentum shells j into consideration, the complete expansion basis $|q\rangle$ is indexed by tuple ranges $q_{aj} = (im)$. The LCAO coefficients, Eq. (3.40), are stored for each a and j either as matrices $d^{(\nu)\kappa aj}(q,\mu)$ or as three-dimensional arrays $d^{(\nu)\kappa aj}(i,m,\mu)$.[7,8]

The symmetrized spinors constructed from the symmetrized orbitals also match the

[6] We make use of Fortran syntax $1:Q$ to denote array bounds and conventional indexing $d^{(\nu\mu)k}$ of different arrays.

[7] It would be sufficient to compute and store LCAO *symmetrization* coefficients for *distinct* types a of "unique" atoms $\{\boldsymbol{a}_i\}$, e.g. for four-fold equatorial atoms, axial atoms and so on.

[8] The Fortran feature, that a three-dimensional array $A(i,j,k)$ of size $M \times N \times K$ may also be accessed as a two-dimensional array $A(ij,k)$ of size $(MN) \times K$, allows seamless switching from one representation to another.

direct product scheme. Indeed, the CG coefficients of the direct product of the vector irrep ν and the spin "irrep" σ, reduced to the projective irrep $\tilde{\nu}$, $c^{(\tilde{\nu}\tilde{\mu})}_{(\nu\,\mu)(\sigma\alpha)}$, Eq. (3.50), stored as arrays $c^{(\tilde{\nu})\nu}(\mu,\alpha,\tilde{\mu})$ with triple index $(\mu,\alpha,\tilde{\mu})$ of corresponding irrep partners, may be equally well viewed as the α-component ($\alpha = \pm 1/2$) of the $(\tilde{\nu}\tilde{\mu})$ spinor, expanded over the partners μ of the orbital representation space (ν).

The general CG coefficients $c^{(\nu\mu)\kappa}_{(\nu_1\mu_1)(\nu_2\mu_2)}$ for the (vector or projective) irrep product $(\nu_1)\otimes(\nu_2) \rightarrow (\nu)_\kappa$ are similarly represented by arrays of coefficients $c^{(\nu)\kappa\nu_1\nu_2}(\mu_1,\mu_2,\mu)$, indexed by the three indices (μ_1,μ_2,μ), two of which, $(\mu_1\mu_2)$, label basis functions $|\mu_1\rangle|\mu_2\rangle$ of the product space $(\nu_1)\otimes(\nu_2)$.

The index structures of the symmetrized bases $d^{(\nu\mu)k}_q$, symmetry transformation matrices $u^{(\nu\mu)k}_q$, and CG coefficients $c^{(\nu\mu)\kappa}_{(\nu_1\mu_1)(\nu_2\mu_2)}$ based on their common origin as basis transformations —, they all allow sharing of processing methods and storage structures between at first glance different objects.

The two basic structures used in ParaGauss for symmetry adaptation are transformation matrices $u^{(\nu)\kappa}(q,\mu)$ in general and CG coefficients $c^{(\nu)\kappa}(\mu_1,\mu_2,\mu)$ as a special case for direct product spaces (tuple index $q = (\mu_1\mu_2)$ implemented as double index). The diversity of objects used in the symmetry part of the code, the symmetrized spherical harmonics and the atomic positions, the symmetrized orbitals, large- and small-component spinors, the CG coefficients for vector and projective irreps, — including the special case of projective representation $SU(2)$, not necessarily irreducible —, may be represented by these structures and processed by unified methods.

In the following, we will discuss the details of the symmetrization in cases where spin-orbit interaction is treated explicitly. Then three types of the CG coefficients are computed and stored in module `clebsch_gordan.f90`:

`cg`(ν,ν_1,ν_2) — structure to store CG coefficients $c^{(\nu\mu)\kappa}_{(\nu_1\mu_1)(\nu_2\mu_2)}$ for vector-vector irrep products $(\nu_1)\otimes(\nu_2) \rightarrow (\nu)_\kappa$. The coefficients for particular subspace κ of the reduced product are stored in the structure component[9] `%sub(`κ`)%c(`μ,μ_1,μ_2`)`. The array of subspaces `%sub(:)` is of size `%mult` which may be zero. This type of the CG coefficients is used when symmetrized spherical harmonics of integer angular momentum l and symmetrized atomic positions are coupled to build symmetrized molecular orbitals.

`vpcg`$(\tilde{\nu},\nu_1,\tilde{\nu}_2)$ — structure to store CG coefficients $c^{(\tilde{\nu}\tilde{\mu})\kappa}_{(\nu_1\mu_1)(\tilde{\nu}_2\tilde{\mu}_2)}$ for vector-projective irrep products $(\nu_1)\otimes(\tilde{\nu}_2) \rightarrow (\tilde{\nu})_\kappa$. The coefficients for particular subspaces of the reduced

[9] Modern Fortran implementations allow structured variables of user-defined types with several components of arbitrary types. The typed variable `A` may be declared with integer and real components `A%Int` and `A%Real`.

product are stored in the structure components `%sub(`κ`)%c(`$\tilde{\mu}, \mu_1, \tilde{\mu}_2$`)`. The complex coefficients may be accessed via `%z(`$\tilde{\mu}, \mu_1, \tilde{\mu}_2$`)` or via the real and imaginary parts `%re(`$\tilde{\mu}, \mu_1, \tilde{\mu}_2$`)` and `%im(`$\tilde{\mu}, \mu_1, \tilde{\mu}_2$`)`, respectively. This type of the CG coefficients is used when symmetrized spherical harmonics of half-integer angular momentum j (spherical spinors) and symmetrized atomic positions are coupled to build the symmetrized molecular spinors.

`vsu2cg(`$\tilde{\nu}, \nu$`)` — structure to store CG coefficients $c^{(\tilde{\nu}\tilde{\mu})}_{(\nu_1\mu_1)(\sigma\alpha)}$ for vector-projective representation products $(\nu_1) \otimes (\sigma) \rightarrow (\nu)$, where $(\sigma) \equiv SU(2) \downarrow G$ is a pure spin rotation representation. The coefficients for particular subspaces of the reduced product are stored in the structure components `%sub(`κ`)%c(`$\tilde{\mu}, \mu_1, \alpha$`)`. The complex coefficients may be accessed via `%z(`$\tilde{\mu}, \mu_1, \alpha$`)` or via the real and imaginary parts `%re(`$\tilde{\mu}, \mu_1, \alpha$`)` and `%im(`$\tilde{\mu}, \mu_1, \alpha$`)`, respectively. This type of the CG coefficients is used to couple properly symmetrized (molecular) orbitals with the spin components; such coupling also results in symmetrized (molecular) spinors.

Algorithm 3.1 represents the pseudo-code used for generating the symmetrized spinor coefficients $d^{(\tilde{\nu})k}(q, \alpha, \tilde{\mu})$ of the expansion in the basis of products $|\alpha\rangle|q\rangle$ [cp. Eq. (3.50)] from the previously obtained orbital coefficients $d^{(\nu)k}(q, \mu)$ of the expansion in some basis $|q\rangle$ with the help of the spin coupling CG coefficients $c^{(\tilde{\nu}\tilde{\mu})\kappa}_{(\nu\mu)(\sigma\alpha)}$ which are stored as $c^{(\tilde{\nu})\kappa\nu}(\mu, \alpha, \tilde{\mu})$. The orbital coefficients were assumed to be taken for a particular atomic shell $\{\boldsymbol{a}_i\} \otimes \{C_{lm}\}$, Eqs. (3.39), (3.40); however, this is not necessary as the coefficients may represent any set of symmetrized orbitals.

3.4.2 Transformation from an Orbital Representation to a Spinor Representation

The ordering of the basis functions used by ParaGauss to store operator matrix representations is outlined in Algorithm 3.2. Basis sets for different irreps are handled separately and, most of the time, the distinction of the partners within an irrep may be ignored. The coarsest division is by the group of symmetry equivalent atoms $\{\boldsymbol{a}_i\}$. This range of basis functions is partitioned into atomic shells of different angular momentum $\{\boldsymbol{a}_i\} \otimes \{C_{lm}\}$. The latter may be eventually split into several independent subspaces k of the same symmetry $\{\boldsymbol{a}_i\} \otimes \{C_{lm}\} \rightarrow (\nu)_k$. Finally the radial dependence of the functions is addressed, which, depending on the situation, is the number of uncontracted exponents of the basis or the number of contracted functions. The only essential difference of the pseudo-code between orbital and spinor bases is the origin of the number of irrep instances within an atomic shell. For orbitals, this is the number of times a (vector) irrep appears in the direct

Algorithm 3.1: Pseudo-code for obtaining symmetrized spinors from symmetrized orbitals.

!! INPUT: symmetrized molecular orbitals $d^{(\nu)k}(q,\mu)$
!! combined index $q=(im)$ *runs over pairs* $i\in\{\boldsymbol{a}_i\}$, $m\in\{C_{lm}\}$ *of a shell* $\{\boldsymbol{a}_i\}\otimes\{C_{lm}\}$
!! OUTPUT: symmetrized molecular spinors $d^{(\tilde{\nu})k}(q,\alpha,\tilde{\mu})$
!! $\alpha=\pm1/2$ *is the spinor component*

```
forall ProjectiveIrreps ν̃ do:                          !! irrep of resulting spinor
   k_proj = 0                                           !! no instances of ν̃ yet
   forall VectorIrreps ν and
   forall IrrepInstances k_vec in d^(ν)k_vec and        !! over instances of (ν) ∈ {a_i} ⊗ {C_lm}
   forall IrrepInstances κ in c^(ν̃μ̃)κ_(νμ)(σα) do:     !! is empty if (ν̃) ∉ (ν) ⊗ (σ)
    k_proj = k_proj + 1                                 !! there will be one more instance of (ν̃)
    forall SpinorComponents α in (±1/2) and             !! obtain spinor expansion coefficients
    forall ProjectivePartners μ̃ in ProjectiveIrrep ν̃ and
    forall BasisFunctions q do:                         !! d^(ν̃)k_proj(q,α,μ̃) for all partners μ̃
      d^(ν̃)k_proj(q,α,μ̃) = Σ_μ d^(ν)k_vec(q,μ)c^(ν̃)κν(μ,α,μ̃)   !! is a matrix product
    done forall                                         !! over (μ̃,α,q)
 done forall                                            !! over (ν,k_vec,κ)
done forall                                             !! over (ν̃)
```

product $\{\boldsymbol{a}_i\}\otimes\{C_{lm}\}$; for spinors, it *may* be computed as number of (projective) irrep instances in $\{\boldsymbol{a}_i\}\otimes[\{C_{l+1/2,m}\}+\{C_{l-1/2,m}\}]$, or, preferentially, determined by counting instances in $[\{\boldsymbol{a}_i\}\otimes\{C_{lm}\}]\otimes(\sigma)$; the latter strategy is consistent with the way the spinors are generated.

This particular ordering of the basis functions actually destroys the clear block structure of the spin-free operators in the spinor representation.[10] The spinor ordering by atomic shells is a straightforward extension of the ordering of orbitals. However, atomic basis functions of each shell are combined into molecular orbitals of several (vector) irreps. When coupled with spin to spinors of certain projective irrep, such a shell may in general contain spinors of several *spatial* symmetries. The spinors of the next atomic shell in a sequence will be also of different spatial symmetries. The ordering of spinors by atomic shells and the ordering by their spatial symmetry are, in effect, two exclusive ordering schemes. Thus, the block structure of spin-free operators which was implied, for example, in Figure 3.1 is not immediately visible in the default ordering. To preserve such a block structure, spinors have to be ordered according to their spatial symmetry. Algorithm 3.3

[10] Indeed, it renders the matrix *sparse*, but not *full*. Selection rules still hold, of course.

Algorithm 3.2: Pseudo-code to order orbital basis functions and spinor basis functions.

```
for Irreps ν = 1..N_irr do:                    !! irrep bases are largely independent
  k = 0                                        !! reset counter for irrep ν
  for AtomGroups a = 1..N_a do:                !! loop over atomic ...
    for AngularMomentumShells l = 0..l_max(a) do:   !! ... shells
      !! here access to symmetry reduced orbitals or spinors of atomic shell required
      for IrrepInstances κ in {a_i} ⊗ {C_lm} → (ν)_κ do:  !! this may be empty
        for RadialFunctions r = 1..N_cont do:    !! fully contracted basis
          !! irrep partners μ not counted!
          k = k + 1                            !! add another function to counter
          !! k is the order of |νμ; a, l, κ, r⟩ = |νμ; k⟩
        done for
      done for
    done for
  done for
  SizeOf(ν) = k                                !! final number of functions for irrep ν
done for
```

Algorithm 3.3: Pseudo-code to generate an alternative order of the spinor basis functions which emphasizes block structure of matrix representation of spin-free operator as in Figure 3.1.

```
for ProjectiveIrreps ν̃ = 1..N_proj do:         !! irrep bases are largely independent
  k = 0                                        !! reset counter for irrep ν̃
  for VectorIrreps ν = 1..N_vec do:            !! vector irreps of orbitals
    for Instances κ in (ν) ⊗ (σ) → (ν̃)_κ do:   !! typically 1 or 0, one or none
      for Orbitals q = 0..SizeOf(ν) do:        !! already ordered orbitals
        !! irrep partners μ̃ not counted!
        k = k + 1                              !! add another spinor to counter
        !! k is the order of |νν̃μ̃; k⟩ built of {|νμ; q⟩, μ = 1 ... h_ν}
      done for
    done for
  done for
  SizeOf(ν̃) = k                                !! final number of spinors for irrep ν̃
done for
```

displays the pseudo-code for such alternative ordering of the basis spinors. There, it is assumed that the basis orbitals are already somehow ordered, e.g. by Algorithm 3.2.

For historical reasons, the spinors in ParaGauss are not ordered as just described in Algorithm 3.3, but rather analogous to Algorithm 3.2. However, the "clean" ordering of the spinors according to the spatial symmetry is used as an intermediate step on the way from the orbital representation of the spin-free operator to its spinor representation. With an alternatively ordered spinor basis, this transformation is carried out just by copying the orbital representation matrices to the proper position within the spinor representation matrix. Then, one only needs to apply twice a permutation to rows and columns of the resulting matrix to obtain the representation in the spinor basis which is ordered according to atomic shells. In this way, the representation matrix V_{xc}[11] is generated, but any other spin-free operator may be treated in the same way.[12]

3.5 Application to Numerical Integration of the Exchange-Correlation Potential

One of the most time-consuming tasks in Kohn–Sham calculations is the construction of the matrix representation of the exchange-correlation (xc) potential V_{xc}. The nonlinear dependence of the xc functional

$$E_{xc} = \int d^3\boldsymbol{r}\, e_{xc}(\rho, \boldsymbol{\nabla}\rho) \tag{3.69}$$

and of the resulting potential

$$V_{xc} = \left[\frac{\partial}{\partial\rho} - \boldsymbol{\nabla}\frac{\partial}{\partial\boldsymbol{\nabla}\rho}\right] e_{xc} \tag{3.70}$$

on the density and the density gradients makes a numerical integration over a spatial grid indispensable. To avoid higher derivatives of the density by explicit evaluation of V_{xc}, one transforms integrals involving the potential to

$$\int d^3\boldsymbol{r}\, V_{xc} g = \int d^3\boldsymbol{r} \left(\frac{\partial e_{xc}}{\partial\rho} g + \frac{\partial e_{xc}}{\partial\boldsymbol{\nabla}\rho}\boldsymbol{\nabla} g\right) =: \int d^3\boldsymbol{r}\, (ag + \boldsymbol{b}\boldsymbol{\nabla} g) \tag{3.71}$$

[11] Implemented for triangular storage mode of symmetric matrices in module `xc_ham_trafo.f90`.

[12] The emphasis of this work was the efficient evaluation of V_{xc} matrix elements since it has to be repeated every SCF iteration. Other operators, e.g. kinetic energy or potential of density fit functions are only evaluated once. Of course, all spin-free operators are represented as real block-diagonal matrices similarly to V_{xc}. This fact is, however, exploited only for V_{xc}.

where the scalar a and the vector $\boldsymbol{b}$ represent (real) functions of $\boldsymbol{r}$. After discretization, the integral $\int d^3\boldsymbol{r}$ turns into a weighted sum $\sum_i w(\boldsymbol{r}_i)$ over the grid points $\boldsymbol{r}_i$; the discretized weight function $w(\boldsymbol{r}_i)$ may be conveniently integrated into the definition of $a(\boldsymbol{r}_i)$ and $\boldsymbol{b}(\boldsymbol{r_i})$. Then the matrix elements $V(m,n) = \langle\psi_m|V_{xc}|\psi_n\rangle$ of the potential V_{xc} are evaluated approximately as the sum

$$\sum_i \left(\psi^\dagger_{mi} a_i \psi_{ni} + \boldsymbol{b}_i \boldsymbol{\nabla}(\psi^\dagger_{mi}\psi_{ni})\right) = \sum_i \psi^\dagger_{mi}\left(\frac{1}{2} a_i \psi_{ni} + \boldsymbol{b}_i \boldsymbol{\nabla}\psi_{ni}\right) + \text{c.c. of } m \leftrightarrow n \qquad (3.72)$$

Subscript i indicates the point $\boldsymbol{r}_i$ at which the function to be integrated is evaluated. The omitted term on the r.h.s. is obtained by complex conjugation of the first term after interchanging indices m and n. Thus, one may efficiently obtain all the matrix elements $V(m,n)$ by a single matrix multiplication step of quantities indexed by (m,i) and (n,i) and subsequent rendering to a Hermitean quantity: $V(m,n) := V(m,n) + V^*(n,m)$. Very efficient implementations of such a matrix multiplication are available in special libraries [126, 127]. The integration is performed for all partners within each irrep. The target quantity is the "average over partners" $\sum_\mu \langle\psi^{(\nu\mu)}_m|V_{xc}|\psi^{(\nu\mu)}_n\rangle$, see Eq. (3.42); at the price of having to deal with all partners μ of an irrep, one is able to reduce the number of grid points to be processed to only the "unique" wedge of the grid, i.e. to those points that are not equivalent by symmetry.

The derivation above is applicable irrespective of what the basis functions are, symmetrized two-component complex spinors $\psi^{(\tilde\nu\tilde\mu)}_m$ or symmetrized real orbitals $\phi^{(\nu\mu)}_n$. In the latter case, complex conjugation has no effect, of course. The computational expense of the integration is quite different in these two cases: every multiplication of two real numbers in case of an orbital integration corresponds to a sum of four products for both the real and the imaginary parts of the result in case of two-spinors. The number of memory references increases accordingly: instead of fetching two real numbers one needs two numbers (real and imaginary parts) for each of the two spinor components of both participating operands. These simple arithmetic does not take into account the fact that the dimension of the problem (basis size of the irrep) is often larger in a spin-orbit calculation than in a standard run, i.e. a non-relativistic or a scalar relativistic calculation. Therefore, the integration step is a promising candidate for applying the formalism discussed above to exploit the spin-free character of operators, V_{xc} being such an operator.

Let the real functions a and $\boldsymbol{b}$ be given; they are characteristic of the spin-free potential V_{xc}. The computational task of computing the representation $V^{(\nu)}(m,n)$ of V_{xc} in the orbital basis $\phi^{(\nu\mu)}_m$ is independent of the origin of a and $\boldsymbol{b}$; these "parameters" may be computed using non-relativistic or spin-orbit densities (density gradients). In a spin-orbit calculation, the matrix $V^{(\nu)}(m,n)$ is exactly the representation $V^{(\nu\tilde\nu)}(m,n)$ one is after,

Table 3.2: Timings of essential parts of relativistic calculations for the example of Au_{13} in O_h symmetry.[a] Comparison of various types of calculations: SO, SO exploiting the spin-free character of V_{xc}, and scalar relativistic (SR) variants. The columns "Integration", "Orbitals", and "Density" correspond to the separate parts of the SCF procedure: integration of V_{xc}, evaluation of the basis orbitals on the grid and the density,[b] respectively. "SCF" refers to the whole SCF part. "Total" is the total time for the calculation; the number of SCF iterations is given in parentheses. Percentages are relative to the total time of the run. SO speed up factors compare SO with and without special treatment of V_{xc}; SR speed up factors compare the SR to the faster SO variant.

	Integration	Orbitals	Density	SCF	Total
SO plain	7802	1066	877	9843	10221 (23)
	76%	10%	9%	96%	
SO spin-free	63	1296	883	2340	2711 (23)
	2%	48%	33%	86%	
SR	52	193	23	276	303 (21)
	17%	64%	8%	91%	
SO speed up	124.8	0.8	1.0	4.2	3.8
SR speed up	1.1	6.1	35.3	7.7	8.2

a) CPU timings in seconds for a parallel run on 3 Pentium 4 (833 MHz) processors.
b) most time consuming step is evaluation of eigenfunctions from the basis functions.

provided the spinor-basis $\psi_m^{(\nu\tilde{\nu}\tilde{\mu})}$ is constructed from the orbital basis $\phi_n^{(\nu\mu)}$ by adding spin coordinates in the fashion described above: $(\nu)\otimes(\sigma) \rightarrow (\tilde{\nu})$. To compute the representation $V^{(\nu)}(m,n)$ in the orbital basis one may re-use the non-relativistic procedure and concentrate on optimizations at a single place.

In Table 3.2 we present timings of three calculations on Au_{13}: SO with a "totally symmetric V_{xc}", SO with "totally symmetric and spin-free V_{xc}", and an SR calculation. Although they give exactly the same results, the total time of the two SO calculations differ by a factor of 3.8. Three major numerical integration tasks, namely the integration of the *xc* matrix, the evaluation of basis orbitals/spinors, and the evaluation of the density, determine the SCF performance to a large extent; together, they take 80–90% of the total time. Of those three numerical tasks in a plain SO calculation, the integration consumes 76% of the total time; the two other tasks, evaluation of the orbitals and the density require 10% and 9%, respectively. If one exploits the implications of the spin-free character of the potential V_{xc}, these relations change drastically: in a "SO spin-free" approach, the integration takes less than 2% of the time, the evaluation of the orbitals and the density consume 48% and 33%, respectively. The integration step shows a speed up of more than a factor of hundred, partly because of the reuse of the highly optimized non-relativistic code;

in absolute terms, it takes hardly more time than in a SR calculation. The requirement of both spinors and orbitals to be computed on the grid in the "SO spin-free" case increases the time for that part by about 20%. With the option to exploit the spin-free character of the potential V_{xc}, SO calculations are still about 8–9 times more expensive than SR calculations.[13]

Finally we note that in noncollinear spin-density functional theory with the energy functional $E_{xc} = \int d^3\boldsymbol{r}\, e_{xc}(\rho, s)$ where $s = |\boldsymbol{s}|$ is the spin-density $\boldsymbol{s} = (1/2)\sum_{\varepsilon}^{occ} \psi_{\varepsilon}^{\dagger}\boldsymbol{\sigma}\psi_{\varepsilon}$, the potential V_{xc} has spin-coupling terms (which may also lower the symmetry):

$$V_{xc} = \left[\frac{\partial}{\partial\rho} + \frac{\boldsymbol{\sigma}\boldsymbol{s}}{s}\frac{\partial}{\partial s}\right] e_{xc} \; . \tag{3.73}$$

The commutator of V_{xc} and the Pauli matrices is

$$[V_{xc}, \boldsymbol{\sigma}] = 2\mathrm{i}\frac{[\boldsymbol{\sigma} \times \boldsymbol{s}]}{s}\frac{\partial e_{xc}}{\partial s} \neq 0 \tag{3.74}$$

Such a potential is not invariant under rotations in spin space, i.e. it is not a spin-free operator. Hence, the strategy discussed above for spin-free operators is not applicable in the case of noncollinear SO.

3.6 Further Applications

In this section, we discuss applications of the symmetry formalism developed above which have not yet been implemented in the code.

Two-component spin-orbit implementations in the spirit of the DKH approach (see Chapter 3) allow one to explore the symmetry of spin-free operators at several stages. The only spin-coupling contribution of the DKH transformation is $\boldsymbol{\sigma}[\boldsymbol{p}V_{nuc} \times \boldsymbol{p}]$. For other operators, e.g. the spin-free counterpart $\boldsymbol{p}V_{nuc}\boldsymbol{p}$ of this operator, the kinetic energy, the nuclear attraction, the Coulomb field of the electron density, and the overlap, one may use representation in the orbital basis. One advantage is immediate: a representation in the orbital basis requires less storage because the matrices are real and of lower dimensions.

Further advantages may be illustrated when one considers the diagonalization of the kinetic energy matrix $T = p^2/2$ which is an essential step in the DKH strategy, Section 2.2.2. The solution of the eigenvalue problem is performed in three steps: diagonalization of overlap matrix S required for the canonical orthogonalization of the basis, transformation of the kinetic matrix T to this orthogonal representation, and diagonalization of T (Section

[13] Further improvement may be expected if calculation of the basis spinors (spinor gradients) at grid points is avoided. Basis spinors are later combined into (spinor) eigenfunctions to obtain the density (density gradients). Alternatively, basis orbitals may be combined into eigenfunctions directly.

2.2.2). The overlap S as a spin-free "operator" is represented in spinor basis by a block-diagonal matrix:

$$S = \bigoplus_{\tilde{\nu}} S^{(\tilde{\nu})} = \bigoplus_{\tilde{\nu}} {\bigoplus_{\nu}}' S^{(\nu)} \tag{3.75}$$

where the sum $\bigoplus'_\nu$ is over those irreps ν that fulfill $(\tilde{\nu}) \in (\nu) \otimes (\sigma)$, Section 3.3.3. Diagonalization of the block diagonal (and real) matrix S is achieved by a real orthogonal matrix U which is also block-diagonal:

$$U = \bigoplus_{\tilde{\nu}} {\bigoplus_{\nu}}' U^{(\nu)} \tag{3.76}$$

Here, each $U^{(\nu)}$ diagonalizes corresponding $S^{(\nu)}$:

$$U^{(\nu)\dagger} S^{(\nu)} U^{(\nu)} = s^{(\nu)} \tag{3.77}$$

with diagonal matrices $s^{(\nu)}$. The orthogonalization of the kinetic energy matrix

$$T \to s^{-1/2} U^\dagger T U s^{-1/2} \tag{3.78}$$

and the subsequent diagonalization are performed block-wise.

The matrix of the transformation to momentum space

$$P = \bigoplus_{\tilde{\nu}} {\bigoplus_{\nu}}' P^{(\nu)} \tag{3.79}$$

may thus be obtained block-wise by operating with the real matrices of the orbital representation. This transformation may be applied to transform the block-diagonal representation of the *spin-free* potential operator V, with a block structure equivalent to that of S in Eq. (3.75):

$$V \to P^{-1} V P \tag{3.80}$$

Moreover, the real-valued block-diagonal transformation matrix P allows savings also when one has to transform the matrix representation of a general (spin-coupling) operator V. To see that, one separates the matrix representation $V^{(\tilde{\nu})}$ into sub-blocks $V^{(\tilde{\nu})}_{\nu_1,\nu_2}$ according to the spatial symmetry of the spinors; for a spin-free V, only the blocks with $\nu_1 = \nu_2$ are non-zero. The transformation to momentum space may be performed as

$$V^{(\tilde{\nu})}_{\nu_1,\nu_2} \to [P^{(\nu_1)}]^{-1} V^{(\tilde{\nu})}_{\nu_1,\nu_2} P^{(\nu_2)} \tag{3.81}$$

where, in general, a complex matrix $V^{(\tilde{\nu})}_{\nu_1,\nu_2}$ is multiplied by the real matrices $P^{(\nu_2)}$ and

$[P^{(\nu_1)}]^{-1}$. The back-transformation of the relativistic DKH Hamiltonian may be performed similarly.

Another application, where a coherent treatment of orbital and spinor bases is advantageous, could be, for instance, a perturbation (or any other post-SCF) treatment of the SO interaction, where solutions of a converged scalar relativistic Hamiltonian are re-used in a post-SCF treatment of the SO interaction.

Chapter 4

Density Functional Study of Small Molecules and Transition Metal Carbonyls Using Revised PBE Functionals

By now, density functional theory (DFT) is a widely accepted framework for calculating ground state electronic state properties of molecules, clusters, and solids. In the Kohn–Sham (KS) approach to DFT, in principle only the exchange-correlation (xc) energy $E_{xc} = E_x + E_c$ needs to be approximated as a functional of the electron density and many variants arise from different choices of approximate xc functionals [13, 179]. For most applications in chemistry, the local (spin) density approximation (L(S)DA) has now been superceded by functionals that also depend on the local value of the density gradient (generalized gradient approximation, GGA) [13, 179, 180]. In comparison to LDA, GGA functionals tend to improve total energies, atomization energies, and energy barriers [179, 180]. GGA functionals in general yield chemical bonds slightly longer and less strong than LDA, an effect that corrects (and sometimes overcorrects) LDA predictions. Well-known and widely used gradient-corrected functionals (for short, termed conventional GGAs in the following) are combinations of Becke's gradient-corrected exchange functional [135] with correlation functionals of Perdew [136] (BP) or Lee, Yang, and Parr [181] (BLYP), or a GGA functional proper (PW91) [182].

In 1996 Perdew, Burke, and Ernzerhof (PBE) [23] presented a generalized gradient approximation for the exchange-correlation functional which exhibits a simple functional form, and where all parameters (except those the of LSDA it is based on) are fundamental constants. Only the general features of the detailed construction underlying the PW91 GGA were invoked. Improvements over PW91 include an accurate description of the linear

response of the homogeneous electron gas, the correct behavior under uniform scaling, and a smoother potential [23].

Subsequently Zhang and Yang [24] revised the original PBE functional (revPBE) to systematically improve molecular atomization energies. They suggested to discard the *local* Lieb-Oxford bound [183], an inequality linking the exchange energy density per particle to the electron density ρ at all positions $\boldsymbol{r}$:

$$\epsilon_x(\boldsymbol{r}) \geq -1.68\rho^{1/3}(\boldsymbol{r}) \tag{4.1}$$

In this way, they gained freedom for optimizing the parameter κ of the exchange energy density enhancement factor $F_x(s)$ (relative to the corresponding LSDA value),

$$F_x(s) = 1 + \mu s^2/(1 + \mu s^2/\kappa) \tag{4.2}$$

This is the general form suggested earlier by Becke [184]. Here, $s(\boldsymbol{r})$ is a dimensionless function of the density gradient which serves as a measure of "non-locality":

$$s(\boldsymbol{r}) = |\nabla\rho|/[2(3\pi^2)^{1/3}\rho^{4/3}] \tag{4.3}$$

In the original PBE functional κ is 0.804 [23], while Zhang and Yang suggested κ=1.254 [24]. Zhang and Yang chose the value of κ by fitting atomic exchange energies to "exact" values obtained by the optimized exchange potential method [185]. Becke's value is κ=0.967 [184]; his partially empirical exchange approximation also features a different value of μ=0.235 instead of 0.220 in the PBE functional. Although the revPBE functional does not obey the *local* Lieb-Oxford bound, Zhang and Yang emphasize [24] that for atoms and molecules they have found the Lieb-Oxford constraint to be fulfilled in the *integral* sense.

In 1999 Hammer, Hansen, and Nørskov [25] developed an alternative revision of the PBE functional, RPBE, which provides the same improvement of the energetics as the revPBE functional and at the same time also fulfills the Lieb-Oxford criterion locally. The construction of the RPBE functional does not involve any parameter fitting. Rather, a functional form is chosen for the exchange enhancement factor that obeys the Lieb-Oxford bound by construction,

$$F_x(s) = 1 + \kappa[1 - \exp(-\mu s^2/\kappa)], \tag{4.4}$$

with the same value κ=0.804 as in original PBE functional. Thus, $F_x(s)$ features the same asymptotic value for $s \to \infty$ as the PBE functional. In the range of small and mid-range values of s, the exchange enhancement factors of both functionals, revPBE and RPBE, are very similar and this similarity translates into very close results for molecular calculations, as we shall see in the following.

When introduced the PBE functional was shown to provide results in close similarity to the functional PW91 using a test suite of small molecules [23]. The revised functional revPBE was tested for a slightly extended set of molecules [24]. On the other hand, Hammer, Hansen, and Nørskov applied their functional RPBE only to adsorption of O_2, CO, and NO on metal surfaces using slab models. They also compared the two revised PBE functionals to the original PBE functional and to the PW91 functional. Thus, we felt that a more systematic comparison between older GGA functionals and revised PBE functionals is advisable. The present work compares the GGA functionals BP, PW91, and PBE to the two revised functionals revPBE and RPBE based on a set of small molecules. Furthermore, we extend this comparison to common test systems of organometallic chemistry, namely to carbonyl compounds of first-row transition metal atoms.

4.1 Computational Details

The calculations reported here were carried out at the all-electron level using the parallel DF program ParaGauss [20, 21]. For the small molecules, we employed rather large uncontracted Gaussian-type molecular orbital basis sets of the following sizes [186, 140]: (8s,4p,3d) for the H, (14s,9p,4d,3f) for elements of the second row, and (17s,12p,5d,4f) for elements of the third row of the periodic table. The transition metal carbonyl metals were calculated using flexible contracted Gaussian-type orbital basis sets of high quality: (21s,15p,10d,6f,4g) → [6s,5p,4d,3f,2g] for the metal atoms Cr, Fe, and Ni; (14s,9p,4d,3f) → [5s,4p,3d,2f] for C and O. All contractions were of general type based on atomic natural orbitals optimized over several states (excited, charged) [186, 140]. Although these contractions were not generated within a DF approach, a comparison of observable properties of CO as test molecule showed that contracted and uncontracted orbital basis sets yield very similar results, even for a smaller number of contracted functions.

ParaGauss employs a fitting strategy for the electron charge density to simplify the evaluation of the Coulomb contributions to the KS potential and the total energy [90, 59, 60]. The fitting basis set was derived from the orbital basis set by scaling the exponents [60]. In this way, s- and p-type functions of the molecular orbital basis set give rise to s- and d(r^2)-type fitting functions [60]. Furthermore, the fitting basis sets were augmented by polarization functions of p- and d-type located on every atom with five exponents chosen as geometrical series; p-type: 0.1 (× 2.5), and d-type: 0.2 (× 2.5) [60].

The exchange-correlation contributions to the KS Hamiltonian were evaluated by an accurate numerical integration and treated self-consistently in the Kohn–Sham procedure. For the LDA approximation, we employed the widely used VWN functional [134] as well as a very similar functional due to Perdew and Wang (PWL) [187]. All gradient-corrected

functionals contain as a primary part one or the other LDA. The *xc* functional of Becke and Perdew (BP) [135, 188, 136] is based on the VWN LDA functional; the other *xc* functionals (PW91 [182], PBE [23], revPBE [24], and RPBE [25]) are based on PWL.

Atomization energies of small molecules were calculated for experimental geometries [189, 190] to permit a consistent comparison with previous benchmark studies of the functionals PBE [23] and revPBE [24]. However, to investigate effects of the revised PBE functionals on structures and to achieve a broader comparison of various PBE-type functionals with previous GGAs (BP and PW91), we also optimized the structures of the molecules with the various *xc* functionals. All geometry optimizations were performed under appropriate symmetry constraints using gradients of the total energy.

Spin unrestricted molecular and atomic calculations were carried out for open-shell systems. In these cases the natural (spatial) symmetry of the electronic wave functions was allowed to break; for atoms this approach implies a non-spherical electron density distribution and results in a lower total energy.

4.2 Results and Discussion

4.2.1 Small Molecules

The quality of various exchange-correlation approximations as well as general trends and relations between different *xc* functionals can to some extent be illustrated by a statistical analysis of experimental and calculated results. For this purpose the same evaluation set of 19 small molecules (see Table 4.1) was used as in previous studies of PBE-type functionals [23, 24]. It comprises molecules which contain hydrogen atoms and atoms from the second row of the periodic table as well as P and Cl of the third row. Although this test set is not particularly large it provides sufficient data to draw some useful general conclusions on trends. We expect that the observed trends to be discussed in the following will hold up for other test sets albeit the average deviations among the various sets of results will change, of course.

We begin by discussing the calculated atomization energies. In Table 4.1 these results are displayed together with the corresponding experimental values. To analyze these data, we show in Table 4.2 the average deviations (AD) and the absolute average deviations (AAD) between these calculated data sets and experiment as well as among the data sets of various *xc* functionals. According to the AAD values relative to experiment (column 1, Table 4.2), the various *xc* functionals can be grouped into three set of roughly equivalent accuracy. In increasing order of accuracy these groups are LDAs (PWL, VWN) with AAD values of more than 30 kcal/mol, conventional GGAs (BP, PW91, PBE) with about 8

Table 4.1: Atomization energies (in kcal/mol) calculated with different exchange-correlation functionals.[a]

Molecule	PWL	VWN	BP	PW91	PBE	revPBE	RPBE	exp.[b]
HF	162.0	162.1	144.3	142.7	142.1	138.2	137.6	140.8
CO	299.2	299.0	264.6	269.1	269.1	259.6	258.2	259.3
LiF	156.3	156.3	138.9	140.6	138.9	133.6	133.3	138.9
LiH	60.8	60.9	58.4	54.5	53.5	53.1	53.4	57.8
N_2	267.9	267.5	238.4	243.2	243.9	234.4	233.4	228.6
F_2	78.1	78.1	51.2	53.6	53.2	46.4	45.4	38.5
H_2O	266.4	266.5	238.6	235.4	234.4	227.8	226.9	232.2
CH_4	462.1	462.4	428.9	421.5	420.2	411.9	411.0	419.3
OH	124.1	124.2	112.1	110.5	110.0	106.9	106.5	106.4
C_2H_2	459.9	459.9	414.5	415.6	415.0	402.1	400.5	405.4
P_2	144.1	144.3	119.5	122.3	121.6	115.6	114.7	117.3
C_2H_4	632.4	632.5	576.9	573.3	572.0	556.8	555.1	562.6
H_2	113.0	113.1	111.7	105.2	104.6	105.5	105.5	109.2
Cl_2	84.3	84.2	64.0	66.9	66.8	61.4	60.7	58.0
NH_3	337.3	337.4	308.4	303.1	302.2	294.5	293.7	297.4
Li_2	23.8	23.6	20.2	21.0	19.9	19.1	20.2	24.4
HCN	360.9	360.6	323.5	326.4	326.4	315.1	313.9	311.9
NO	199.6	199.3	168.2	172.4	172.9	163.8	162.7	152.9
O_2	175.3	175.2	140.2	143.8	144.3	135.3	133.9	120.5

a) Experimental geometries used throughout [189, 190]. See text for explanations of the various *xc* functionals. b) Experimental estimate corrected for the zero point vibrational energy [24, 191, 192].

Figure 4.1: Deviations of atomization energies from experiment for the test suite of small molecules as calculated by various exchange-correlation functionals: PWL, BP, PBE, RPBE, and M-GGA (see text for an explanation of the acronyms).

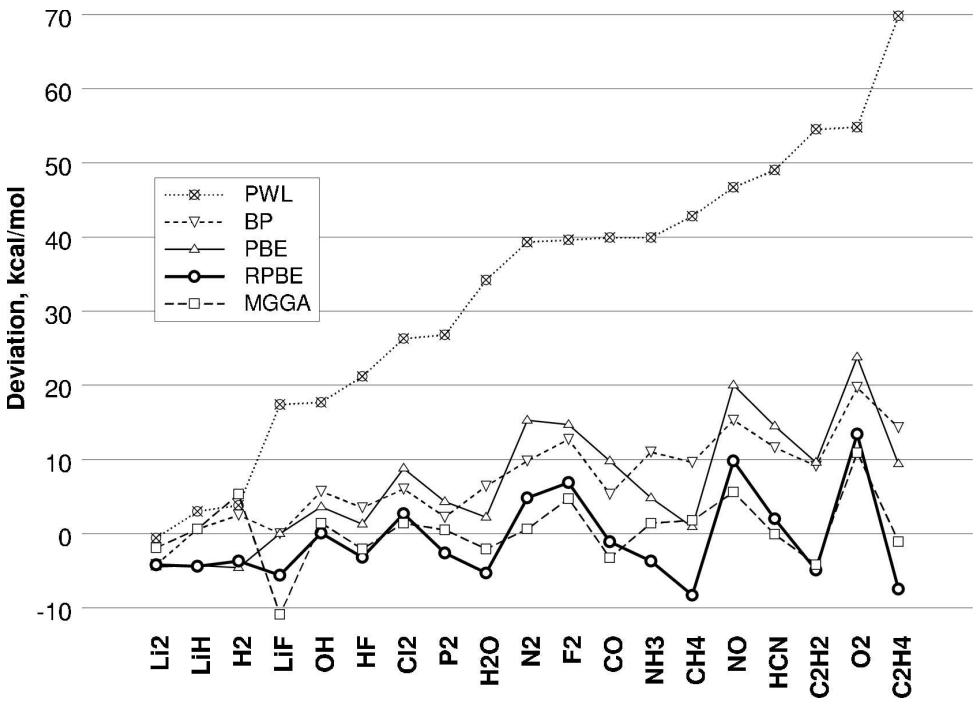

Table 4.2: Cross correlation of average absolute deviations (AAD) and average deviations (AD)[a] of atomization energies (in kcal/mol) between experiment and results of various exchange-correlation functionals.

	exp.	PWL	VWN	BP	PW91	PBE	revPBE
PWL	33.0/-33.0	0/0					
VWN	33.0/-32.9	0.2/0.1	0/0				
BP	7.9/-7.4	25.5/25.5	25.5/25.5	0/0			
PW91	8.5/-7.3	25.6/25.6	25.5/25.5	3.4/0.1	0/0		
PBE	8.2/-6.8	26.1/26.1	26.1/26.1	3.7/0.6	0.7/0.5	0/0	
revPBE	4.9/0.0	33.0/33.0	32.9/32.9	7.4/7.4	7.4/7.4	6.9/6.8	0/0
RPBE	5.0/0.8	33.7/33.7	33.7/33.7	8.2/8.2	8.2/8.1	7.7/7.6	0.9/0.8

a) Calculated as $\Delta = X_{col} - X_{row}$, where Δ is the deviation between the quantities X_{col} and X_{row} referred to by the column and row designators, respectively.

kcal/mol, and the two revised PBE functionals (revPBE, RPBE) with 5 kcal/mol. For the LDAs and conventional GGAs these facts are well known [13, 179, 180, 23]. Although not of chemical accuracy (1-2 kcal/mol), both revised PBE functionals afford a noticeable improvement of molecular energetics over conventional GGAs and they correct their general tendency to a small overbinding.

From the AD (signed, in contrast to absolute) values (Table 4.2, column 1, denominator) one concludes that LDAs and conventional GGAs on average all overestimate the atomization energies while the results of the revised PBE functionals oscillate around the experimental values. This implies another improvement introduced by the two revised PBE functionals, namely the resulting atomization energies seem almost unbiased — in a statistical sense — with respect experiment. This is demonstrated by the very small AD values, 0.0 and 0.8 kcal/mol, and becomes evident by the graphical comparison (Figure 1). In Figure 1, we also display results obtained with the meta-GGA *xc* functional that has been proposed by Perdew et al. [193] in 1999. This functional goes beyond conventional GGAs by incorporating also the kinetic energy density (via the gradients of the KS orbitals). The functional has an AAD value of 3.5 kcal/mol over the present test set of small molecules [193].

The data assembled in Table 4.2 also allow a quantification of the differences and similarities of the various *xc* functional among each other. In fact, the grouping of the various *xc* functionals into three subsets, as stated above, is convincingly supported by the corresponding AAD (and AD) values. Most obvious from the AAD value of 0.2 kcal/mol is the fact that both LDAs, PWL and VWN, indeed yield almost identical results. The

Table 4.3: Cross correlations of average absolute deviations (AAD) and average deviations (AD) of nearest-neighbor bond distances (in 10^{-3} Å) between experiment and results of various exchange-correlation functionals.[a]

	exp.	PWL	VWN	BP	PW91	PBE	revPBE
PWL	11/-3	0/0					
VWN	11/-3	0.2/-0.2	0/0				
BP	13/-12	12/-9	12/-9	0/0			
PW91	11/-10	11/-7	11/-7	2/2	0/0		
PBE	12/-11	11/-8	11/-8	1/1	1/-1	0/0	
revPBE	16/-16	15/-13	15/-13	4/-3	6/-6	5/-4	0/0
RPBE	16/-16	16/-13	16/-14	4/-4	7/-6	6/-5	1/-1

a) Layout as in Table 4.2.

conventional GGAs also exhibit rather small AADs among each other, e.g. PW91 and PBE with AAD = 0.7 kcal/mol. Yet, one also notes certain differences among them. Different construction principles underlying BP and PBE (and PW91) result in noticeable pointwise deviations which are reflected in the AAD values of 3.4-3-7 kcal/mol. Furthermore, binding energies calculated with PW91 are slightly larger than those of PBE, as shown by the PBE AD value of 0.5 kcal/mol (Table 4.2). Finally, and most important for the goal of the present study, both revised PBE functionals, revPBE and RPBE, furnish very similar molecular binding energies, with an average absolute deviation of only 0.9 kcal/mol; the RPBE AD value of 0.8 kcal/mol shows that atomization energies calculated with revPBE are on average somewhat smaller (see also Fig. 4.1).

The main improvement of revised PBE functionals over conventional GGAs seems to be more accurate molecular binding energies. Nevertheless it is interesting to also compare the geometries calculated with the various *xc* functionals and to subject these results to a similar statistical analysis. For this purpose we have carried out geometry optimizations of the same set of small molecules (see Table 4.1); the statistical analysis of these results is summarized in Table 4.3. When comparing AAD values relative to experiment (Table 4.3, column 1), we find that the members of the three classes of *xc* functionals (LDAs, GGAs, and revised PBE functionals), defined above by their increasing energy accuracy, yield AAD values for bond distances in reverse order. As noticed before [13, 179, 180], LDA structural parameters are often in better agreement with experimental data than geometries obtained by GGA functionals. Here, they show the smallest AAD value, 0.011 Å relative to experiment, while the AAD values of the conventional GGAs are slightly larger, 0.012±0.001 Å. The revised PBE *xc* functionals yield a noticeably larger value,

AAD = 0.016 Å; bond distances obtained by revised PBE functionals are on average by about 0.006 Å longer than those of GGA calculations (Table 4.3).

Compared to experiment, bond distances of all *xc* functionals investigated here turn out to be somewhat too long on average, as demonstrated by the negative AD values (Table 4.3, column 1, denominator). Bond distances within the three classes of *xc* functionals turn out to be very similar, with relative AAD values of at most 0.002 Å.

Summarizing the results for the test suite of 19 small molecules, one notes that the two goals, accurate molecular energies and structures, apparently are to some extent in conflict. Improvement of the energetics comes at the prize of slightly worse structural results. However, it is fair to say that the bond elongation of GGAs and revised PBE functionals relative to LDAs is rather moderated compared to the significant improvement achieved for molecular bond energies.

4.2.2 Transition Metal Carbonyls

While DF methods have been extensively evaluated for molecules of main group elements, much fewer tests are available for transition metal compounds (for a review see e.g. Ref. [179]). The scarcity of reliable experimental data renders benchmark studies of such systems difficult. Therefore, calculations of high accuracy may significantly ameliorate this situation.

After the overview of general features and accuracy of revised PBE *xc* functionals and their relation to conventional GGAs presented above, we now turn to applications of revised PBE functionals to transition metal carbonyl complexes. Transition metal carbonyls have been studied extensively by a variety of quantum-chemical methods [194, 195, 196, 197, 198, 199]. As a matter of fact, the first successful application of the RPBE functional was devoted to the adsorption of small molecules at transition metal surfaces where it was shown to yield significantly reduced and thus improved adsorption energies [25].

In the present work we investigated structural parameters and ligand bonding energies of the transition metal carbonyls $Cr(CO)_6$, $Fe(CO)_5$, and $Ni(CO)_4$. These species are all of high symmetry: O_h, D_{3h}, and T_d, respectively. Removal of one CO ligand leads to fragments of reduced symmetry. $Cr(CO)_5$ exhibits C_{4v} symmetry, $Fe(CO)_4$ C_{2v} symmetry, and $Ni(CO)_3$ appears to have D_{3h} symmetry.

Several *xc* functionals were employed for the calculations, PWL, PBE, revPBE, and RPBE. This choice embraces members of all three classes of *xc* functionals as established in the previous section: LDA, conventional GGA, and the two revised PBE functionals. The first bond dissociation energies calculated for the three transition metal carbonyls are summarized in Table 4.4 and compared to results of other DF calculations [198] and to

Table 4.4: First metal carbonyl bond dissociation energy (in kcal/mol) of various transition metal carbonyls.

	$Cr(CO)_6$	$Fe(CO)_5$[a]		$Ni(CO)_4$
		S	T	
VWN[b]	62.1	65.9	69.5	44.9
PWL	58.6	66.0	69.9	43.6
BP[b]	45.9	44.8	43.0	28.7
PBE	43.0	50.2	48.1	29.8
revPBE	36.9	44.2	40.4	24.6
RPBE	36.1	43.2	39.2	23.8
exp.	37±2[c]	42[c]	—	25±2[d]

a) Results for $Fe(CO)_4$ in singlet (S) and triplet (T) states. b) Ref. [196]. c) Ref. [200]. d) Ref. [201].

experiment [200, 201]. The present results were determined as total energy differences of structures that were optimized with the appropriate *xc* functional. From these data it is obvious that the LDA functionals overestimate the metal-carbonyl bonds by about 20-25 kcal/mol, as they often do for small molecules (Table 4.2). The two conventional GGAs BP and PBE significantly improve the first ligand dissociation energy, with errors of about 4-8 kcal/mol. Again, in accordance with the previous discussion for small molecules, the two revised PBE functionals reduce the bond strength by about 5-6 kcal/mol with respect to PBE and BP and bring the calculated dissociation energies in excellent agreement with experiment. The revPBE functional yields first carbonyl disassociation energies of 36.9, 40.4, and 24.6 kcal/mol for $Cr(CO)_6$, $Fe(CO)_5$, and $Ni(CO)_4$, respectively; the corresponding experimental values are 37±2, 42, and 25±2 kcal/mol [200, 201]. The alternative revision RPBE furnishes somewhat smaller dissociation energy, by about 1 kcal/mol, just as for the test suite of small molecules (Table 4.2).

The fragment $Fe(CO)_4$ presents a difficult case since it features states rather close to the ground state [196, 199, 202]. We have investigated two states, $^3B_2$ and $^1A_1$. The LDA functionals fails to correctly predict the ground state which experiment suggests to be a triplet state [203]. According to LDA, the triplet state is by about 3.6 kcal/mol higher than the singlet. GGAs correct this and furnish a stabilization of the triplet over the singlet state by 1.8 (BP of [199]), 2.1 (PBE) or even about 4 kcal/mol (revPBE, RPBE). In a conventional quantum chemical treatment this difference has been estimated to 15±5 kcal/mol [196].

For the nickel complex, we also calculated the second, third, and forth carbonyl dissoci-

Table 4.5: First metal carbonyl bond dissociation energy (in kcal/mol) of $Ni(CO)_n$ (n = 1–4) fragments.

	$Ni(CO)_4$	$Ni(CO)_3$	$Ni(CO)_2$	Ni(CO)	average
PWL	43.6	52.0	59.6	78.2	58.3
PBE	29.8	39.1	48.2	55.7	43.2
revPBE	24.6	34.2	43.3	49.1	37.8
RPBE	23.8	33.4	42.7	48.2	37.0
CCSD[a]	23.2	29.8	39.0	19.2	27.8
CCSD(T)[a]	29.8	34.6	42.6	34.5	35.4
B3LYP[b]	20.6	29.0	40.7	31.6	30.4
exp. A[c]	25±2	13±10	54±15	29±15	30±3
exp. B	25±2[c]	29±2[d]	51±4[d]	35±3[e]	35[f]
exp. C	25±2[c]	28.3±2.3[g]	47.1±5.8[g]	40.5±5.8[g]	35.2
exp. D[h]					35.3±0.6

a) Coupled clusters results of Ref. [204]. b) Ref. [205]. c) Ref. [201]. d) Ref. [206] of Ref. [204]. e) Derived from the other results of this row; see Ref. [204]. f) Ref. [206]. g) Ref. [207]. h) Ref. [208].

ation energies (Table 4.5). Experimentally, these energies seem difficult to determine; they vary noticeably from one experiment to another. Data set B (Table 4.5) originates from four different sources [201, 204, 206, 208]. Data set C, although incomplete, is likely to be most reliable [207]. While increasingly more energy is required to remove the first three ligands, the dissociation energy of the last carbonyl ligand, Ni(CO)→Ni+CO, is found drop by about 7-16 kcal/mol relative to the previous ligand (data sets B and C, Table 4.5). This difference can be rationalized if one considers the formation of the Ni-CO bond of the monocarbonyl as a combination of two steps: excitation of a free Ni atom to the bonding state d^{10} and successive ligand association [209]. For the second carbonyl the first step is not necessary and thus a stronger (second) Ni-CO bond results.

CCSD(T) results [208] reproduce the first three dissociation energies (DE) quite well; the deviation from experiment is about 4-8 kcal/mol (Table 4.5). The average dissociation energy is also well reproduced. B3LYP results [205] are of comparable quality although there is a noticeable tendency to underestimate the ligand binding energies as illustrated by the low value of the average binding energy (Table 4.5). All "pure" DF *xc* functionals fail to reproduce the drop-off of the last carbonyl dissociation energy (Table 4.5). The LDA values are much too large, but PBE values are significantly smaller, the first three DEs by about 12-14 kcal/mol and the forth DE by about 23 kcal/mol. Revised PBE functionals reduce the PBE dissociation energies even further, by a rather uniform amount

Table 4.6: Structural parameters (distances in Å, angles in degree) of $Cr(CO)_6$[a] and $Cr(CO)_5$.[b]

	$Cr(CO)_6$		$Cr(CO)_5$				
	M-C	C-O	M-C_{ax}	M-C_{bs}	C-O_{ax}	C-O_{bs}	$C_{ax}MC_{bs}$
HF[c]			1.968	1.982	1.136	1.137	91.9
MP2[c]			1.759	1.880	1.213	1.186	87.7
PWL	1.870	1.143	1.803	1.871	1.151	1.146	90.1
VWN[d]	1.866	1.145					
BP[d]	1.910	1.153					
PBE	1.909	1.152	1.842	1.910	1.159	1.154	90.8
revPBE	1.921	1.155	1.853	1.922	1.162	1.157	91.0
RPBE	1.925	1.156	1.857	1.925	1.163	1.158	91.0
exp.[e]	1.918	1.141					

a) Calculated in O_h symmetry. b) Calculated in C_{4v} symmetry with angles MCO fixed to 180°. The subscripts 'ax' and 'bs' indicate ligand atoms on the main axis and in the basal plane of the square pyramid, respectively. c) Hartree–Fock and many-body perturbation theory 2nd order; Ref. [197]. d) Ref. [199]. e) Ref. [210].

of about 5-7 kcal/mol. It is interesting to note that these revised PBE values of the second and third DEs agree very well with the corresponding CCSD(T) results (Table 4.5). It seems that the dissociation energy of Ni(CO) is particularly difficult to determine by a DF method [179] since it involves an open-shell atom with two nearly degenerate configurations d^8s^2 and d^9s^1 as well as a configuration change of the transition metal (to d^{10}) as a consequence of the bond formation (see above). Most likely the shortcomings of the DF functionals which impact the dissociation energy of Ni(CO) are due to the representation of the exchange energy, since the B3LYP method (which features a contribution of "exact" single-determinant exchange [179]) yields a drop-off of about 9 kcal/mol compared to the experimental value of about 7 kcal/mol. We refrain from further discussing these aspects in the context of the present benchmark study of revised PBE functionals; more theoretical and experimental investigations of the nickel carbonyl fragments are desirable.

Finally, we briefly describe the optimized geometries of the transition metal carbonyl complexes. The structures of saturated metal carbonyls and of the corresponding dissociation fragments were determined by imposing appropriate symmetry constraints. In addition, all angles M-C-O were fixed to 180°. This additional constraint may to some extent affect the structures of the fragments $Cr(CO)_5$ (C_{4v}) and $Fe(CO)_4$ (C_{2v}). Elimination of this degree of freedom will increase the total energy of these species and thus presumably implies a small increase of the ligand binding energy of the corresponding sat-

Table 4.7: Structural parameters (distances in Å) of $Fe(CO)_5$.[a]

	M-C_{ax}	M-C_{eq}	C-O_{ax}	C-O_{eq}
PWL	1.777	1.772	1.142	1.145
LDA[b]	1.769	1.789	1.145	1.149
PBE	1.814	1.808	1.150	1.154
BP[b]	1.819	1.816	1.153	1.157
revPBE	1.825	1.819	1.153	1.157
RPBE	1.828	1.822	1.154	1.158
exp.[c]	1.807	1.827	1.152	1.152

a) Calculated in D_{3h} symmetry with angles MCO fixed to 180°. The subscripts 'ax' and 'eq' indicate ligand atoms on the main axis and in equatorial plane of the trigonal bipyramid, respectively. b) Ref. [199]. c) See Ref. [211].

Table 4.8: Structural parameters (distances in Å, angles in degree) of $Fe(CO)_4$ in the triplet and singlet state.[a]

	State	M-C_{ax}	M-C_eq	C-O_{ax}	C-O_{eq}	$C_{ax}MC_{ax}$	$C_{eq}MC_{eq}$
PWL	$^3B_2$	1.804	1.763	1.145	1.146	151.6	97.0
LDA[b]		1.800	1.756	1.147	1.148	154.6	95.0
BP[b]		1.859	1.820	1.156	1.160	147.4	99.4
PBE		1.846	1.813	1.153	1.154	149.3	98.1
revPBE		1.859	1.827	1.155	1.156	148.7	98.3
RPBE		1.864	1.832	1.156	1.157	148.4	98.4
PWL	$^1A_1$	1.780	1.750	1.144	1.150	178.3	136.5
LDA[b]		1.775	1.746	1.146	1.152	177.0	130.2
BP[b]		1.834	1.793	1.153	1.160	167.7	129.8
PBE		1.818	1.783	1.152	1.159	172.5	134.2
revPBE		1.829	1.793	1.155	1.162	171.0	133.5
RPBE		1.832	1.796	1.155	1.163	170.6	133.3

a) Calculated in C_{2v} symmetry with angles MCO fixed to 180°. The subscripts 'ax' and 'eq' indicate atoms X of ligands which subtend the larger and smaller angle XMX, respectively, with the metal center and their symmetry equivalent partner. The bonds C_{eq}-M-C_{eq} were chosen to lie in the xz plane. b) Ref. [199].

Table 4.9: Structural data of $Ni(CO)_4$[a] and $Ni(CO)_3$[b] (distances in Å).

	$Ni(CO)_4$		$Ni(CO)_3$	
	M-C	C-O	M-C	C-O
PWL	1.786	1.140	1.768	1.142
LDA[c]	1.779	1.140	1.765	1.145
BP[c]	1.830	1.150	1.829	1.153
PBE	1.824	1.148	1.803	1.151
revPBE	1.836	1.151	1.814	1.154
RPBE	1.840	1.152	1.817	1.155
exp.[d]	1.838	1.141		

a) Calculated in T_d symmetry. b) Calculated in C_{3v} symmetry; the resulting structure exhibits essentially D_{3h} symmetry. c) Ref. [199]. d) Ref. [212].

urated species. The species $Ni(CO)_3$ was calculated in C_{3v} symmetry, but was found to adopt a planar structure and thus features an effective D_{3h} symmetry. Characteristic bond distances and angles of the optimized structures as obtained for various *xc* functionals are collected in Tables 4.6 to 4.9 together with available experimental data [210, 211, 212]. As in previous calculations [180, 194, 198] metal-carbon distances at the LDA level are found too short compared to experiment, but in good agreement at the GGA level. The metal-carbon bond distances determined with GGA *xc* functionals increase in the order PBE < revPBE < RPBE, with overall changes of up to about 0.02 Å. On the other hand, the C-O bond distances are in general best described at the LDA level (just as for the other small molecules discussed in the previous section). The only exception is $Fe(CO)_5$ where the GGA values of the C-O distance are closer to the experiment than the LDA values.

4.3 Conclusions

We have examined two recently developed revisions of the PBE exchange-correlation functional, revPBE and RPBE, for molecular calculations. For a set of small molecules these two functionals were compared with widely used conventional functionals such as BP, PW91, and PBE as well as with two LDA functionals. In general, both revised PBE functionals yield improved molecular atomization energies; average absolute deviations from experiment of both functionals are about 5 kcal/mol. The values of the RPBE functional are on average about 1 kcal/mol smaller than those obtained with the revPBE functional. Application of the revised PBE functionals to the metal carbonyls $Cr(CO)_6$, $Fe(CO)_5$, and $Ni(CO)_4$ corroborates their superiority over other conventional GGA. With errors of about

2 kcal/mol, revised PBE functionals furnish first ligand dissociation energies in excellent agreement with experiment. Overall, revised PBE functionals result in somewhat longer, less strong bonds than those calculated with conventional GGAs (BP, PW91, PBE). Bond distances are on average about 0.006 Å longer than those obtained with the parent PBE functional. Both revised PBE functionals represent a good compromise between accurate binding energies and bond distances. As their results are very similar, the RPBE functional may be chosen if one wants to employ a functional that also obeys the local Lieb-Oxford bound.

The present work supports the statement of Perdew et al. [23] that consistent, systematic improvement of *xc* functionals is possible. Revised PBE functionals provide so far the best energetics of all exchange-correlation functionals that depend locally only on the electron density and the density gradient.

Of course, one should keep in mind that all these statements about trends are based on a statistical analysis of results of a rather small set of molecules with atoms of the first to third rows of the periodic table. Clearly, broadening of the data base to include more and a larger variety of systems (e.g. to include transition metal compound as well as energy barriers) is highly desirable.

Chapter 5

Summary

The presented work was devoted to extending and optimizing the relativistic options of the parallel quantum chemical density functional program ParaGauss. Three major tasks of different complexity and problem background were addressed in the course of the work. However, they serve a common goal, namely they are intended to improve the quality and the efficiency of simulations of molecular systems in the framework of Density-Functional Theory (DFT) with a strong emphasis on those systems, where relativistic effects are important. These tasks, addressed in chronological sequence, were:

- Integration of the Perdew–Burke–Ernzerhof (PBE) exchange-correlation (xc) functional family into ParaGauss and investigation of the quality of the novel, and ultimately improved approximation for small molecular systems and the bonding of ligands to transition metals.

- Derivation and implementation of a variational formalism to "screen" the nuclear potential by the Hartree potential in the relativistic framework based on the Douglas–Kroll–Hess (DKH) approach. A procedure to generate four-spinor bases optimal for representing operators invariant to "charge conjugation"[1] was developed specifically for subjecting the Hartree potential to a relativistic transformation.

- Analysis and optimization of the way orbitals and spinors are symmetrized in a spin-orbit calculation to fully exploit the symmetry properties of spin-free operators. For this purpose, a new formalism to generate symmetrized spinors that uses point group symmetry and the corresponding double group symmetry was developed and implemented.

[1] Including but not limited to operators of the type $V(\boldsymbol{r})\delta_{\alpha\beta}$, i.e. diagonal in all four spinor components, α and β, and *independent* of them. In general, "charge conjugation" is equivalent to the permutation of large and small components.

The family of the PBE *xc* functionals includes the exchange and correlation functionals due to Perdew, Burke, and Ernzerhof [23], and the two alternative exchange functionals, one due to Zhang and Wang [24], and another one due to Hammer, Hansen, and Nørskov [25]. All of them are gradient corrections to the corresponding local density approximation (LDA). The correlation functional is based on the LDA parametrization of Perdew and Wang [187], an alternative to the well known Vosko–Wilk–Nusair parametrization [134]. Thus, the former also needed to be incorporated into the program. At the time all these approximations emerged, there was some discussion about which functional matches more rigorously the restrictions on the asymptotic behavior of the exact functional and which one has a better performance in practical applications [23, 24, 213, 25]. The present work contributed to this discussion by comparing the performance of these functionals to each other and to the several conventional ones in prediction of structure and energetics of transition metal carbonyls and a set of the small molecules [22]. It was shown that the performance of the PBE functionals family is often better then that of the de-facto standard Becke–Perdew functional; subtle differences within the family of gradient corrected functionals were systematically investigated and documented. Adding these functionals to the codebase significantly increased the flexibility of the code with respect to the choice of *xc* functionals.

To treat relativistic systems, the program ParaGauss implements the DKH scalar relativistic Hamiltonian and four flavors of spin-orbit (SO) Hamiltonian: with an untransformed Hartree term and with three variants of a relativistically transformed Hartree term of different accuracy. In its simplest form (DKnuc), the DKH approach completely neglects relativistic effects due to the electron-electron interaction. The present work released this limitation for the first time by introducing a relativistic expression for the Hartree energy. This was done in a way that is consistent with the DKH philosophy [27]. The formalism is variationally consistent; this ensures that the potential can be obtained from the energy expression by variation. In a simplified formulation this approach accounts for the relativistic effects on the Coulomb (Hartree) "screening" by the electron density repulsion field. The approach was adjusted to the special procedure in which the Hartree term is treated in the program ParaGauss: the fitting procedure where the electron density is represented as a linear combination of auxiliary basis functions. Three approximations of the method were implemented: first-order DKH transformation of the Hartree terms (DKee1), and two variants of the second-order DKH transformation, DKee2 and DKee3. In addition, the code was adjusted for use on parallel machines. The applicability and the quality of the novel approaches were evaluated for the level structure of heavy atoms (here Hg), for structural, vibrational, and energetic properties of diatomic molecules (PbO, Pb_2, Bi_2, and TlH), as well as for *g*-tensor shifts (NO_2). It was demonstrated that the

new approaches improve the level structure of atoms to yield very good agreement with fully relativistic (four-component) Dirac–Kohn–Sham results; also, g-tensor values were predicted in significantly better agreement with experiment. Some molecular properties, like the geometry and vibrational frequencies are hardly affected by the DKee models when compared to DKnuc results. The atomization energy may, however, change substantially, e.g. by several tenths of an eV. The DKee methods in the current implementation were found to be more sensitive to the quality of the orbital basis set than "standard" DKnuc or non-relativistic models, requiring very flexible basis sets. It was also demonstrated that the two second-order models DKee2 and DKee3 are essentially identical in practical applications. For most purposes, excluding calculations of the total energy and atomization energies, the first-order transformation DKee1 is sufficient and gives essentially the same results as the second-order variants DKee2 and DKee3.

In general, methods that include the SO interaction are substantially more expensive than the analogous non-relativistic or scalar-relativistic calculations. To exploit the symmetry of the SO operator, one has to deal with spinor wavefunctions, double groups, and double-valued representations instead of orbitals, the pertinent point groups and their single-valued representations. On the other hand, only a few operators in an SO calculation really contain the inherent spin-coupling terms, e.g. the operator $[\boldsymbol{p}V \times \boldsymbol{p}]\boldsymbol{s}$ in the DKH Hamiltonian or $\zeta(r)\boldsymbol{ls}$ in the Pauli Hamiltonian. During this work, a general framework for exploiting the symmetry of spin-free operators in any SO calculation was developed. For this purpose, the symmetry part of the program was extended to provide the option of "coherent" symmetry adaption of orbitals and spinors. In such a procedure, the basis spinors are simultaneous eigenfunctions of projective class operators of the double group and of vector class operators of the corresponding point group. The eigenvalues of projective and vector class operators label the symmetry type of any basis spinor. On the other hand, any SO Hamiltonian commutes with projective class operators and any spin-free operator commutes with class operators of both types; these commutation properties allow operators to have common eigenvectors with all implications for selection rules. Thus, the projective and vector symmetry labels as "good quantum numbers" of a basis chosen accordingly provide the symmetry selection rules for the spin-free operators to be exploited *in parallel* to the selection rules for the general spin-coupling ones. The matrix representation of a spin-free operator in a *spinor* basis constructed according to this procedure is block-diagonal with respect to point group irreducible representations and these blocks are equivalent to the (real-valued) representation in the *orbital* basis; this makes transitions from orbital to spinor representations and back a trivial matter.

This symmetry framework was applied to build up the matrix representation of the exchange-correlation potential. The latter is constructed by numerical integration over

a grid of points, which is a very time consuming step, much more time consuming in spinor bases than in orbital bases. The newly developed construction procedure of the spinor representation of the exchange-correlation potential via the intermediate orbital representation, on the other hand, is no more expensive than a construction in the orbital representation itself. Thus, the most time consuming step of an SO calculation was made to perform as efficient as that of a non-relativistic one, which not only removed the bottleneck of the integration of *xc* potential, but made it, in fact, negligible in comparison to the costs of other tasks, e.g. the evaluation of the density.

In summary, this work contributed (i) a novel method to treat the relativistic Hartree terms in a DKH calculation and its implementation in a parallel program, (ii) an efficient symmetry treatment for spin-free operators in any SO calculation and an implementation for the integration of the *xc* potential which removed the most severe bottleneck of SO calculations, and (iii) an implementation of the PBE family of exchange-correlation functionals. Altogether, these contributions added much flexibility, performance and rigor to the program ParaGauss.

Due to the quality of the results demonstrated in this work, in combination with the considerably increased computational efficiency, new fields of quantum-chemical studies are now accessible, which before had not been addressed due to methodological as well as computational limitations. Examples are the study of the chemistry of lower oxidation states of the actinides, the effects of SO interaction on the magnetism of transition metal clusters, or more accurate predictions of EPR parameters.

Appendix A

An Interface to Matrix Arithmetics

A set of modules has been added to the source of ParaGauss to deal efficiently and transparently with matrix arithmetics. The primary focus was the DKH SO implementation; however, other applications are possible.[1] The package defines several matrix types and operations associated with them. Currently matrix types include general complex matrix, real matrix, and real diagonal matrix. Operations defined for these types of matrices are usual arithmetic operations: multiplication by a scalar, addition and multiplication of matrices. Interfaces to the LAPACK subroutine for the eigenvalue problem and to the MPI packing/unpacking subroutines are also available. The main idea was to create an interface to the efficient BLAS (LAPACK) kernels which is easily read by programmers. There is definitely no need to argue that the efficiency of the code is important. However, for a project with more than 10^5 lines of code, maintainability of the code is at least as important. The latter depends much on the ease of reading and understanding of the code.

There are also other advantages of an interface between performance optimized libraries and the main code. With the new concept of (*multi-dimensional*) zero-sized arrays, the bodies of wrapper routines are the best place to catch different kinds of exceptions. For some purposes it may be useful to "extend" the definition of a matrix multiplication to zero-sized matrices. Examples of such more "physical" rather than mathematical definitions are

$$A(0 \times K) * B(K \times N) = C(0 \times N) \tag{A.1}$$

$$A(M \times K) * B(K \times 0) = C(M \times 0) \tag{A.2}$$

$$A(M \times 0) * B(0 \times N) = ZERO(M \times N) \tag{A.3}$$

where zero-sized matrices of different ranks have 0 as one of the dimensions and $ZERO(M\times$

[1] Meanwhile the package is also used by the modules which implement the calculation of g-tensor and hyperfine coupling constants.

N) is a $M \times N$ matrix of zeros. With help of these definitions it is possible to avoid separate branches of the code when treating empty irrep bases while processing two coupled irreps in the module which transforms the contributions of charge fitting functions.

In the following, we present a short description of the interface of the package:

- Supported matrix types

  `cmatrix` general complex matrix with the following components

  - `%n` dimension of the matrix. Defined for square matrices. For rectangular matrices use `%n1` and `%n2` instead
  - `%n1, %n2` dimensions of the matrix, always defined
  - `%re(:,:), %im(:,:)` real and imaginary parts of the complex matrix elements

  `rmatrix` general real matrix with the following components

  - `%n, %n1, %n2` dimensions, see above
  - `%m(:,:)` storage

  `rdmatrix` A real diagonal matrix with the following components

  - `%n` dimension of the matrix.
  - `%d(:)` diagonal elements of the matrix

- Creation and destruction of matrices

  `subroutine alloc(n,A1,A2,...)` allocates (square) matrices; generic, implemented for `cmatrix :: A1`, `rmatrix :: A1`, and `rdmatrix :: A1`; accepts up to 10 matrix arguments.

  `subroutine alloc(n1,n2,A)` allocates a rectangular `cmatrix :: A` or a `rmatrix :: A`.

  `subroutine free(A1,A2,...)` deallocates memory associated with matrix A; generic, implemented for `cmatrix :: A1`, `rmatrix :: A1`, `rdmatrix :: A1`; accepts up to 10 matrix arguments.

- Arithmetic operations

  `assignment(=)` used in the assignment statement `L=R`. For `cmatrix :: L` the expression `R` on the r.h.s. may be another `cmatrix` or an array `real(:,:,2)` holding real and imaginary parts in `real(:,:,1)` and `real(:,:,2`, respectively. For the `rdmatrix :: L` the expression `R` has to be an array `real(:)`.

`operator(*), mult(A,B)` is used to construct expressions of the type `A * B`. For most combinations of `typeA :: A` and `typeB :: B` this operator is defined intuitively. Arrays `real(:)` are treated as diagonal matrices, not as vectors. Types `typeA` and `typeB` may be `real`, `real(:)`, `real(:,:,2)`, `rdmatrix`, `rmatrix`, and `cmatrix`. An escape interface `mult()` to the `operator(*)` is provided for cases where the built-in Fortran array multiplication rules prevent one from using the operator notation.

`operator(+), operator(-)` is used to construct expressions of the type `A` $\pm$ `B` and $-$`B`. Extends the built-in definitions to several matrix operand types.

`function tr(A)` returns the transposed or the Hermitean conjugate of a matrix `A`.

`subroutines eigs(H,e,V), geigs(H,S,e,V),...` generic interfaces to the LAPACK subroutines for the (generalized) eigenvalue problem.

- other matrix methods for special cases of matrix multipliers, inquiries and consistency checks, packing and unpacking.

In the following, we provide an example which uses some functionality of the package; it represents code used in the relativistic transformations of the Hartree potential of the fitted density:

```
use matrix_module
! declare arrays of matrices; LL=1,SS=2,LS=1,SL=2
type(cmatrix)  :: AFA(LL:SS), ARFRA(LL:SS), F(LL:SS)
type(cmatrix)  :: AR(LS:SL)
type(rdmatrix) :: Ap(LL:SS)
! ...
! allocate storage:
call alloc(nL,AFA(LL))
call alloc(nS,AFA(SS))
! ...
! do some work:
AFA(LL)   = Ap(LL) * F(LL) * Ap(LL)
ARFRA(LL) = AR(LS) * (F(SS) * tr(AR(LS)))
AFA(SS)   = Ap(SS) * F(SS) * Ap(SS)
ARFRA(SS) = AR(SL) * (F(LL) * tr(AR(SL)))
! ...
! free the storage:
```

```
call free(AFA(LL),AFA(SS))
```

This type of code combines the readability of the operator notation for the arithmetics and the efficiency of the computational kernel underneath.

Appendix B

Group-Theoretical Information: Generators, Canonical Subgroup Chains, CSCO

Figure B.1: Point group generators.

Polyhedral groups

I_h	$C^+_{5,1}$, $C^+_{3,1}$, C_{2z}, i
I	$C^+_{5,1}$, $C^+_{3,1}$, C_{2z}
O_h	$C^+_{3,1}$, C^+_{4z}, i
O	$C^+_{3,1}$, C^+_{4z}
T_h	$C^+_{3,1}$, C_{2z}, i
T_d	$C^+_{3,1}$, S^+_{4z}
T	$C^+_{3,1}$, C_{2z}
D_2	C_{2z}, C_{2x}

Axial groups

C_{nv}	C^+_n, σ_v
D_n	C^+_n, $C_{2,1}$
D_{nd}	S^+_{2n}, $C_{2,1}$
D_{nh}	C^+_n, $C_{2,1}$, σ_h
C_n	C^+_n
S_{2n}	S^+_{2n}
C_{nh}	C^+_n, σ_h
C_s	σ_v
C_2	$C_{2,1}$

Figure B.2: Canonical subgroup chains for polyhedral and axial groups [77]. Dashed lines indicate subduction to real vector representations.

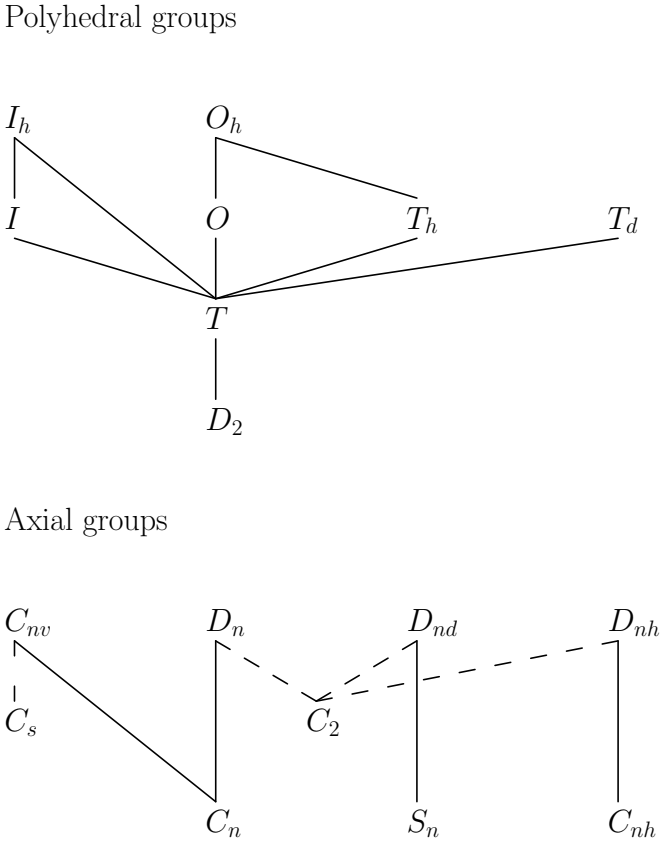

Table B.1: Complete set of commuting operators (CSCO) for point groups.

#	Group	vector CSCO	projective CSCO
1	C_1	E	E
2	C_2	C_2	C_2
3..10	C_n, $n = 3..10$	C_n^+	C_n^+
11	C_i	i	i
12	C_s	σ_h	σ_h
13..21	S_{2n}, $n = 2..10$	S_{2n}^+	S_{2n}^+
22	D_2	$2C_{2z} + C_{2x}$	$2E$
23	D_3	$C'_{2,1}$	$C'_{2,1}$
24	D_4	$2C_4^+ + C'_{2,1}$	$2C_4^+$
25	D_5	$2C_5^+ + C'_{2,1}$	$2C_5^+ + C'_{2,1}$
26	D_6	$2C_6^+ + C'_{2,1}$	$2C_6^+$
27	D_7	$2C_7^+ + C'_{2,1}$	$2C_7^+ + C'_{2,1}$
28	D_8	$2C_8^+ + 2C'_{2,1}$	$2C_8^+$
29	D_9	$2C_9^+ + C'_{2,1}$	$2C_9^+ + C'_{2,1}$
30	D_{10}	$2C_{10}^+ + C'_{2,1}$	$2C_{10}^+$
31	D_{2h}	$6C_{2z} + 2C_{2x} + i$	i
32	D_{3h}	$C'_{2,1} + \sigma_h$	S_3^-
33	D_{4h}	$4C_4^+ + C'_{2,1} + i$	$4C_4^+ + i$
34	D_{5h}	$4C_5^+ + C'_{2,1} + \sigma_h$	$4C_5^+ + S_5^-$
35	D_{6h}	$4C_6^+ + C'_{2,1} + i$	$4C_6^+ + i$
36	D_{7h}	$4C_7^+ + C'_{2,1} + \sigma_h$	$4C_7^+ + S_7^+$
37	D_{8h}	$2C_8^+ + 2C'_{2,1} + i$	$2C_8^+ + 2i$
38	D_{9h}	$2C_9^+ + C'_{2,1} + \sigma_h$	$2C_9^+ + \sigma_h$
39	D_{10h}	$4C_{10}^+ + 2C'_{2,1} + i$	$4C_{10}^+ + i$
40	${D_{\infty h}}^a$	$2C_8^+ + 2C'_{2,1} + i$	$2C_8^+ + 2i$
41	D_{2d}	$2S_4^- + \sigma_{d_1}$	$2S_4^-$
42	D_{3d}	$2i + \sigma_{d_1}$	$2i + \sigma_{d_1}$
43	D_{4d}	$3S_8^- + \sigma_{d_1}$	$3S_8^-$
44	D_{5d}	$2S_{10}^- + \sigma_{d_1}$	$2S_{10}^- + \sigma_{d_1}$
45	D_{6d}	$4S_{12}^- + \sigma_{d_1}$	$4S_{12}^-$
46	D_{7d}	$2S_{14}^- + \sigma_{d_1}$	$2S_{14}^- + \sigma_{d_1}$
47	D_{8d}	$2S_{16}^- + \sigma_{d_1}$	$2S_{16}^-$
48	D_{9d}	$2S_{18}^- + \sigma_{d_1}$	$2S_{18}^- + \sigma_{d_1}$

Table B.1: (continued)

#	Group	vector CSCO	projective CSCO
49	D_{10d}	$2S_{20}^{-} + \sigma_{d_1}$	$2S_{20}^{-}$
50	C_{2v}	$2C_2 + \sigma_x$	$2E$
51	C_{3v}	σ_{v_1}	σ_{v_1}
52	C_{4v}	$2C_4^{+} + \sigma'_{v_1}$	$2C_4^{+}$
53	C_{5v}	$2C_5^{+} + \sigma_{v_1}$	$2C_5^{+} + \sigma_{v_1}$
54	C_{6v}	$2C_6^{+} + \sigma'_{v_1}$	$2C_6^{+}$
55	C_{7v}	$2C_7^{+} + \sigma_{v_1}$	$2C_7^{+} + \sigma_{v_1}$
56	C_{8v}	$2C_8^{+} + 2\sigma'_{v_1}$	$2C_8^{+}$
57	C_{9v}	$2C_9^{+} + \sigma_{v_1}$	$2C_9^{+} + \sigma_{v_1}$
58	C_{10v}	$2C_{10}^{+} + \sigma'_{v_1}$	$2C_{10}^{+}$
59	C_{4v}	$2C_4^{+} + \sigma'_{v_1}$	$2C_4^{+}$
60	C_{2h}	$2C_2 + i$	$2C_2 + i$
61	C_{3h}	$C_3^{+} + 5\sigma_h$	$C_3^{+} + 5\sigma_h$
62	C_{4h}	$2C_4^{+} + 5i$	$2C_4^{+} + 5i$
63	C_{5h}	$2C_5^{+} + 5\sigma_h$	$2C_5^{+} + 5\sigma_h$
64	C_{6h}	$2C_6^{+} + 5i$	$2C_6^{+} + 5i$
65	C_{7h}	$2C_7^{+} + 5\sigma_h$	$2C_7^{+} + 5\sigma_h$
66	C_{8h}	$2C_8^{+} + 5i$	$2C_8^{+} + 5i$
67	C_{9h}	$2C_9^{+} + 5\sigma_h$	$2C_9^{+} + 5\sigma_h$
68	C_{10h}	$2C_{10}^{+} + 5i$	$2C_{10}^{+} + 5i$
69	O	C'_{2a}	C_{4x}^{+}
70	T	$C_{3,1}^{+}$	$C_{3,1}^{+}$
71	O_h	$2C'_{2a} + i$	$2C_{4x}^{+} + i$
72	T_h	$C_{3,1}^{+} + 5i$	$C_{3,1}^{+} + 5i$
73	T_d	σ_{d_1}	S_{4x}^{-}
74	I	$2C_{5,1}^{+} + C_{2a}$	$2C_{5,1}^{+}$
75	I_h	$2C_{5,1}^{+} + C_{2a} + i$	$2C_{5,1}^{+} + i$

a) $D_{\infty h}$ when required in input is internally treated as D_{8h} which is equivalent to the former for angular momentum eigenfunctions with $l \leq 4$.

Bibliography

[1] D. R. Hartree, Proc. Camb. Phil. Soc. **24**, 89 (1928).

[2] V. Fock, Z. Phys. **61**, 126 (1930).

[3] V. Fock, Z. Phys. **62**, 765 (1930).

[4] L. H. Thomas, Proc. Camb. Phil. Soc. **23**, 542 (1926).

[5] E. Fermi, Z. Phys. **48**, 73 (1928).

[6] F. Jensen, *Introduction to Computational Chemistry* (John Wiley & Sons, Chichester, 1998).

[7] I. N. Levine, *Quantum Chemistry* (Prentice Hall, Upper Saddle River, New Jersey, 2000), 5th edition.

[8] P. Pyykkö, *Relativistic Theory of Atoms and Molecules. III. A Bibliography 1993-1999*, Vol. 76 of *Lecture Notes in Chemistry* (Springer-Verlag, Berlin, 2000).

[9] W. G. Richards, H. P. Trivedi, and D. L. Cooper, *Spin-Orbit Coupling in Molecules* (Clarendon, Oxford, 1981).

[10] C. M. Marian, in *Reviews in Computational Chemistry*, edited by K. B. Lipkowitz and D. B. Boyd (Wiley-VCH, John Wily and Sons, Inc., New York, 2001), Vol. 17, p. 99.

[11] A. Lund and M. Shiotani, (eds.), *EPR Spectroscopy of Free Radicals in Solids. Trends in Methods and Applications* (Kluwer, Dordrecht, 2002).

[12] M. Douglas and N. M. Kroll, Ann. Phys. (NY) **82**, 89 (1974).

[13] R. G. Parr and W. Yang, *Density-Functional Theory of Atoms and Molecules* (Oxford University Press, Oxford, 1989).

[14] W. Kohn and L. J. Sham, Phys. Rev. A **140**, 1133 (1965).

[15] E. Engel, S. Keller, and R. M. Dreizler, in *Electronic Density Functional Theory: Recent Progress and New Directions*, edited by J. F. Dobson, G. Vignale, and M. P. Das (Plenum Press, New York, 1998), p. 149.

[16] N. Rösch, S. Krüger, M. Mayer, and V. A. Nasluzov, in *Recent Developments and Applications of Modern Density Functional Theory*, edited by J. M. Seminario (Elsevier, Amsterdam, 1996), p. 497.

[17] N. Rösch, A. Matveev, V. A. Nasluzov, K. M. Neyman, L. Moskaleva, and S. Krüger, in *Relativistic Electronic Structure Theory — Applications*, *Theoretical and Computational Chemistry Series*, edited by P. Schwerdtfeger (Elsevier, Amsterdam, 2003), in press.

[18] B. A. Hess, R. J. Buenker, and P. Chandra, Int. J. Quantum Chem. **29**, 737 (1986).

[19] B. A. Hess, (ed.), *Relativistic Effects in Heavy-Element Physics and Chemistry* (Wiley, Chichester, 2003).

[20] T. Belling, T. Grauschopf, S. Krüger, M. Mayer, F. Nörtemann, M. Staufer, C. Zenger, and N. Rösch, in *High Performance Scientific and Engineering Computing*, Vol. 8 of *Lecture Notes in Computational Science and Engineering*, edited by H.-J. Bungartz, F. Durst, and C. Zenger (Springer, Heidelberg, 1999), p. 439.

[21] T. Belling, T. Grauschopf, S. Krüger, F. Nörtemann, M. Staufer, M. Mayer, V. A. Nasluzov, U. Birkenheuer, A. Hu, A. Matveev, A. V. Shor, M. S. K. Fuchs-Rohr, K. M. Neyman, D. I. Ganyushin, T. Kerdcharoen, A. Woiterski, and N. Rösch, ParaGauss, Version 2.2, Technische Universität München, 2001.

[22] A. Matveev, M. Staufer, M. Mayer, and N. Rösch, Int. J. Quantum Chem. **75**, 863 (1999).

[23] J. P. Perdew, K. Burke, and M. Ernzerhof, Phys. Rev. Lett. **77**, 3865 (1996).

[24] Y. Zhang and W. Yang, Phys. Rev. Lett. **80**, 890 (1998).

[25] B. Hammer, L. B. Hansen, and J. K. Nørskov, Phys. Rev. B **59**, 7413 (1999).

[26] M. Mayer, S. Krüger, and N. Rösch, J. Chem. Phys. **115**, 4411 (2001).

[27] A. Matveev and N. Rösch, J. Chem. Phys. **118**, 3997 (2003).

[28] P. Pyykkö, Chem. Rev. **88**, 563 (1988).

[29] K. Balasubramanian, *Relativistic Effects in Chemistry. Part B* (Wiley-Interscience, New York, 1997).

[30] M. V. Ramana and A. K. Rajagopal, Adv. Chem. Phys. **54**, 231 (1983).

[31] E. Engel, H. Müller, C. Speicher, and R. M. Dreizler, in *Density Functional Theory*, Vol. 337 of *NATO ASI Series B*, edited by E. K. U. Gross and R. M. Dreizler (Plenum, New York, 1995), p. 65.

[32] P. Hohenberg and W. Kohn, Phys. Rev. B **136**, 864 (1964).

[33] A. K. Rajagopal and J. Callaway, Phys. Rev. B **7**, 1912 (1973).

[34] A. K. Rajagopal, J. Phys. C **11**, L943 (1978).

[35] A. H. MacDonald and S. H. Vosko, J. Phys. Chem. **12**, 2977 (1979).

[36] M. Mayer, O. D. Häberlen, and N. Rösch, Phys. Rev. A **54**, 4775 (1996).

[37] L. L. Foldy and S. A. Wouthuysen, Phys. Rev. **78**, 29 (1950).

[38] B. A. Hess, Phys. Rev. A **32**, 756 (1985).

[39] E. van Lenthe, E. J. Baerends, and J. G. Snijders, J. Chem. Phys. **99**, 4597 (1993).

[40] E. van Lenthe, E. J. Baerends, and J. G. Snijders, J. Chem. Phys. **101**, 9783 (1994).

[41] W. Kutzelnigg, Z. Phys. D **11**, 15 (1989).

[42] W. Kutzelnigg, Z. Phys. D **15**, 27 (1990).

[43] L. Visscher and E. van Lenthe, Chem. Phys. Lett. **306**, 357 (1999).

[44] O. D. Häberlen and N. Rösch, Chem. Phys. Lett. **199**, 491 (1992).

[45] B. A. Hess, C. M. Marian, and S. D. Peyerimhoff, in *Modern Electronic Structure Theory*, edited by D. R. Yarkony (World Scientific, Singapore, 1995), p. 152.

[46] O. L. Malkina, B. Schimmelpfennig, M. Kaupp, B. A. Hess, P. Chandra, U. Wahlgren, and V. G. Malkin, Chem. Phys. Lett. **296**, 93 (1998).

[47] O. L. Malkina, J. Vaara, B. Schimmelpfennig, M. Munzarová, V. G. Malkin, and M. Kaupp, J. Am. Chem. Soc. **122**, 9206 (2000).

[48] M. Blume and R. E. Watson, Proc. Roy. Soc. A **270**, 127 (1962).

[49] J. Tatchen and C. M. Marian, Chem. Phys. Lett. **313**, 351 (1999).

[50] M. Blume and R. E. Watson, Proc. Roy. Soc. A **271**, 565 (1963).

[51] S. R. Langhoff and C. W. Kern, in *Applications of Electronic Structure Theory*, Vol. 4 of *Modern Theoretical Chemistry*, edited by H. F. Schaefer III (Plenum, New York, 1977), p. 381.

[52] M. Dolg, H. Stoll, H.-J. Flad, and H. Preuss, J. Chem. Phys. **97**, 1162 (1992).

[53] D. G. Fedorov and M. S. Gordon, J. Chem. Phys. **112**, 5611 (2000).

[54] J. Vaara, K. Ruud, O. Vahtras, H. Ågren, and J. Jokisaari, J. Chem. Phys. **109**, 1212 (1998).

[55] K. M. Neyman, D. I. Ganyushin, A. V. Matveev, and V. A. Nasluzov, J. Phys. Chem. A **106**, 5022 (2002).

[56] B. A. Hess, C. M. Marian, U. Wahlgren, and O. Gropen, Chem. Phys. Lett. **251**, 365 (1996).

[57] J. C. Boettger, Phys. Rev. B **62**, 7809 (2000).

[58] E. J. Baerends, D. E. Ellis, and P. Ros, Chem. Phys. **2**, 41 (1973).

[59] B. I. Dunlap, J. W. D. Connolly, and J. R. Sabin, J. Chem. Phys. **71**, 3396 (1979).

[60] B. I. Dunlap and N. Rösch, Adv. Quantum Chem. **21**, 317 (1990).

[61] M. V. Ramana and A. K. Rajagopal, Phys. Rev. A **24**, 1689 (1981).

[62] R. Samzow, B. A. Hess, and G. Jansen, J. Chem. Phys. **96**, 1227 (1992).

[63] E. Engel, S. Keller, and R. M. Dreizler, Phys. Rev. A **53**, 1367 (1996).

[64] K. G. Dyall and E. van Lenthe, J. Chem. Phys. **111**, 1366 (1999).

[65] F. Wang, G. Hong, and L. Li, Chem. Phys. Lett. **316**, 318 (2000).

[66] G. Hardekopf and J. Sucher, Phys. Rev. A **30**, 703 (1984).

[67] P. Knappe and N. Rösch, J. Chem. Phys. **92**, 1153 (1990).

[68] J.-L. Heully, I. Lindgren, E. Lindroth, S. Lundqvist, and A.-M. Martensson-Pendrill, J. Phys. B **19**, 2799 (1986).

[69] G. Jansen and B. A. Hess, Phys. Rev. A **39**, 6016 (1989).

[70] T. Nakajima and K. Hirao, J. Chem. Phys. **113**, 7786 (2000).

[71] T. Nakajima and K. Hirao, Chem. Phys. Lett. **329**, 511 (2000).

[72] A. Wolf, M. Reiher, and B. A. Hess, J. Chem. Phys. **117**, 9215 (2002).

[73] L. Gagliardi, N. C. Handy, A. G. Ioannou, C.-K. Skylaris, S. Spencerand, A. Willetts, and A. M. Simper, Chem. Phys. Lett. **283**, 187 (1998).

[74] W. A. de Jong, R. J. Harrison, and D. A. Dixon, J. Chem. Phys. **114**, 48 (2001).

[75] M. Barysz, A. J. Sadlej, and J. G. Snijders, Int. J. Quantum Chem. **65**, 225 (1997).

[76] S. L. Altmann, *Rotations, Quaternions and Double Groups* (Clarendon Press, Oxford, 1986).

[77] M. Mayer, *A Parallel Implementation of the Density Functional Method: Implementation of the Two-Component Douglas–Kroll–Hess Method and Application to Relativistic Effects in Heavy Element Chemistry*, Dissertation, Technische Universität München, 1999.

[78] J. D. Bjorken and S. D. Drell, *Relativistic Quantum Mechanics* (Mc Graw-Hill, New York, 1964).

[79] K. G. Dyall, J. Chem. Phys. **100**, 2118 (1994).

[80] O. Vahtras, J. Almlöf, and M. W. Feyereisen, Chem. Phys. Lett. **213**, 514 (1993).

[81] K. Eichkorn, O. Treutler, H. Öhm, M. Häser, and R. Ahlrichs, Chem. Phys. Lett. **240**, 283 (1995).

[82] B. I. Dunlap, J. Phys. Chem. **90**, 5524 (1986).

[83] B. Dunlap and M. Cook, Int. J. Quantum Chem. **29**, 767 (1986).

[84] Y. C. Zheng and J. Almlöf, Chem. Phys. Lett. **214**, 397 (1993).

[85] Y. C. Zheng and J. Almlöf, J. Mol. Struct.: THEOCHEM **388**, 277 (1998).

[86] K. S. Werpetinski and M. Cook, Phys. Rev. A **52**, R3397 (1995).

[87] K. S. Werpetinski and M. Cook, J. Chem. Phys. **106**, 7124 (1997).

[88] U. Birkenheuer, A. B. Gordienko, V. A. Nasluzov, M. Fuchs-Rohr, and N. Rösch, in preparation.

[89] M. Staufer, *A Parallel Implementation of the Density Functional Method: Analytical Energy Gradients, DF Quadrature and Applications to Chemisorption*, Dissertation, Technische Universität München, 1999.

[90] T. Belling, *A Parallel Implementation of the Density Functional Method. Integral Evaluation and External Potentials. Application to Thiolate Adsorption on Gold Surfaces*, Dissertation, Technische Universität München, 1998.

[91] F. Nörtemann, *A Parallel Implementation of the Density Functional Method: SCF Part, Optimization Package and Application to Gold Clusters*, Dissertation, Technische Universität München, 1998.

[92] N. Rösch, P. Knappe, P. Sandl, A. Görling, and B. I. Dunlap, in *The Challenge of d and f Electrons. Theory and Computation*, Vol. 394 of *ACS symposium series*, edited by D. R. Salahub and M. C. Zerner (American Chemical Society, Washington, DC, 1989), p. 180.

[93] B. I. Dunlap, J. Andzelm, and J. W. Mintmire, Phys. Rev. A **42**, 6354 (1990).

[94] T. Živković and Z. Maksić, J. Chem. Phys. **49**, 3083 (1968).

[95] E. O. Steinborn and K. Ruedenberg, Adv. Quantum Chem. **7**, 1 (1973).

[96] E. O. Steinborn and K. Ruedenberg, Adv. Quantum Chem. **7**, 83 (1973).

[97] H. Sambe and R. H. Felton, J. Chem. Phys. **61**, 3862 (1974).

[98] H. Sambe and R. H. Felton, J. Chem. Phys. **62**, 1122 (1975).

[99] H. Jörg, N. Rösch, J. R. Sabin, and B. I. Dunlap, Chem. Phys. Lett. **114**, 529 (1985).

[100] S. Obara and A. Saika, J. Chem. Phys. **84**, 3963 (1986).

[101] S. Obara and A. Saika, J. Chem. Phys. **89**, 1540 (1988).

[102] B. I. Dunlap, Phys. Rev. A **42**, 1127 (1990).

[103] J. Andzelm and E. Wimmer, J. Chem. Phys. **96**, 1280 (1992).

[104] D. R. Salahub, R. Fournier, P. Mylnarski, I. Papai, A. St-Amant, and J. Usiho, in *Density Functional Methods in Chemistry*, edited by J. Labanowski and J. Andzelm (Springer, New York, 1991), p. 77.

[105] A. St-Amant and D. Salahub, Chem. Phys. Lett. **169**, 387 (1990).

[106] C. Fonseca Guerra, O. Visser, J. G. Snijders, G. te Velde, and E. J. Baerends, in *Methods and Techniques in Computational Chemistry (METECC-95)*, edited by E. Clementi and G. Corongiu (Université L. Pasteur, Strasbourg, France, 1995), p. 305.

[107] M. J. Frisch, G. W. Trucks, H. B. Schlegel, G. E. Scuseria, M. A. Robb, J. R. Cheeseman, J. A. Montgomery Jr., T. Vreven, K. N. Kudin, J. C. Burant, J. M. Millam, S. S. Iyengar, J. Tomasi, V. Barone, B. Mennucci, M. Cossi, G. Scalmani, N. Rega, G. A. Petersson, H. Nakatsuji, M. Hada, M. Ehara, K. Toyota, R. Fukuda, J. Hasegawa, M. Ishida, T. Nakajima, Y. Honda, O. Kitao, H. Nakai, M. Klene, X. Li, J. E. Knox, H. P. Hratchian, J. B. Cross, C. Adamo, J. Jaramillo, R. Gomperts, R. E. Stratmann, O. Yazyev, A. J. Austin, R. Cammi, C. Pomelli, J. W. Ochterski, P. Y. Ayala, K. Morokuma, G. A. Voth, P. Salvador, J. J. Dannenberg, V. G. Zakrzewski, S. Dapprich, A. D. Daniels, M. C. Strain, O. Farkas, D. K. Malick, A. D. Rabuck, K. Raghavachari, J. B. Foresman, J. V. Ortiz, Q. Cui, A. G. Baboul, S. Clifford, J. Cioslowski, B. B. Stefanov, G. Liu, A. Liashenko, P. Piskorz, I. Komaromi, R. L. Martin, D. J. Fox, T. Keith, M. A. Al-Laham, C. Y. Peng, A. Nanayakkara, M. Challacombe, P. M. W. Gill, B. Johnson, W. Chen, M. W. Wong, C. Gonzalez, and J. A. Pople, *Gaussian 03* Revison A.1, Gaussian Inc., Pittsburgh PA, 2003.

[108] B. Delley, J. Chem. Phys. **94**, 7245 (1991).

[109] B. G. Johnson, C. A. White, Q. Zhang, B. Chen, R. L. Graham, P. M. W. Gill, and M. Head-Gordon, in *Recent Developments and Applications of Modern Density Functional Theory*, Vol. 4 of *Theoretical and Computational Chemistry*, edited by J. M. Seminario (Elsevier, Amsterdam, 1996), p. 441.

[110] M. Häser and R. Ahlrichs, J. Comput. Chem. **10**, 104 (1989).

[111] C. van Wüllen, Chem. Phys. Lett. **219**, 8 (1994).

[112] M. C. Payne, M. P. Teter, D. C. Allan, T. A. Arias, and J. D. Joannopoulos, Rev. Mod. Phys. **64**, 1045 (1992).

[113] B. Hammer, L. B. Hansen und J. K. Nørskov, *The DACAPO Program*, Version 1.35, Center of Atomic-Scale Materials Physics, (Technical University of Denmark, Lyngby, 1998).

[114] P. Blaha, K. Schwarz, and J. Luitz, WIEN97, Vienna University of Technology, Vienna 1997, updated version of P. Blaha, K. Schwarz, P. Sorantin, and S. B. Trickey, Comp. Phys. Commun. **59** 399 (1990).

[115] G. Kresse and J. Hafner, Phys. Rev. B **47**, 558 (1993).

[116] G. Kresse and J. Furthmüller, Phys. Rev. B **55**, 11169 (1996).

[117] T. Grauschopf, *Eine Implementierung der Dichtefunktionalmethode mit einer hybriden Finite–Element–Basis*, Dissertation, Technische Universität München, 1999.

[118] E. O. Steinborn and K. Ruedenberg, Int. J. Quantum Chem. **6**, 413 (1972).

[119] A. Görling, *Zur Verwendung von Dipolmomenten in der LCGTO-DF Methode*, Dissertation, Technische Universität München, 1990.

[120] A. R. Edmonds, *Drehimpulse in der Quantenmechanik* (Bibliographisches Institut, Mannheim, 1964).

[121] M. E. Rose, *Elementary Theory of Angular Momentum* (John Wiley & Sons, New York, 1957).

[122] E. U. Condon and G. H. Shortley, *The Theory of Atomic Spectra* (Cambridge University Press, Cambridge, 1935).

[123] D. Brink and G. Satchler, *Angular Momentum* (Oxford University Press, Oxford, 1968).

[124] T. Nakajima and K. Hirao, J. Chem. Phys. **119**, 4105 (2003).

[125] O. D. Häberlen, *Eine zweikomponentige relativistische Dichtefunktional-Methode für Moleküle und Cluster*, Dissertation, Technische Universität München, 1993.

[126] J. J. Dongarra, J. D. Croz, S. Hammarling, and I. Duff, ACM Transactions on Mathematical Software **16**, 1 (1990).

[127] A. Petitet, R. C. Whaley, J. Horner, D. Aberdeen, N. Coult, K. Goto, C. Maguire, V. Nguyen, P. Strazdins, P. Soendergaard, and C. Staelin, Automatically Tuned Linear Algebra Software (ATLAS), http://math-atlas.sourceforge.net/.

[128] E. Anderson, Z. Bai, C. Bischof, J. Demmel, J. Dongarra, J. D. Croz, A. Greenbaum, S. Hammarling, A. McKenney, and D. Sorensen, *LAPACK Users Guide* (SIAM, Philadelphia, 1999), 3rd edition.

[129] A. Szabo and N. S. Ostlund, *Modern Quantum Chemistry: Introduction to Advanced Electronic Structure Theory* (McGraw-Hill, New York, 1989).

[130] R. J. Buenker, P. Chandra, and B. A. Hess, Chem. Phys. **84**, 1 (1984).

[131] E. Anderson, Z. Bai, C. Bischof, J. Demmel, J. Dongarra, J. D. Croz, A. Greenbaum, S. Hammarling, A. McKenney, and D. Sorensen, *LAPACK: A Portable Linear Algebra Library for High-Performance Computers* (University of Tennessee, Knoxville, TN, 1990).

[132] J.-L. Heully, I. Lindgren, E. Lindroth, and A.-M. Martensson-Pendrill, Phys. Rev. A **33**, 4426 (1986).

[133] A. S. Davydov, *Quantum Mechanics* (Pergamon, Oxford, 1976).

[134] S. H. Vosko, L. Wilk, and M. Nusair, Can. J. Phys. **58**, 1200 (1980).

[135] A. D. Becke, Phys. Rev. A **38**, 3098 (1988).

[136] J. P. Perdew, Phys. Rev. B **33**, 8822 (1986).

[137] F. B. van Duijnefeldt, IBM Res. Report RJ945 (1971).

[138] O. Gropen, J. Comp. Chem. **8**, 982 (1987).

[139] S. Huzinaga and M. Klobukowski, Chem. Phys. Lett. **212**, 260 (1993).

[140] P.-O. Widmark, P.-Å. Malmqvist, and B. O. Roos, Theoretica Chimica Acta **77**, 291 (1990).

[141] I. V. Yudanov, V. A. Nasluzov, and N. Rösch, unpublished.

[142] A. D. Becke, J. Chem. Phys **88**, 2547 (1988).

[143] V. I. Lebedev, Sib. Math. J. **18**, 99 (1977).

[144] E. Engel, S. Keller, A. F. Bonetti, H. Müller, and R. M. Dreizler, Phys. Rev. A **52**, 2750 (1995).

[145] M. Plato and K. Möbius, Chem. Phys. **197**, 745 (1995).

[146] J. T. Törring, S. Un, M. Knüpling, M. Plato, and K. Möbius, J. Chem. Phys. **107**, 3905 (1997).

[147] G. H. Lushington, P. Bündgen, and F. Grein, Int. J. Quantum Chem. **55**, 377 (1995).

[148] G. H. Lushington and F. Grein, J. Chem. Phys. **106**, 3292 (1997).

[149] O. Vahtras, B. Minaev, and H. Ågren, Chem. Phys. Lett. **281**, 186 (1997).

[150] E. van Lenthe, P. E. S. Wormer, and A. van der Avoird, J. Chem. Phys. **107**, 2488 (1997).

[151] G. Schreckenbach and T. Ziegler, J. Phys. Chem. A **101**, 3388 (1997).

[152] P. Belanzoni, E. van Lenthe, and E. J. Baerends, J. Chem. Phys. **114**, 4421 (2001).

[153] J. M. Brown, T. C. Steimle, M. E. Coles, and R. F. Curl, J. Chem. Phys. **74**, 3668 (1981).

[154] E. van Lenthe, J. G. Snijders, and E. J. Baerends, J. Chem. Phys. **105**, 6505 (1996).

[155] W. Liu, C. van Wuellen, Y. K. Han, Y. J. Choi, and Y. S. Lee, Adv. Quantum Chem. **39**, 325 (2001).

[156] W. Liu, C. van Wüllen, F. Wang, and L. Li, J. Chem. Phys. **116**, 3626 (2002).

[157] K. P. Huber and G. Herzberg, *Molecular Spectra and Molecular Structure* (Van Nostrand, New York, 1979), Vol. 4.

[158] F. A. Cotton, *Chemical Application of Group Theory* (Wiley, New York, 1990).

[159] J. Mayer, Int. J. Quantum Chem. **61**, 929 (1997).

[160] A. L. H. Chung and G. Goodman, J. Chem. Phys. **56**, 4125 (1972).

[161] G. Fieck, Theor. Chim. Acta **49**, 144 (1978).

[162] Q.-E. Zhang, Int. J. Quantum Chem. **23**, 1479 (1983).

[163] F. Wang and L. Li, J. Mol. Struct.: THEOCHEM **586**, 193 (2002).

[164] H. T. Toivonen and P. Pyykkö, Int. J. Quantum Chem. **11**, 695 (1977).

[165] J. Oreg and G. Malli, J. Chem. Phys. **65**, 1746 (1976).

[166] J. Oreg and G. Malli, J. Chem. Phys. **65**, 1755 (1976).

[167] J. Meyer, Int. J. Quantum Chem. **52**, 1369 (1994).

[168] L. Visscher, Chem. Phys. Lett. **253**, 20 (1996).

[169] G. te Velde, F. M. Bickelhaupt, E. J. Baerends, C. Fonseca Guerra, S. J. A. van Gisbergen, J. G. Snijders, and T. Ziegler, J. Comp. Chem. **22**, 931 (2001).

[170] J.-Q. Chen, J. Ping, and F. Wang, *Group Representation Theory for Physicists* (World Scientific, Singapore, 2002), 2nd edition.

[171] J.-Q. Chen and J.-L. Ping, Comp. Phys. Comm. **120**, 71 (1999).

[172] J.-L. Ping and J.-Q. Chen, Int. J. Quantum Chem. **75**, 67 (1999).

[173] A. Messiah, *Quantum Mechanics* (North-Holland Publishing Company, Amsterdam, 1961), Vol. I.

[174] S. L. Altmann and P. Herzig, *Group Theory and its Application to Physical Problems* (Clarendon Press, Oxford, 1994).

[175] P. A. M. Dirac, *The Principles of Quantum Mechanics* (Clarendon, Oxford, 1958).

[176] B. I. Dunlap, Adv. Chem. Phys. **69**, 287 (1987).

[177] N. Rösch, Chem. Phys. **80**, 1 (1983).

[178] W. Kutzelnigg, Chem. Phys. **225**, 203 (1997).

[179] A. Görling, S. B. Trickey, P. Gisdakis, and N. Rösch, in *Topics in Organometallic Chemistry*, edited by P. Hofmann and J. M. Brown (Springer, Berlin, Heidelberg, New York, 1999), Vol. 3, p. 109.

[180] T. Ziegler, Chem. Rev. **91**, 651 (1991).

[181] C. Lee, W. Yang, and R. G. Parr, Phys. Rev. B **37**, 785 (1988).

[182] J. P. Perdew, J. A. Chevary, S. H. Vosko, K. A. Jackson, M. R. Pederson, D. J. Singh, and C. Fiolhais, Phys. Rev. B **46**, 6671 (1992).

[183] E. H. Lieb and S. Oxford, Int. J. Quantum Chem. **19**, 427 (1981).

[184] A. D. Becke, J. Chem. Phys. **84**, 4524 (1986).

[185] E. Engel and S. H. Vosko, Phys. Rev. A **47**, 2800 (1993).

[186] R. Pou-Amerigo, M. Merchán, I. Nebot-Gil, P.-O. Widmark, and B. Roos, Theor. Chim. Acta **92**, 149 (1995).

[187] J. P. Perdew and Y. Wang, Phys. Rev. B **45**, 13244 (1992).

[188] J. P. Perdew and Y. Wang, Phys. Rev. B **33**, 8800 (1986).

[189] J. DeFeers, B. A. Levi, S. K. Pollack, W. J. Hehre, J. S. Binkley, and J. A. Pople, J. Am. Chem. Soc. **101**, 4085 (1979).

[190] K. S. Krasnov, (ed.), *Structural Constants of Inorganic Molecules* (Khimija, Leningrad, 1979), in Russian.

[191] J. A. Pople, M. Head-Gordon, D. J. Fox, K. Raghavachari, and L. A. Curtiss, J. Chem. Phys. **90**, 5622 (1989).

[192] L. A. Curtiss, C. Jones, G. W. Trucks, K. Raghavachari, and J. A. Pople, J. Chem. Phys. **93**, 2537 (1990).

[193] J. P. Perdew, S. Kurth, A. Zupan, and P. Blaha, Phys. Rev. Lett. **82**, 2544 (1999), see erratum *ibid.* **82**, 5179 (1999).

[194] T. Ziegler, V. Tschinke, and C. Ursenbach, J. Am. Chem. Soc. **109**, 4825 (1987).

[195] C. W. Bauschlicher, S. R. Langhoff, and L. A. Barnes, Chem. Phys. **129**, 431 (1989).

[196] L. A. Barnes, M. Rosi, and J. C. W. Bauschlicher, J. Chem. Phys. **94**, 2031 (1991).

[197] A. W. Ehlers and G. Frenking, J. Am. Chem. Soc. **116**, 1514 (1994).

[198] V. Jonas and W. Thiel, J. Chem. Phys. **102**, 8474 (1995).

[199] J. Li, G. Schreckenbach, and T. Ziegler, J. Am. Chem. Soc. **117**, 486 (1995).

[200] K. E. Lewis, D. M. Golden, and G. P. Smith, J. Am. Chem. Soc. **106**, 3905 (1984).

[201] A. E. Stevens, C. S. Feigerle, and W. C. Lineberger, J. Am. Chem. Soc. **104**, 5026 (1982).

[202] C. Daniel, M. Bernard, A. Dedieu, R. Wiest, and A. Veillard, J. Phys. Chem. **88**, 4805 (1984).

[203] M. Poliakoff and E. Weitz, Acc. Chem. Res. **20**, 408 (1987).

[204] M. R. A. Blomberg, P. E. M. Siegbahn, T. J. Lee, A. P. Rendell, and J. E. Rice, J. Chem. Phys. **95**, 5898 (1991).

[205] M. R. A. Blomberg, P. E. M. Siegbahn, and M. Svensson, J. Chem. Phys. **104**, 9546 (1996).

[206] A. K. Fisher, F. A. Cotton, and G. Wilkinson, J. Am. Chem. Soc. **79**, 2044 (1957).

[207] L. S. Sunderlin, D. Wang, and R. R. Squires, J. Am. Chem. Soc. **114**, 2788 (1992).

[208] G. Distefano, J. Res. Natl. Bur. Stand., Sect. A **74**, 2333 (1970).

[209] S. C. Chung, S. Krüger, G. Pacchioni, and N. Rösch, J. Chem. Phys. **102**, 3695 (1995).

[210] A. Jost and B. Rees, Acta Crystallogr. **B31**, 2649 (1975).

[211] H. P. Lüthi, P. E. M. Siegbahn, and J. Almlöf, J. Phys. Chem. **89**, 2156 (1985).

[212] L. Hedberg, T. Ijima, and K. Hedberg, J. Chem. Phys. **70**, 3224 (1979).

[213] J. P. Perdew, K. Burke, and M. Ernzerhof, Phys. Rev. Lett. **80**, 890 (1998).

Publications

1 A. V. Matveev, M. Mayer, N. Rösch, *An Efficient Symmetry Treatment for Molecular Electronic Structure Calculations. The Symmetry Module of the Program* PARAGAUSS *for Solving the Nonrelativistic and Relativistic Kohn–Sham Problem*, in preparation.

2 S. Majumder, A. V. Matveev, N. Rösch, *Spin-Orbit Interaction in the Douglas–Kroll Approach to Relativistic Density Functional Theory: The Screened Nuclear Potential Approximation for Molecules*, in preparation.

3 N. Rösch, A. Matveev, V. A. Nasluzov, K. M. Neyman, L. Moskaleva, S. Krüger, *Quantum Chemistry with the Douglas–Kroll–Hess Approach to Relativistic Density Functional Theory: Efficient Methods for Molecules and Materials*, in *Relativistic Electronic Structure Theory — Applications, Theoretical and Computational Chemistry Series*, edited by P. Schwerdtfeger, (Elsevier, Amsterdam, 2003), in press.

4 A. V. Matveev and N. Rösch, *The Electron-Electron Interaction in the Douglas–Kroll–Hess Approach to the Dirac–Kohn–Sham Problem*, J. Chem. Phys. **118**, 3997 (2003).

5 M. Garcia Hernández, C. Lauterbach, S. Krüger, A. Matveev and N. Rösch, *Comparative Study of Relativistic Density Functional Methods Applied to the Actinide species AcO_2^{2+} and AcF_6 for Ac = U, Np*, J. Comput. Chem. **23**, 834 (2002).

6 K. M. Neyman, D. I. Ganyushin, A. V. Matveev, V. A. Nasluzov, *Calculation of Electronic g-Tensors Using a Relativistic Density Functional Douglas-Kroll Method*, J. Phys. Chem. A, **106**, 5022 (2002).

7 A. Matveev, M. Staufer, M. Mayer, and N. Rösch, *Density Functional Calculations on Small Molecules and Transition Metal Carbonyls with Revised PBE Functionals*, Int. J. Quantum Chem. **75**, 863 (1999).

8 A. V. Matveev, K. M. Neyman, I. V. Yudanov, and N. Rösch, *Adsorption of Transition Metal Atoms on Oxygen Vacancies and Regular Sites of the $MgO(001)$ Surface*, Surf. Sci. **426**, 123 (1999).

9 A. V. Matveev, K. M. Neyman, G. Pacchioni, and N. Rösch, *Density Functional Studies of M_4 Clusters (M = Cu, Ag, Ni, Pd) Deposited on the Regular $MgO(001)$ Surface*, Chem. Phys. Lett. **299**, 603 (1999).

Parts of this dissertation have been (or will be) be published in publications no. 1, 3, 4, 6, and 7.

Thanks

A work of this length would not have been possible without the support of many people around me. This section is dedicated to them. I would like to thank all of them, especially ...

- Prof. Dr. Notker Rösch, for constant support and interest, the opportunities to attend conferences and schools, and, last but not least, the occasional reminder that I could still do better.

- Markus Mayer, my collaborator whose work provided a solid fundament for mine, from whom I learned a lot, for countless hot debates, insightful ideas, and good company all along.

- Philip Gisdakis, my roommate, colleague, and my tutor in system administration for friendly atmosphere he always managed to maintain around him.

- Markus Staufer, my other collaborator, for sharing his programming experience with me and his superlative patience at explaining me the right way to do things.

- My other friends, colleagues, and guests of the group for the pleasure of working with them and many other reasons: K. Albert, W. Alsheimer, T. Belling, U. Birkenheuer, C. Bussai, S.-H. Cai, Z. Chen, P. Chuichay, N. Cruz Hernández, C. Di Valentin, D. Egorova, M. Fuchs-Rohr, D. Ganyushin, M. Garcia Hernández, A. Genest, M. Girju, A. Görling, A. Gordienko, U. Gutdeutsch, H. Heinze, A. Hu, V. Igoshin, C. Inntam, E. Ivanova-Shor, T. Kerdcharoen, R. Kosarev, S. Krüger, C. Lauterbach-Willnauer, E. Le Gentil, K.-H. Lim, A.-M. Ferrari, S. Majumder, D. Mamaluy, L. Moskaleva, S. Nagel, V. Nasluzov, K. Neyman, F. Nörtemann, G. Pacchioni, J. Rak, T. Rathmann, Z. Rinkevicius S. Ruzankin, R. Sahnoun, F. Schlosser, T. Seemüller, A. Shor, K. Siriwong, M. Suzen, G. Vayssilov, S. Vent, A. Voityuk, A. Woiterski, I. Yudanov, and all the people not mentioned here by name.

- My mother for everything.

Last but not least, I thank the patient reader who has come this far.